# CHEMICAL COMPOSITION DISTRIBUTION OF BINARY AND MULTICOMPONENT COPOLYMERS

**Siripon Anantawaraskul**

Department of Chemical Engineering
McGill University
Montreal, Quebec, Canada

A thesis submitted to the Faculty of Graduate Studies and Research
in partial fulfillment of the requirements for the
degree of Doctor of Philosophy

*Your file Votre référence*
*ISBN: 0-612-98195-9*
*Our file Notre référence*
*ISBN: 0-612-98195-9*

ให้คุณแม่ครับ

*To my mother*

# PREFACE

This thesis was prepared using the manuscript-based thesis option following the guidelines for thesis preparation provided by the Faculty of Graduate Studies and Research.

*As an alternative to the traditional thesis format, the dissertation can consist of a collection of papers of which the student is an author or co-author. These papers must have a cohesive, unitary character making them a report of a single program of research. The structure of the manuscript-based thesis must conform to the following:*

*Candidates have the option of including, as part of the thesis, the text of one or more papers submitted, or to be submitted, for publication, or the clearly duplicated text (not the reprints) of one or more published papers. These texts must conform to the "Guidelines for Thesis Preparation" with respect to font size, line spacing and margin sizes and must be bound together as an integral part of the thesis.*

*The thesis must be more than a collection of manuscripts. All components must be integrated into a cohesive unit with a logical progression from one chapter to the next. In order to ensure that the thesis has continuity, connecting texts that provide logical bridges preceding and following each manuscript are mandatory.*

*The thesis must conform to all other requirements of the "Guidelines for Thesis Preparation" in addition to the manuscripts. The thesis must include the following: a table of contents; a brief abstract in English and French; an introduction, which clearly states the rational, and objectives of the research; a comprehensive review of the literature (in addition to that covered in the introduction to each paper); and a thorough bibliography.*

*As manuscripts for publication are frequently very concise documents, where appropriate, additional materials must be provided (e.g., in appendices) in sufficient detail to allow a clear and precise judgment to be made of the important and originality of the research reported in the thesis.*

*In general, when co-authored papers are included in a thesis the candidate must have made a substantial contribution to all papers included in the thesis. In addition, the candidate is required to make an explicit statement in the thesis as to who contributed to such work and to what extent. This statement should appear in a single section entitled "Contributions of Authors" as a preface to the thesis. The supervisor must attest to the accuracy of this statement at the doctoral oral defense. Since the task of the examiners is made more difficult in these cases, it is in the candidate's interest to clearly specify the responsibilities of all the authors of the co-authored papers.*

This thesis is based on 4 manuscripts:

- Anantawaraskul S., Soares J.B.P. and Wood-Adams P.M., "Chemical Composition Distribution of Multicomponent Copolymers", *Macromolecular Theory and Simulation*, **2003**, *12*, p. 229-236.
- Anantawaraskul S., Soares J.B.P., Wood-Adams P.M. and Monrabal B., "Effect of Molecular Weight and Average Comonomer Content on the Crystallization Analysis Fractionation (Crystaf) of Ethylene α-Olefin Copolymers", *Polymer*, **2003**, *44*, p. 2393-2401.
- Anantawaraskul S., Soares J.B.P. and Wood-Adams P.M., "Effect of Operation Parameters on Temperature Rising Elution Fractionation and

Crystallization Analysis Fractionation", *Journal of Polymer Science: Part B: Polymer Physics*, **2003**, *41*, p.1762-1778.

- Anantawaraskul S., Soares J.B.P. and Wood-Adams P.M., "A Study on the Cocrystallization of Blends of Ethylene/1-Olefin Copolymers during Crystallization Analysis Fractionation (Crystaf)", submitted to *Macromolecular Chemistry and Physics*.

## CONTRIBUTIONS OF AUTHORS

The author of this thesis, Siripon Anantawaraskul, is the principal investigator of the research work reported in all the manuscripts. The author carried out the experimental, computational, and theoretical studies, performed the data analysis, and prepared the first draft of each manuscript.

Dr. João B.P. Soares and Dr. Paula M. Wood-Adams are research directors. They provided guidance, useful discussions, as well as editorial assistance for all manuscripts. Dr. João B.P. Soares also provided laboratory space and access to the specialized experimental apparatus involved in this study.

Dr. Benjamin Monrabal provided Crystaf and GPC data of samples fractionated using a preparative fractionation apparatus (PREP) and gave useful suggestions during the manuscript preparation.

# ABSTRACT

Chemical composition distribution (CCD) of copolymers describes the distribution of average comonomer content among copolymer chains. This information is very important as CCD can significantly influence physical properties of copolymers. The main goal of this study is to further our understanding of the CCD of copolymers.

The present understanding of CCD of multicomponent copolymers is very limited and there are no analytical equations capable of describing this distribution. In the present study, analytical expressions for describing the CCDs of random multicomponent copolymers are developed using a statistical approach. The results from this theoretical expression are validated with the results from Stockmayer's distribution and Monte Carlo simulations for limiting cases.

In the case of semi-crystalline binary copolymers, temperature rising elution fractionation (Tref) and crystallization analysis fractionation (Crystaf) can be used for the estimation of CCD. The effects of chain microstructure and operating conditions on these techniques are investigated using a series of ethylene/α-olefin copolymers with well-defined microstructures. Both molecular weight and comonomer content are shown to significantly affect the shape of Crystaf profiles. Fortunately, comonomer content is the main determining factor for Crystaf peak temperature, permitting the use reliable calibration curves for this technique. A Crystaf model

based on the average ethylene sequence distribution in the chains is proposed and the results from this model show very good agreement with the present and previously reported experimental data.

The typical operating conditions used in Tref and Crystaf analyses are found to lead to fractionation conditions that are far from the thermodynamic equilibrium. Consequently, crystallization kinetics can strongly influence the CCD estimated with Tref and Crystaf. Sample cocrystallization during analysis is also considered as it may interfere with the fractionation processes of both techniques. The similarity of chain crystallizabilities and fast cooling rates are found to promote cocrystallization. Cocrystallization under a certain conditions can be so strong that it can seriously affect the interpretation of the CCD measured with Crystaf and Tref.

# RÉSUMÉ

La distribution de la composition chimique (DCC) des copolymères décrit la distribution du contenu moyen en comonomère parmi des chaînes copolymères. La connaissance de la DCC est importante car elle influence grandement les propriétés physiques des copolymères.

La compréhension actuelle de la DCC des copolymères à composants multiples est limitée. Il n'y a pas d'expressions analytiques capables de décrire cette distribution. Dans cette étude, des expressions analytiques pour décrire les DCCs des copolymères aléatoires à composants multiples sont développées en utilisant une approche statistique. Les résultats de cette expression théorique sont validés par les résultats de la distribution de Stockmayer et des simulations Monte Carlo pour des cas limités.

Pour les copolymères semicristallins binaires, la fractionnement par élution (Tref) et la fractionnement par cristallisation (Crystaf) peuvent être utilisées pour l'estimation de la DCC. Les effets de la microstructure des chaînes et des conditions expérimentales sur ces techniques sont étudiés pour une série de copolymères d'éthylène/α-oléfine à microstructures bien définies. Il est trouvé que la masse moléculaire et le contenu en comonomère influencent, tous les deux, grandement la forme des profils de Crystaf. Heureusement, le contenu en comonomère est le facteur

principal déterminant la température de crête du Crystaf, permettant ainsi une utilisation fiable de courbes de calibrage pour cette technique. Un modèle basé sur la distribution de la séquence d'éthylène moyenne est proposé pour la technique de Crystaf. Les résultats de ce modèle sont en accord avec les résultats présentés ici et antérieurement.

Il a été trouvé que les conditions expérimentales typiques utilisées pour les analyses Tref et Crystaf aboutissent à des conditions de fractionnement loin de l'équilibre thermodynamique. En conséquence, la cinétique de cristallisation peut fortement influencer la DCC estimée par Tref et Crystaf. La co-cristallisation de l'échantillon pendant l'analyse a été aussi étudiée, puisque cela peut interférer avec le fractionnement pour les deux techniques. Il a été trouvé que la similitude du pouvoir de cristallisation des chaînes et des vitesses de refroidissement rapides favorisent la co-cristallisation. La co-cristallisation dans certaines conditions peut être tellement forte que cela peut sérieusement affecter l'interprétation de la DCC mesurée par Crystal et Tref.

# ACKNOWLEDGEMENTS

*A master can tell you what he expects of you.*
*A teacher, though, awakens your own expectations.*

*Patricia Neal*

I would like to express gratitude to my academic advisors, Prof. João B.P. Soares (University of Waterloo), Prof. Paula M. Wood-Adams (Concordia University), and Prof. John M. Dealy (McGill University), for their advice and continuous encouragement throughout the course of my work. I am very thankful to Prof. João B.P. Soares for giving me the opportunity to work in his laboratory at University of Waterloo and to learn from his fascinating research.

I would also like to thank Dr. Daryoosh Beigzadeh, Dr. Stéphane Costeux, Dr. Márcio Nele, and Lijun Feng for interesting discussions and useful suggestions in various stages of this works.

I extend many thanks to my co-workers at polymer rheology and structure research group at McGill University and polyolefin research group at University of Waterloo: Deborah M. Sarzotti and William Ripmeester, for teaching me how to use various characterization techniques and to synthesize my own polymers; Chunxia He and Hee Eon Park, for their help and suggestions on many small issues that sum up to be enormous; Sang-Yang A. Shin, Fabio Mota, Miguel Baqueiro, Matthew Campbell, Fabricio Smillo, Jen S. Tiang, and Junke Xu, for their friendship and for being with me in the lab, even at some times pass midnight.

I would also like to thank Dr. Ludovic Capt for his help in the preparation of the French version of the thesis abstract.

Living as an international student in the country that is half way across the world for more than half a decade is not easy. Friendship and continuous moral support from Thai student communities at both McGill University and the University of Waterloo made my life in Canada much more pleasant and is greatly appreciated. I have always felt welcome no matter which city I was in.

Thanks to the Department of Chemical Engineering, Kasetsart University, and government of Thailand for allowing me to pursue this degree. I am really looking forward to going back to rejoin the team there.

Last, but not least, I would like to thank my family for their love and continuous support thought out my career as a graduate student.

# TABLE OF CONTENTS

## CHAPTER 3 CHEMICAL COMPOSITION DISTRIBUTION OF MULTICOMPONENT COPOLYMERS



## CHAPTER 4 EFFECT OF MOLECULAR WEIGHT AND COMONOMER CONTENT ON CRYSTAF

# LIST OF FIGURES

**CHAPTER 4**

**CHAPTER 5**

**CHAPTER 6**

# LIST OF TABLES

CHAPTER 1

# INTRODUCTION

*A science is any discipline in which a fool of this generation can go beyond the point reached by the genius of the last generation.*

***Max Gluckman***

## 1.1 BACKGROUND

The unique properties of polymers come from the large size of their molecules and the fact that they are composed of molecules having a distribution of chain microstructures. It is generally known that the properties of polymers depend not only on their average microstructural characteristics, but also on the detailed distribution of their microstructures. Both average chain length and chain length distribution, for example, significantly affect the physical properties of polymers.

In the case of copolymers, the properties are also influenced by how comonomer units are distributed on the copolymer chains. Comonomer incorporation gives rise to two different distributions: The monomer sequence length distribution (SLD) and the chemical composition distribution (CCD). Figure 1.1 illustrates these distributions for a typical Ziegler-Natta linear low-density polyethylene (ZN-LLDPE). The SLD describes how the monomers are distributed within the copolymer chains and reflects intramolecular heterogeneity. On the other hand, the CCD describes the distribution of the average comonomer content among the copolymer chains, thus reflecting intermolecular heterogeneity.

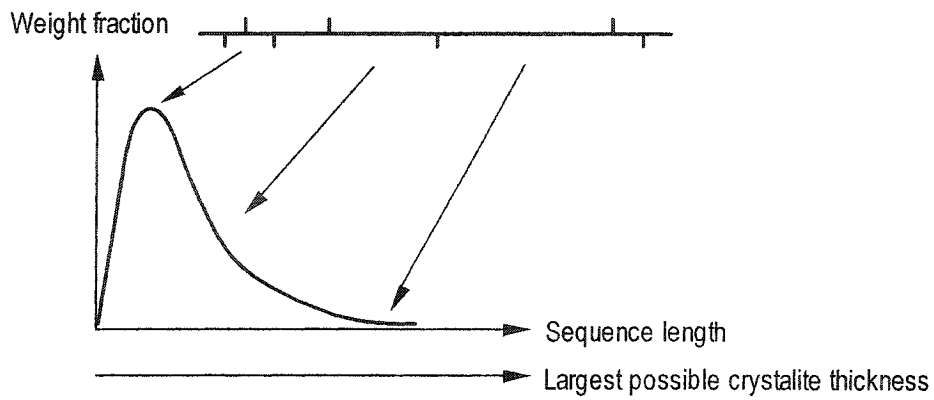


(a) Sequence length distribution (SLD)

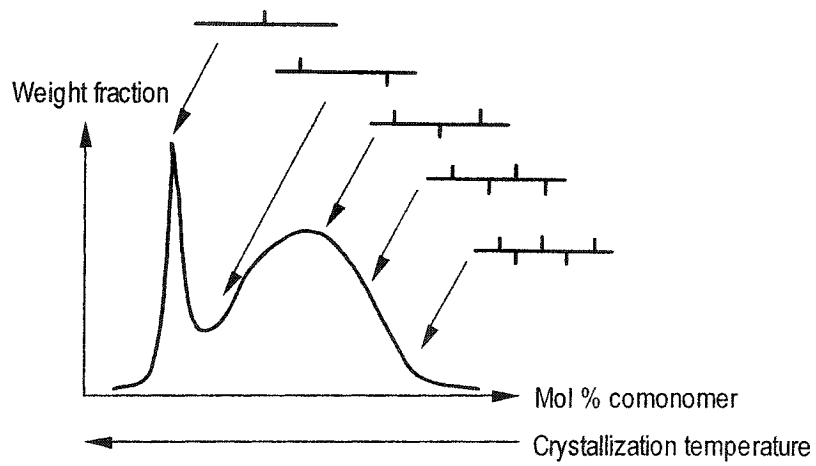


(b) Chemical composition distribution (CCD)

Figure 1.1 Illustration of sequence length and chemical composition distributions of a typical Ziegler-Natta linear low-density polyethylene (ZN-LLDPE), reflecting the intramolecular and intermolecular heterogeneity of these copolymers

The knowledge of these distributions is of great important for constructing structure-property relationships, tailor-making polymers with predetermined properties, and understanding the nature of polymerization mechanisms. The present study intends to further the current understanding of these distributions.

The theory describing the SLD for various copolymerization models, for both binary and multicomponent copolymers, is well developed. However, a general

analytical equation for the CCD of multicomponent copolymers is not yet available. The first objective of this study is to develop a general theoretical expression using a statistical approach. Experimental methods for determining the CCD of multicomponent copolymers are not available; therefore, the results from this theoretical expression are validated by comparison with the results from Monte Carlo simulations.

In the case of semi-crystalline binary copolymers, two techniques are widely used for the estimation of CCD: temperature rising elution fractionation (Tref) and crystallization analysis fractionation (Crystaf). Both of these techniques fractionate polymer chains of different crystallizabilities via crystallization from dilute solutions. Details of the operations of both techniques will be discussed in the subsequent chapters.

This study examines these two techniques to determine the factors governing the fractionation process and how these factors can influence the CCD estimated using both techniques. The effects of both chain microstructure and operating conditions are considered. Cocrystallization during the analyses can interfere with the fractionation process and may, therefore, affect the estimated CCD. Therefore, cocrystallization phenomena in Tref and Crystaf are also investigated in this study. An attempt is also made to develop a mathematical model for Crystaf based on a distribution of chain microstructures using Monte Carlo simulations.

## 1.2 RESEARCH OBJECTIVES

The main goal of this study is to further our understanding of the CCD of copolymers. In the case of binary copolymers, where experimental measurements are possible, this study also investigates the details of the fractionation process to better understand these analytical techniques and identify the potential factors that may affect the estimated CCD. More specifically, the objectives of this work can be summarized as follows:

(1) To develop an analytical expression for the CCD of multicomponent copolymers.

(2) To establish a mathematical model for Crystaf analysis using a statistical method and Monte Carlo simulation.

(3) To identify key parameters governing the fractionation process in Tref and Crystaf analysis and to understand the effect of these parameters on the analysis results.

(4) To investigate the cocrystallization phenomenon during Crystaf analysis and to determine the factors influencing this phenomenon.

## 1.3 THESIS OUTLINE

This thesis is divided into 7 chapters. Chapter 2 presents the research background and a summary of the published literature on CCD, Tref, and Crystaf analyses. In Chapter 3, a rigorous derivation of the CCD of terpolymers using a statistical approach is presented. The extension of this expression to the case of random multicomponent copolymers is also presented.

In Chapter 4, the effect of chain microstructure on Crystaf profiles, specifically average molecular weight and comonomer content, are examined experimentally. These experimental results are then used to validate the proposed Crystaf models. Chapter 5 discusses the effects of crystallization kinetics and cocrystallization on Tref and Crystaf data. The investigation of cocrystallization during Crystaf analysis is described in more detail in Chapter 6. Finally, Chapter 7 summarizes the conclusions and notes the original contributions of the present study.

## 1.4 GUIDE TO MANUSCRIPTS

This thesis is written using the manuscript-based thesis option following the guidelines for thesis preparation provided by the Faculty of Graduate Studies and Research. The thesis is based on 4 manuscripts. It is prepared in such a way that each chapter is as self-contained as possible with sufficient introduction, research rational, and references provided. However, readers who go through this thesis in order will find a logical connection from one chapter to the next. The following list provides a guide for the readers to the manuscripts related to each chapter:

*Chapter 3*

- Anantawaraskul S., Soares J.B.P. and Wood-Adams P.M., "Chemical Composition Distribution of Multicomponent Copolymers", *Macromolecular Theory and Simulation*, **2003**, *12*, p. 229-236.

*Chapter 4*

- Anantawaraskul S., Soares J.B.P., Wood-Adams P.M. and Monrabal B., "Effect of Molecular Weight and Average Comonomer Content on the Crystallization Analysis Fractionation (Crystaf) of Ethylene α-Olefin Copolymers", *Polymer*, **2003**, *44*, p. 2393-2401.

*Chapter 5*

- Anantawaraskul S., Soares J.B.P. and Wood-Adams P.M., "Effect of Operation Parameters on Temperature Rising Elution Fractionation and Crystallization Analysis Fractionation", *Journal of Polymer Science: Part B: Polymer Physics*, **2003**, *41*, p.1762-1778.

*Chapter 6*

- Anantawaraskul S., Soares J.B.P. and Wood-Adams P.M., "A Study on the Cocrystallization of Blends of Ethylene/1-Olefin Copolymers during Crystallization Analysis Fractionation (Crystaf)", submitted to *Macromolecular Chemistry and Physics*.

CHAPTER 2

# RESEARCH BACKGROUND AND LITERATURE REVIEW

*Science is built up with facts, as a house is with stones.*
*But a collection of facts is no more a science than a heap of stones is a house.*
***Henri Poincaré***

This chapter presents a brief literature review and provides some theoretical background relevant to the present study. Research works related to the chemical composition distribution (CCD) of copolymers are summarized first. The published literature on two analytical techniques for measuring CCD of binary semi-crystalline copolymers, temperature rising elution fractionation (Tref) and crystallization analysis fractionation (Crystaf), are then reviewed. Finally, polymer-diluent systems, which are related to Tref and Crystaf operations, are considered from a theoretical viewpoint using the Flory-Huggins theory.

## 2.1 CHEMICAL COMPOSITION DISTRIBUTION

The chemical composition distribution (CCD) of copolymers is a microstructural characteristic that reflects the composition heterogeneity of copolymer chains. This term has also been referred to in the literature as comonomer composition distribution and short chain branching distribution (SCBD). However, the term SCBD is generally restricted to linear low-density polyethylene (LLDPE), where α-olefin comonomers (e.g., 1-butene, 1-octene) act as short branches in the chain topology. Therefore, the

term CCD, which is more general and applicable to all copolymer systems, is more appropriate and will be used in the thesis.

### 2.1.1 Stockmayer's bivariate distribution

Stockmayer's bivariate distribution is an analytical expression describing the weight distribution of kinetic chain length and chemical composition for linear binary copolymers. Stockmayer [1] obtained this expression with the aid of some approximations from a general theory of chain copolymerization described earlier by Simha and Branson [2].

Despite its simplifying assumptions, this distribution function has been found to be useful for understanding the chain microstructures of several copolymers [3-5]. It has also been used to model fractionation techniques that are based on CCD, *e.g.* temperature rising elution fractionation (Tref) [6] and crystallization analysis fractionation (Crystaf) [7-9].

Stockmayer's bivariate distribution for linear binary copolymers can be expressed as follows,

$$w(r,y)\cdot dr\cdot dy = r\cdot\tau^2\cdot exp(-r\cdot\tau)\cdot dr\cdot\frac{1}{\sqrt{2\pi\beta/r}}\cdot exp\left(\frac{-y^2}{2\beta/r}\right)\cdot dy \qquad (2.1)$$

$$\beta = \overline{F_1}\cdot(1-\overline{F_1})\cdot\sqrt{1+4\cdot\overline{F_1}\cdot(1-\overline{F_1})\cdot(r_1\cdot r_2-1)} \qquad (2.2)$$

where $\overline{F_1}$ is the average mole fraction of monomer type 1 in the copolymer, $y$ is the chemical composition deviation from $\overline{F_1}$, $r$ is the kinetic chain length, $r_1$ and $r_2$ are the reactivity ratios for copolymerization, and $\tau$ is the ratio of the transfer rate to the propagation rate. This ratio can be easily estimated, as it is equal to the reciprocal of the number average chain length.

Integrating Equation (2.1) over all chain lengths, one obtains the equation describing the CCD component of Stockmayer's distribution, independently of chain length:

$$w(y) = \int_{r=0}^{\infty} w(r,y) \cdot dr = \frac{3}{4\sqrt{2\beta\tau}\left(1+\frac{y^2}{2\beta\tau}\right)^{5/2}} \tag{2.3}$$

Equation (2.3) has been found to be useful for describing polymers synthesized with multi-site type catalysts and for modeling CCDs of polymers synthesized with both multi-site and single-site type catalysts [6-9].

### 2.1.2 Origins and effects of composition heterogeneity in copolymers

Several factors contribute to the composition heterogeneity of the CCD of copolymers [10]. The first cause of deviation from the average comonomer composition is caused by the statistical nature of polymerization and is well described by Stockmayer's bivariate distribution discussed earlier. For chain growth polymerization, the formation of each polymer chain follows a stochastic process governed by the probabilities of chain propagation and comonomer incorporation.

Even if copolymers are produced by single-site type catalysts, polymer chains differ in chain length and comonomer composition. Large variations in comonomer composition are generally observed for shorter polymer chains. The type of the copolymerization statistics also affects the broadening of the CCD. Block copolymers have broader CCD than random copolymers, while perfectly alternating copolymers have an extremely narrow CCD.

The type of catalyst used during polymerization can also greatly influence the shape of the CCD. For multi-site type catalysts, *e.g.* heterogeneous Ziegler-Natta catalysts, each active site type produces polymer chains with a distinct set of polymerization kinetic constants, *i.e.* a different set of probabilities governing the polymerization process [10-12]. Therefore, the polymers synthesized using these catalysts are mixtures of chains of different chain lengths and comonomer compositions from all active site types. This generally produces polymers with an extremely broad and non-unimodal CCD.

This broad CCD of heterogeneous copolymers may induce *microphase separation*, where the highly short chain branched molecules segregate from the less branched chains and form a disperse phase [13-15]. This, of course, significantly affects the crystallization process and influences the mechanical and optical properties of the product.

Another important cause of CCD heterogeneity is nonuniform polymerization conditions, *i.e.* temporal and spatial variations in monomer concentration and temperature during polymerization. This phenomenon can be caused by macro- and micromixing effects in the polymerization reactor. For batch or semibatch reactors, compositional drift can also broaden the CCD.

Composition heterogeneity of copolymers has been reported to significantly influence their physical properties. For example, linear low-density polyethylene (LLDPE) with narrow CCDs can have dramatically improved film properties as compared to LLDPE with broad CCDs [16-17]. The CCDs have also been related to other properties, such as environmental stress crack resistance (ESCR) [18] and the dependence of dynamic mechanical behavior on temperature [19].

## 2.2 TEMPERATURE RISING ELUTION FRACTIONATION (TREF)

Temperature rising elution fractionation (Tref) is an analytical technique that is widely used for determining the distribution of chain crystallizabilities. As chain crystallizabilities are mainly controlled by the chain composition in the case of ethylene/α-olefin copolymers, the results from Tref analysis, together with an appropriate calibration curve, can be used to estimate CCD.

In the case of stereoregular polymers (*e.g.* isotactic or syndiotactic polypropylene), where tacticity is the main factor affecting chain crystallizabilities, Tref can provide information on the distribution of chain tacticities. It has also been applied to determine blend compositions in polyolefins. A number of extensive reviews of this technique have been published [10, 20-23].

A schematic diagram of Tref is shown in Figure 2.1. Tref analysis involves two temperature steps: crystallization and elution. Before the crystallization step, the

sample is dissolved in a thermodynamically good solvent at high temperature and then introduced into a column containing an inert substrate, such as glass beads or steel shots. The temperature in the column is then decreased at a slow, constant rate. This step allows polymer chains to crystallize in an orderly fashion. A molecule with higher crystallizability will precipitate and deposit as a layer on the inert substrate at higher temperatures. Subsequently, chains with lower crystallizabilities, *i.e.* with higher comonomer content, will precipitate at lower temperatures as outer layers on the substrate. The crystallization step is the most important one in Tref, as the fractionation process occurs during this step.

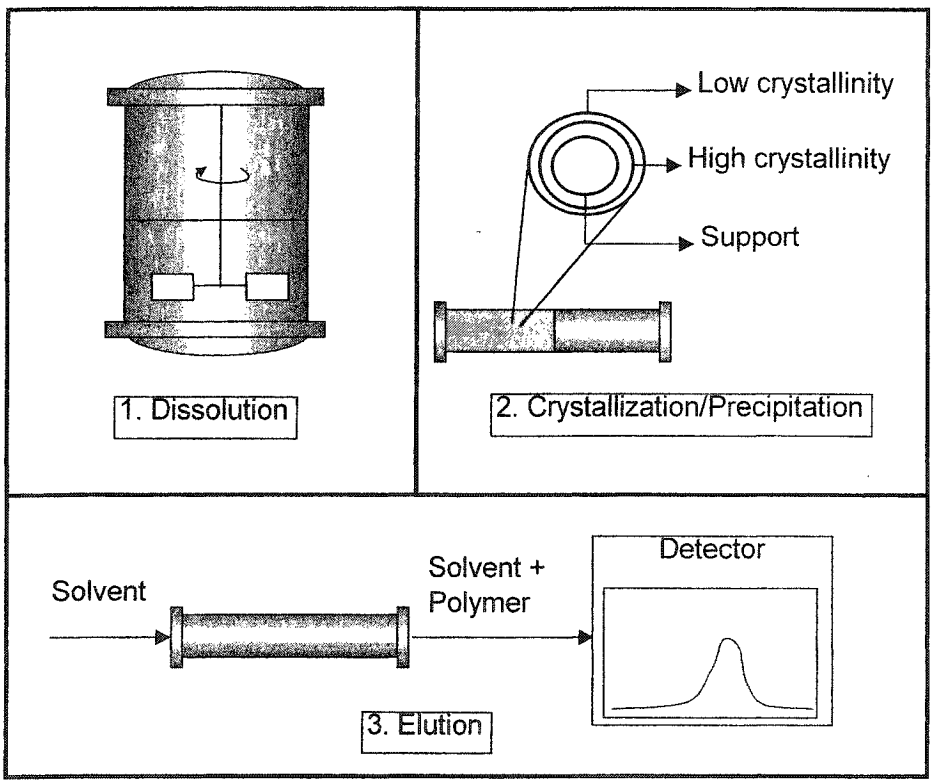


Figure 2.1 Schematic diagram of Tref

In the elution step, pure solvent flows through the column while the temperature is being increased. This allows the outer layers of polymer to dissolve back into the solvent in the reverse order in which they were precipitated. The concentration of polymer eluted from the column by the solvent and the elution temperature are monitored. This step can be carried out in two ways, as described below.

In the first method, called analytical Tref (or A-Tref), the temperature in the elution step is increased at a slow constant rate. This method provides information on the distribution of chain crystallizabilities in terms of the weight fraction of polymer eluted at each temperature, commonly referred to as the Tref profile. The second method is called preparative Tref (or P-Tref). In this case, the temperature is increased as a step function. The second method is used to prepare a series of larger fractions, each containing relatively narrow compositional heterogeneity that can be further investigated by other analytical and characterization techniques.

The effect of molecular weight on the fractionation process in Tref was examined by Wild *et al.* [24]. They reported a very strong molecular weight dependence when polymers with low molecular weight (<10,000) were involved. Tref results become independent of chain length, however, for polymers with higher molecular weights.

Comonomer content is found to significantly affect Tref profiles. This is to be expected, as the comonomer units are known to reduce chain regularity, thus lowering chain crystallizability. A linear relationship between the average comonomer content and the elution peak temperature is generally observed for ethylene/α-olefin copolymers [10, 20-21]. Comonomer type also has an effect on Tref profiles. This effect causes a change in the slope of the calibration curve, which is the plot of comonomer content versus elution temperature [25].

The major difficulty in using Tref analysis to obtain quantitative CCDs is that the calibration curve is material-dependent, *i.e.* it depends on the comonomer type, comonomer content, and comonomer sequence length distribution [26-27]. This means that in addition to the characterization of samples using analytical Tref, preparative Tref has to be performed for each material in order to obtain its correct calibration standards. The compositions of these calibration standards have to be determined using another analytical technique, such as $^{13}C$ NMR, so that the comonomer composition versus elution temperature calibration curve can be determined for each sample type.

Pigeon and Rudin [26] reported a difference between the branching frequencies measured with analytical Tref and with preparative Tref at the same

elution temperature. Their results imply that a calibration curve produced from preparative Tref can not be used for converting raw, analytical Tref results to CCD. It is necessary to modify the analytical Tref results before applying the calibration curve by taking into account the elution time associated with the volumes of the A-Tref and P-Tref columns.

To reduce the complexity of using preparative Tref to obtain calibration curves, Pigeon and Rudin [27] proposed an alternative technique using analytical Tref and a dual infrared spectrometry (dual-IR) detector. The dual-IR system proposed allowed them to measure both concentration and branching frequencies as functions of elution temperature. This eliminated the need to perform preparative Tref on every sample and to correct the analytical Tref results.

Several researchers have attempted to model Tref. Soares and Hamielec [6] used Stockmayer's distributions to simulate the CCD of linear binary copolymers synthesized using multi-site catalysts assuming that the fractionation process of Tref was controlled only by the comonomer composition of copolymer chains. For the case of ethylene/α-olefin copolymers made with multiple-site catalysts, they described the CCD of the whole polymer as the summation of the CCDs of copolymers produced at each active site. Their model, however, did not account for the peak broadening in Tref analysis.

Borrajo *et al.* [28] and Elicabe *et al.* [29-30] proposed a thermodynamic model for Tref based on the Flory-Huggins theory. They attempted to relate the distribution of crystallizable chain lengths with the elution temperature profile. The proposed model assumed extended-chain length crystallization. Therefore, it can not adequately explain the results when long polymer chains are involved, as chain folding effects during crystallization are found to play an important role for such chains.

## 2.3 CRYSTALLIZATION ANALYSIS FRACTIONATION (CRYSTAF)

Crystallization analysis fractionation (Crystaf) is a new thermal characterization technique developed as an alternative to Tref. Crystaf relies on the same fractionation

principle as in Tref, *i.e.* crystallization of chains with different crystallizabilities from a dilute polymer solution. However, Crystaf involves a single polymer solution crystallization step, compared to the two crystallization/elution steps in Tref. Because of this, Crystaf requires a relatively shorter analysis time than Tref to provide the same information. Moreover, Crystaf can also be used to measure the soluble fraction (amorphous polymer fraction) of the polymer being analyzed.

Figure 2.2 is a schematic diagram of Crystaf. In Crystaf analysis, the polymer sample is first dissolved in a good solvent at high temperature to ensure complete dissolution. The temperature of the solution is then decreased at a slow, constant rate to allow polymer chains to crystallize and fractionate according to their crystallizabilities. During this crystallization period, the concentration of the polymer solution is monitored as a function of the crystallization temperature, leading to a cumulative concentration profile (Figure 2.3). The first derivative of this profile is called the derivative profile and represents the fraction of polymer crystallized at each temperature. This derivative profile is generally referred to as the Crystaf profile. As in the case of Tref, Crystaf results can be used to estimate the CCD of copolymers by means of an appropriate calibration curve. More details on the operation of Crystaf are available in the literature [31-34]. The limitations of Tref regarding sample-specific calibration curves also apply to Crystaf.

As a new characterization technique, Crystaf has been compared to other techniques, specifically Tref and DSC [31-33, 35]. It is generally accepted that Crystaf and Tref profiles differ mainly by a temperature shift due to the supercooling effect in Crystaf, similar to the difference between the heating and cooling cycles in DSC.

Gabriel *et al.* [35] compared Crystaf, Tref, and DSC profiles for LLDPE synthesized using a Ziegler-Natta catalyst. Their results showed that these profiles provide the same information and, in fact, can simply be shifted on the temperature axis. Special care should be taken, however, when comparing results from different characterization techniques, because of differences in the typical operating conditions between techniques.

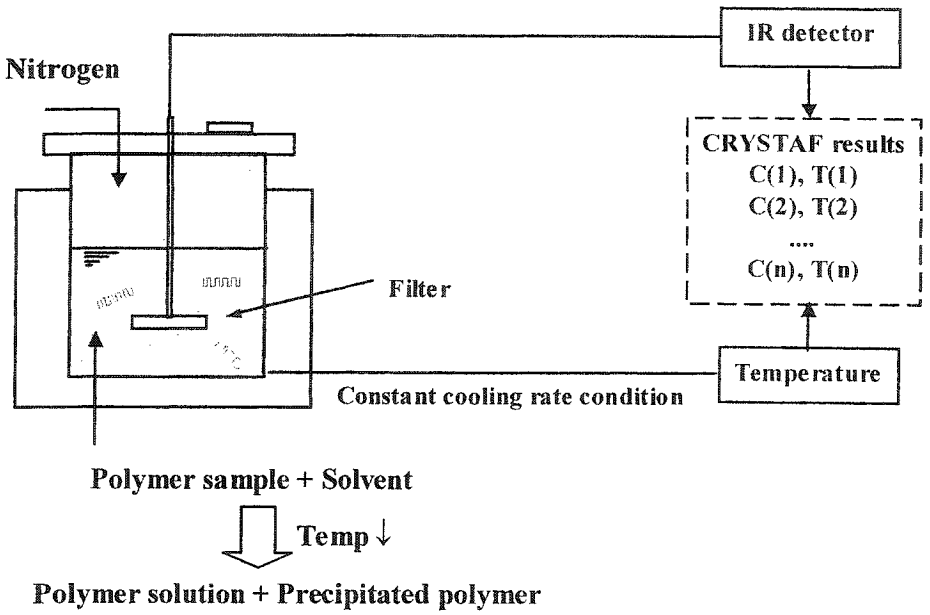


Figure 2.2 Schematic diagram of Crystaf

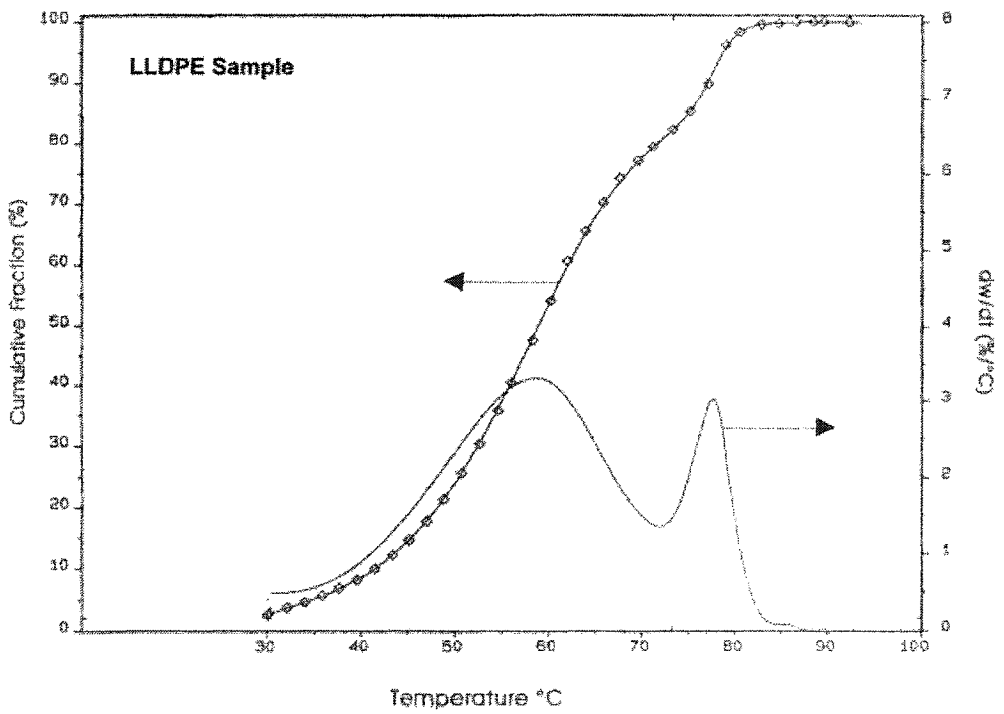


Figure 2.3 Typical cumulative (or integral) and derivative Crystaf profiles of LLDPE synthesized with a Ziegler-Natta catalyst (Monrabal B. [32])

Britto *et al.* [31] compared Crystaf and Tref results for various LLDPE samples. Although qualitatively good agreement between the two techniques was found, quantitative disagreements were observed. Tref analysis clearly revealed the presence of a high-crystallinity double peak, while Crystaf could not detect it. The nature of this double peak is still unclear and the subject of debate in the literature.

All microstructural features affecting chain crystallizability can potentially influence the fractionation process during Crystaf analysis. The main microstructural properties of interests are: (1) number average molecular weight, (2) average comonomer content, and (3) comonomer type.

Nieto *et al.* [36] investigated the effect of chain length on Crystaf profiles using a series of ethylene homopolymers with various molecular weights. A plot of Crystaf peak temperature versus number average molecular weight indicated that the crystallization temperature decreases with molecular weight below a certain chain length threshold ($M_N < 6{,}000$). However, at a reasonably high molecular weight, the crystallization temperature was found to be independent of molecular weight. In addition, the overall Crystaf profiles were found to broaden with decreasing molecular weight.

These results have two main implications. Firstly, Crystaf profiles can reflect the molecular weight distribution when low molecular weight chains are present. (Luckily, it does not significantly affect the Crystaf peak position unless very low molecular weight samples are analyzed.) Secondly, chains with low molecular weight can interfere with the Crystaf profiles, if fractionation due to other microstructural characteristics (*e.g.*, average comonomer content) is the only fractionation mechanism considered. This can lead to discrepancies (most likely widening of the CCD) in the case of the CCD of copolymers with low molecular weights.

The number of comonomer units in the copolymer chains is the most important factor affecting chain crystallizability. This is due to the fact that comonomer units interrupt the chain regularity and thus greatly lower chain crystallizability.

Sarzotti *et al.* [8-9] investigated the effect of comonomer content on Crystaf profiles in great detail using a series of ethylene/1-hexene copolymers having

approximately the same molecular weight, thus eliminating misinterpretations that might arise due to molecular weight effects. As expected, the Crystaf peak temperature was dramatically influenced by the average comonomer content in the copolymer chains. Moreover, the Crystaf profiles became broader with increasing comonomer content.

The effect of comonomer type was studied by Brull *et al.* [37] using propylene/α-olefin copolymers with various comonomers (1-octene, 1-decene, 1-tetradecene, and 1-octadecene). They reported that for their set of samples, not only Crystaf peak temperature but also melting and crystallization temperatures measured by DSC were independent of comonomer type but were strong functions of comonomer content.

Earlier work by da Silva Filho *et al.* [11], however, showed that the comonomer in ethylene/α-olefin copolymers had a significant effect on the relationship between comonomer content and crystallization temperature. Their results from ethylene/1-butene and ethylene/1-octene copolymers give significantly different Crystaf calibration curves. The trend observed in their work is in a good agreement with previous studies that examined the effect of comonomer on Tref calibration curves [25]. A more detailed study is necessary to understand the conflicting conclusions from these two experimental studies. Notice, however, that the work by Brull *et al.* was performed with propylene as the main monomer, not ethylene. It may be that the effect of α-olefin comonomer units on the crystallinity of propylene/α-olefin copolymers is independent of comonomer length, as opposed to the case of ethylene/α-olefin copolymers.

One of the main applications of Crystaf analysis is the estimation of the CCD of semi-crystalline copolymers, particularly LLDPE. The CCD of copolymers can be obtained from the Crystaf profile with the help of a calibration curve relating average comonomer content to crystallization temperature. The renormalization of the transformed CCD is generally required to ensure that the area under the distribution is equal to one. For routine analysis, a calibration curve can also provide a quick estimate of the average comonomer content from the Crystaf peak temperature.

Two methods for preparing Crystaf calibration curves have been reported. Both methods involve performing Crystaf on a series of copolymer samples having known comonomer contents (measured with FTIR or $^{13}C$ NMR) and narrow CCDs, with crystallizabilities covering a broad range of crystallization temperatures. The only difference between these two methods is the type of sample used in the calibration. The first method uses a series of samples synthesized using a single-site catalyst, while the second method uses a series of fractions from broad CCD Ziegler-Natta copolymers obtained by preparative-Tref (P-Tref). After all the samples are analyzed, the relationship between Crystaf peak temperature (or weight-average crystallization temperature) and average comonomer content is plotted and used as a calibration curve.

A number of calibration curves have been reported [32-34, 37]. Unfortunately, as in the case of Tref, calibration curves for Crystaf depend on polymer type, solvent type, cooling rate, and method of sample preparation. Therefore, the calibration curves depend strongly on sample type and analysis conditions. Published calibration curves can still be used, however, if care is taken to replicate as closely as possible the conditions under which they were obtained. These curves are useful for obtaining an approximate CCD or for the relative comparison of CCDs (*e.g.*, the broadness of CCD from different polymers can be compared, provided that the same calibration curve is used).

Although several previous investigations considered the Crystaf analysis of blends, early work was intended only to quantify the limitations of Crystaf due to cocrystallization [32-33]. Only recently has Crystaf been used to provide quantitative information on blend compositions [38-40].

Pasch *et al.* [40] considered Crystaf analyses of blends of commercial HDPE and LDPE. By comparing the known composition of the blends with the blend composition measured by Crystaf, they found that Crystaf was quantitatively accurate over a very wide range of compositions. For instance, Crystaf can detect blend components present in amounts as small as five wt-%. In the analysis of waste plastic samples, Crystaf was found to be superior to conventional DSC for determining blend composition.

Although Crystaf has been established as a good alternative to Tref during the last decade, accurate quantitative models for describing the fractionation process during Crystaf analysis are currently unavailable. Incidentally, they are equally unavailable for Tref. The main difficulty in developing generalized models is the complexity of the crystallization mechanism and fractionation process that occur in both techniques.

Two main approaches have been proposed to model Crystaf fractionation: (1) models based on Stockmayer's bivariate distribution [7-8] and (2) models based on the distribution of chain crystallizabilities using Monte Carlo simulation [41-43]. Sarzotti *et al.* [8-9] used Stockmayer's distribution (Equation 2.3) together with a relationship between crystallization temperature and average comonomer content to model Crystaf profiles. Two variables in Equation (2.3), $\overline{F_1}$ and $\tau$, were used as adjustable parameters to minimize the sum of squares of the residuals between model and experimental profiles. Even though the model fitted the experimental profiles adequately, the molecular weights calculated from the model (easily obtained as $1/\tau$) were significantly underestimated, compared to the molecular weights measured by GPC, indicating that the model was not theoretically sound and provided only a convenient empirical fit of experimental data.

Soares *et al.* [7] proposed a model using Stockmayer's distribution with additional help from a generic instrumental spreading function to account for the instrumental peak broadening in Crystaf. Again, although the model fitted the experimental profiles well, an attempt to determine a general function for the parameters used in the spreading function was not successful.

Although these models are not rigorously correct, the fact that they can fit reasonably well the experimental profiles is surprising, considering that using Stockmayer's distribution to model CCD obtained from Crystaf is based on a number of severe simplifying assumptions. These models assume that: (1) the polymer is prepared under uniform polymerization conditions (*i.e.*, the absence of composition drift and other reactor condition nonuniformities), (2) the fractionation process in Crystaf is controlled only by the average copolymer composition per chain, (3) cocrystallization is completely absent during the analysis, (4) the fractionation

process is independent of molecular weight even for short chains, and (5) crystallization kinetics does not influence Crystaf profiles or, in other words, the fractionation takes place at thermodynamic equilibrium.

Unfortunately, most of these assumptions have recently been proven to be invalid [44-46]. Even though modeling Crystaf profiles using Stockmayer's distribution can provide a reasonable fit of the data, these models are, at best, only semi-empirical. It is clear that a truly physics-based model of the Crystaf fractionation process is essential to predict the correct distribution.

Monte Carlo simulation is a numerical technique for solving stochastic problems that is widely used in polymer science and engineering. Specifically for studies of polymer microstructure, it has been used to predict the CCD of copolymers and the distribution of stereoregularity [47-48]. One of the advantages of this technique is that one can obtain detailed statistical information about chain structures from relatively easy-to-obtain polymer properties such as average comonomer content and molecular weight.

Beigzadeh *et al.* [41-42] proposed the first Monte Carlo model for simulating Crystaf profiles. They assumed that the crystallization of a copolymer chain during Crystaf was solely governed by the length of its longest crystallizable monomer sequence. For the particular case of ethylene/α-olefin copolymers, the longest ethylene sequence per chain was assumed to govern the crystallization process in Crystaf. They proposed that Crystaf profiles could be calculated from the distribution of the longest ethylene sequence instead of the CCD and used Monte Carlo simulation to obtain this distribution. A modified Gibbs-Thompson equation [41] was used as the thermodynamic equilibrium relationship between the crystallization temperature and the length of the longest ethylene sequence, which was assumed to be proportional to the lamella thickness,

$$T_C = \frac{T_S^o(LS-\alpha)}{LS} - \beta \tag{2.4}$$

where $T_C$ is the crystallization temperature measured in Crystaf, $T_S^o$ is the equilibrium melting temperature of a chain with infinite chain length, $\alpha$ is a constant proportional

to $1/\Delta H_u$, $LS$ is the longest ethylene sequence, and $\beta$ is the supercooling temperature in Crystaf. They reported good agreement with the experimental Crystaf profiles for their series of ethylene/1-octene copolymers.

## 2.4 THERMODYNAMIC CONSIDERATIONS OF POLYMER-DILUENT SYSTEMS

The fractionation processes in both Tref and Crystaf analyses are based on differences in chain crystallizabilities in a dilute solution. Therefore, knowledge of polymer-diluent systems is crucial to understanding their operation. In this section, the thermodynamic theory of polymer-diluent systems is reviewed.

### 2.4.1 Thermodynamic considerations for homopolymer-diluent systems

The Flory-Huggins expression for the free energy of mixing can be used to describe the thermodynamic behavior of a concentrated solution where a uniform distribution of diluent and polymer segments can be assumed [49-51]. From the application of the phase equilibrium conditions and the Flory-Huggins mixing expression, one can determine the decrease in the equilibrium melting temperature due to diluent and number of chain segments in homopolymer-diluent systems as follows:

$$\frac{1}{T_m} - \frac{1}{T_m^0} = \left(\frac{R}{\Delta H_u}\right)\left(\frac{V_u}{V_l}\right)\left[-\frac{ln(v_2)}{x} + \left(1 - \frac{1}{x}\right)v_1 - \chi_1 \cdot v_1^2\right] \qquad (2.5)$$

where $T_m^0$ is the melting temperature of the pure polymer, $T_m$ is the equilibrium melting temperature of the polymer-diluent system, $\Delta H_u$ is the heat of fusion per repeating unit, $V_u$ and $V_l$ are the molar volumes of the polymer repeating unit and diluent, respectively, $v_1$ and $v_2$ are the volume fractions of the diluent and polymer, respectively, $x$ is the number of segments, and $\chi_1$ is the Flory-Huggins thermodynamic interaction parameter.

The crystallization step during Tref and Crystaf analysis, however, occurs in dilute solution. Theoretically, this situation is more complicated, as polymer segments

are non-uniformly distributed throughout the medium. Therefore, the Flory-Huggins free energy function is no longer valid. To account for the non-uniform segment distribution, the general theory of dilute solution where the chemical potential of the solvent species is expressed in virial form has to be considered. Fortunately, it has been found that the change in chemical potential of the polymer species with dilution is so small that it does not have any appreciable effect on the equilibrium melting temperature [52]. Therefore, Equation (2.5), derived from the Flory-Huggins theory, is obeyed over the complete concentration range of dilutions.

To examine the effect of chain length on the melting temperature of the polymer in dilute solution, it is useful to rearrange Equation (2.5) as follows:

$$\frac{1}{T_m} - \frac{1}{T_m^0} = \frac{R}{\Delta H_u}\frac{V_u}{V_l}\left[v_1 - \chi_1 \cdot v_1^2\right] - \frac{R}{\Delta H_u}\left[\frac{ln(v_2)}{r} + \frac{v_1}{r}\right] \tag{2.6}$$

Here, the number of repeating units per molecule ($r$) is used instead of the number of segments ($x$). The second term on the right hand side represents the influence of chain length. It indicates that the equilibrium melting temperature decreases with a reduction in molecular weight [53]. However, the second term on the right hand side is important only for chains with low molecular weights. For large values of $r$, the case of polymers with high molecular weight, the melting temperature becomes independent of chain length, and Equation (2.6) can be reduced to:

$$\frac{1}{T_m} - \frac{1}{T_m^0} = \frac{R}{\Delta H_u}\frac{V_u}{V_l}\left[v_1 - \chi_1 \cdot v_1^2\right] \tag{2.7}$$

Equation (2.7) implies that all polymer chains having reasonably large molecular weights will crystallize at the same temperature. In other words, molecular weight effects are negligible in the Tref and Crystaf analysis of high polymers. This is in an agreement with the recent experimental observations of Nieto *et al.* [36].

### 2.4.1 Thermodynamic considerations for copolymer-diluent systems

In the case of copolymer-diluent systems, the change in melting temperature is slightly more complicated, as it also depends on the interactions between various monomeric units and the diluent. Considering the case when the crystalline phase is

pure (*i.e.*, only monomeric units of type A crystallize, and no diluent is present in the lattice), the decrease in melting temperature can be derived in a similar manner as for homopolymer-diluent systems using the same Flory-Huggins theory with an appropriate modification [52].

Taking into account the interactions between both monomer types and diluent, the net interaction free energy between binary copolymers and diluent has to be modified as follows:

$$\chi_1 = v_A \cdot \chi_{1A} + v_B \cdot \chi_{1B} - v_A \cdot v_B \cdot \chi_{AB} \tag{2.8}$$

where $\chi_1$ is the interaction parameter of a binary copolymer with pure solvent, $\chi_{1A}$ and $\chi_{1B}$ are the interaction parameters of the corresponding homopolymers in the same solvent, $\chi_{AB}$ is the interaction parameter between A and B units in the copolymer chain, and $v_A$ and $v_B$ are the volume fractions of the monomer A and B in copolymer molecules, respectively.

In the case when the steric structures of both units in random copolymers are similar, the melting temperature depression equation will be in the same form as Equation (2.5), with the new interaction parameter expressed by Equation (2.8). For a given copolymer, the crystallizabilities of copolymer chains in dilute solution strongly depend on the chain composition. From thermodynamic considerations, this can be explained by the fact that the change in composition of copolymer chains also alters the net interaction parameter as shown in Equation (2.8).

**REFERENCES:**


1. Stockmayer W.H., "Distribution of Chain Lengths and Compositions in Copolymers", *Journal of Chemical Physics*, **1945**, *13*, 199.
2. Simha R. and Branson H., "Theory of Chain Copolymerization Reactions", *Journal of Chemical Physics*, **1944**, *12*, 253.
3. Thomann Y., Sernetz F.G., Thomann R, Kressler J. and Mulhaupt R., "Temperature Rising Elution Fractionation of a Random Ethylene/Styrene Copolymer", *Macromolecular Chemistry and Physics*, **1997**, *198*, 739.

4. Montaudo M.S. and Montaudo G., "Bivariate Distribution in PMMA/PBA Copolymers by Combined SEC/NMR and SEC/MALDI Measurements", *Macromolecules*, **1999**, *32*, 7015.
5. Gordon M., "Universality of the Stockmayer Distribution", *Macromolecules*, **1984**, *17*, 514.
6. Soares J.B.P. and Hamielec A.E., "Analyzing TREF Data by Stockmayer's Bivariate Distribution", *Macromolecular Theory and Simulation*, **1995**, *4*, 305.
7. Soares J.B.P., Monrabal B., Nieto J. and Blanco, "Crystallization Analysis Fractionation (CRYSTAF) of Poly(Ethylene-co-1-Octene) Made with Single-Site-Type Catalysts: A Mathematic Model for the Dependence of Composition Distribution on Molecular Weight", *Macromolecular Chemistry and Physics*, **1998**, *199*, 1917.
8. Sarzotti D.M., Soares J.B.P. and Penlidis A., "Ethylene/1-Hexene Copolymers Synthesized with a Single-Site Catalyst: Crystallization Analysis Fractionation, Modeling, and Reactivity Ratio Estimation", *Journal of Polymer Science: Part B: Polymer Physics*, **2002**, *40*, 2595.
9. Sarzotti D.M., "Heterogeneous Metallocene Catalysts for Olefin Polymerization: Effects of Support Material on Microstructure", *Master Thesis*, University of Waterloo, Canada, 2001.
10. Soares J.B.P. and Hamielec A.E., "Temperature Rising Elution Fractionation", in: *Modern Techniques for Polymer Characterization*, R.A. Pethrick, J.V. Dawkins, Eds., John Wiley&Sons, 1999, p. 15-55.
11. da Silva Filho A.A., Soares J.B.P. and de Galland G.B., "Measurement and Mathematical Modeling of Molecular Weight and Chemical Composition Distributions of Ethylene/1-Olefin Copolymers Synthesized with A Heterogeneous Ziegler-Natta Catalyst", *Macromolecular Chemistry and Physics*, **2000**, *201*, 1226.
12. Soares J.B.P. and Hamielec A.E., "Deconvolution of Chain-Length Distribution of Linear Polymers Made by Multi-Site-Type Catalysts", *Polymer*, **1995**, *36*, 2257.

13. Nesarikar A., Crist B., and Davidovich A., "Liquid-liquid Phase Separation in Linear Low-Density Polyethylene", *Journal of Polymer Science: Part B Polymer Physics*, **1994**, *32*, 641.
14. Wardhaugh L.T. and Williams M.C., "Blockiness of Olefin Copolymers and Possible Microphase Separation in the Melt", *Polymer Engineering and Science*, **1995**, *35*, 18.
15. Wignall G.D., Alamo R.G., Londono J.D., Mandelkern L. and Stehling F.C., "Small-Angle Neutron Scattering Investigations of Liquid-Liquid Phase Separation in Heterogeneous Linear Low-Density Polyethylene", *Macromolecules*, **1996**, *29*, 5332.
16. Cady L.D., "LLDPE Properties Tied to Branch Distribution", *Plastics Engineering*, **1987**, 25.
17. Gownder M., "Branching of LLDPE as Studied by Crystallization Analysis Fractionation and Its Effect on Mechanical Properties of Films", *Journal of Plastic Film and Sheeting*, **2001**, *17*, 53.
18. Soares J.B.P., Abbott R.F. and Kim J.D., "Environmental Stress Cracking Resistance of Polyethylene: the Use of CRYSTAF and SEC to Establish Structure-Property Relationships", *Journal of Polymer Science: Part B: Polymer Physics*, **2000**, *38*, 1267.
19. Simon L.C., de Souza R.F., Soares J.B.P. and Mauler R.S., "Effect of Molecular Structure on Dynamic Mechanical Properties of Polyethylene Obtained with Nickel-Diimine Catalysts", *Polymer*, **2001**, *42*, 4885.
20. Soares J.B.P. and Hamielec A.E., "Temperature Rising Elution Fractionation of Linear Polyolefins", *Polymer*, **1995**, *36*, 1639.
21. Wild L., "Temperature Rising Elution Fractionation", *Advances in Polymer Science*, **1990**, *98*, 1.
22. Wild L. and Blatz C., "Development of High Performance Tref for Polyolefin Analysis", in: *New Advances in Polyolefins*, T.C. Chung, Eds, Plenum Press 1993, p. 147-157.

23. Fonseca C.A. and Harrison I.R., "Temperature Rising Elution Fractionation", in: Modern Techniques for Polymer Characterization, R.A. Pethrick, J.V. Dawkins, Eds., John Wiley&Sons, **1999**, p. 1-14.
24. Wild L., Ryle D., Knobeloch D. and Peat I., "Determination of Branching Distributions in Polyethylene and Ethylene Copolymers", *Journal of Polymer Science: Part B: Polymer Physics*, **1982**, *20*, 441.
25. Savitski E.P., Caflisch G.B., Killian C.M., Meadows M., Merkley J.H. and Huff B.J., "Influence of the Short-Chain Branch Length on the Calibration of Temperature Rising Elution Fractionation Systems", *Journal of Applied Polymer Science*, **2003**, *90*, 722.
26. Pigeon M.G. and Rudin A., "Comparison of Analytical and Preparative TREF Analysis: A Mathematical Approach to Correcting Analytical TREF Data", *Journal of Applied Polymer Science*, **1993**, 47, 685.
27. Pigeon M.G. and Rudin A., "Branching Measurement by Analytical TREF: A Fully Quantitative Technique", *Journal of Applied Polymer Science*, **1994**, *51*, 303.
28. Borrajo J., Cordon C., Carella J.M., Toso S. and Goizueta G, "Modelling the Fractionation Process in TREF System: Thermodynamic Simple Approach", *Journal of Polymer Science: Part B: Polymer Physics*, **1995**, *33*, 1627.
29. Elicabe G., Carella J. and Borrajo J., "Modelling the Fractionation Process in TREF System II. Numerical Analysis", *Journal of Polymer Science: Part B: Polymer Physics*, **1996**, *34*, 527.
30. Elicabe G., Borrajo J. and Carella J., "Modelling the Fractionation Process in TREF System III. Model Validation With Low Molecular Weight Homopolymers", *Journal of Polymer Science: Part B: Polymer Physics*, **1996**, *34*, 1147.
31. Britto L.J.D., Soares J.B.P., Penlidis A. and Monrabal B., "Polyolefin Analysis by Single-Step Crystallization Fractionation", *Journal of Polymer Science: Part B: Polymer Physics*, **1999**, *37*, 539.

32. Monrabal B., "Crystallization Analysis Fractionation: A New Technique for the Analysis of Branching Distribution in Polyolefins", *Journal of Applied Polymer Science,* **1994**, *52*, 491.
33. Monrabal B., "CRYSTAF: Crystallization Analysis Fractionation. A New Approach to the Composition Analysis of Semicrystalline Polymers", *Macromolecular Symposia,* **1996**, *110*, 81.
34. Monrabal B., Blanco J., Nieto J. and Soares J.B.P, "Characterization of Homogeneous Ethylene/1-Octene Copolymers Made with a Single-Site Catalyst. CRYSTAF Analysis and Calibration", *Journal of Polymer Science: Part A: Polymer Chemistry*, **1999**, *37*, 89.
35. Gabriel C. and Lilge D., "Comparison of Different Methods for the Investigation of the Short-Chain Branching Distribution of LLDPE", *Polymer*, **2001**, *42*, 297.
36. Nieto J., Oswald T., Blanco F., Soares J.B.P. and Monrabal B., "Crystallizability of Ethylene Homopolymers by Crystallization Analysis Fractionation", *Journal of Polymer Science: Part B: Polymer Physics*, **2001**, *39*, 1616.
37. Brull R., Pasch H., Ruaubenheimer H.G., Sanderson R., van Reenen A.J. and Wahner U.M., "Investigation of the Melting and Crystallization Behavior of Random Propane/1-Olefin Copolymers by DSC and CRYSTAF", *Macromolecular Chemistry and Physics*, **2001**, *202*, 1281.
38. Brull R., Grumel V., Pasch H., Raubenheimer H.G., Sanderson R. and Wahner U.M., "Analysis of Polyolefin Blends by CRYSTAF", *Macromolecule Symposium*, **2002**, *178*, 81.
39. Pasch H., "Recent Developments in Polyolefin Characterization", *Macromolecular Symposium*, **2001**, *165*, 91.
40. Pasch H., Brull R., Wahner U. and Monrabal B., "Analysis of Polyolefins by Crystallization Analysis Fractionation", *Macromolecular Materials and Engineering*, **2000**, *279*, 46.
41. Beigzadeh D., Soares J.B.P. and Duever T.A., "Modeling of Fractionation in CRYSTAF Using Monte Carlo Simulation of Crystallizable Sequence

Lengths: Ethylene/1-Octene Copolymers Synthesized with Single-Site-Type Catalysts", *Journal of Applied Polymer Science*, **2001**, *80*, 2200.

42. Beigzadeh D., "Long Chain Branching in Ethylene Polymerization Using Combined Metallocene Catalyst Systems", *PhD thesis*, University of Waterloo, Canada, 2000.
43. Costeux S., Anantawaraskul S., Wood-Adams P.M. and Soares J.B.P., "Distribution of the Longest Ethylene Sequence in Ethylene/1-Olefin Copolymers Synthesized with Single-Site-Type Catalysts", *Macromolecular Theory and Simulation*, **2002**, *11*, 326.
44. Anantawaraskul S., Soares J.B.P., Wood-Adams P.M. and Monrabal B., "Effect of Molecular Weight and Average Comonomer Content on the Crystallization Analysis Fractionation (Crystaf) of Ethylene α-Olefin Copolymers", *Polymer*, **2003**, *44*, 2393.
45. Anantawaraskul S., Soares J.B.P. and Wood-Adams P.M., "Effect of Operation Parameters on Temperature Rising Elution Fractionation and Crystallization Analysis Fractionation", *Journal of Polymer Science: Part B: Polymer Physics*, **2003**, *41*, 1762.
46. Anantawaraskul S., Soares J.B.P. and Wood-Adams P.M., "An Experimental and Numerical Study on Crystallization Analysis Fractionation (Crystaf)", to appear in *Macromolecular Symposia.*
47. Cheng H.N., Tam S.B. and Kasehagen L.J., "Compositional Heterogeneity in Polymers: Computer Simulation Approaches", *Macromolecules*, **1992**, *25*, 3779.
48. Cheng H.N. and Kasehagen, "Tacticity Distribution and Simulation", *Macromolecules*, **1993**, *26*, 4774.
49. Flory P.J., "Thermodynamics of High Polymer Solution", *Journal of Chemical Physics*, **1942**, *10*, 51.
50. Flory P.J., "Thermodynamics of Crystallization in High Polymers IV. A Theory of Crystalline States and Fusion in Polymers, Copolymers, and Their Mixtures with Diluents", *Journal of Chemical Physics,* **1949**, *17*, 223.

51. Flory P.J., "*Principles of Polymer Chemistry*", 1st edition, Cornell University Press **1953**.
52. Mandelkern L., "*Crystallization of Polymers*", 2nd edition, Cambridge University Press **2002**.
53. Prasad A. and Mandelkern L., "Equilibrium Dissolution Temperature of Low Molecular Weight Polyethylene Fractions in Dilute Solution", *Macromolecules*, **1989**, *22*, 914.

CHAPTER 3

# CHEMICAL COMPOSITION DISTRIBUTION OF MULTICOMPONENT COPOLYMERS

*This is the remarkable paradox of mathematics:*
*no matter how determinedly its practitioners ignore the world,*
*they consistently produce the best tools for understanding it.*
***Henri Poincaré***

This chapter presents the development of analytical expressions for the number and weight chemical composition distributions (CCD) of multicomponent copolymers using a statistical approach. As an experimental method for measuring CCD of multicomponent copolymers is not yet available, the results of the derivation will be validated by comparing with results calculated using Stockmayer's distribution for the case of binary copolymers and with results of Monte Carlo simulations for the case of terpolymers.

## 3.1 INTRODUCTION

Sequence length distribution (SLD) and chemical composition distribution (CCD) are important structural characteristics of copolymers as they govern several physical and mechanical properties of these materials. The average comonomer sequence length and sequence length distribution can be determined experimentally. Theories for various copolymerization models (*e.g.*, terminal, penultimate, and pen-penultimate) and for both binary and multi-component copolymers are well developed [1]. On the other hand, a general theory for the CCD of multicomponent copolymers is not yet

available, even though terpolymers and higher copolymers have found a number of practical applications, and their CCDs are relevant for the understanding of their properties.

For linear binary copolymers, the analytical expression for describing the weight distribution of kinetic chain length and chemical composition developed by Stockmayer is useful for understanding their microstructure [2-6]. Stockmayer [7] obtained this simplified expression with the aid of some approximations from the more general theory of copolymerization described earlier by Simha and Branson [8]. Later, Tacx *et al.* [9] presented an extension from the original Stockmayer distribution that includes the effect of the molar masses of different monomer types on the final distribution. This distribution function has also been modified for special cases [10-12].

An equation similar to Stockmayer's distribution was developed by Costeux *et al.* [13] using a statistical approach. They investigated the CCD of random binary copolymers using Monte Carlo simulation and developed an analytical expression describing this distribution function. The results from their analytical expression agree well with the ones from Monte Carlo simulations and from Stockmayer's distribution.

Recently, Xu [14] attempted to develop an equation describing the CCD for random terpolymers using the same strategy used by Stockmayer. The equations are, however, too complex for convenient use.

In the present study, a more convenient equation for terpolymers is developed using the approach of Costeux *et al.* [13]. This result is then generalized to the case of multi-component copolymers. The analytical solution obtained in the present study is validated using results from the Monte Carlo simulations. Even though some copolymers do not follow random copolymerization statistics, there are a significant number of new copolymers, notably those made with single-site coordination catalysts such as metallocenes, that are random or nearly random. The distributions derived in this chapter can be used to describe the microstructures of these important new copolymers.

## 3.2 MONTE CARLO SIMULATIONS

The CCD of random terpolymers was investigated numerically using Monte Carlo simulations. Starting with random numbers between 0 and 1, each polymer molecule is simulated by comparing these random numbers with a chain propagation probability and the probabilities of incorporating each monomer type.

The probability of chain propagation, defined as *PP*, is used to decide if propagation takes place. Polymer chains propagate if the random number is less than *PP* and terminate if it is greater than *PP*. This parameter is related to the number average kinetic chain length ($r_N$) as follows:

$$PP = \frac{r_N - 1}{r_N} \tag{3.1}$$

If the chain propagates, another random number is generated and used to decide which monomer type reacts. Considering A-B-C terpolymers, *P[A]*, *P[B]*, and *P[C]* are the probabilities that monomer of type A, B, or C will be incorporated into the molecule (note that *P[A]+P[B]+P[C]* = 1). Figure 3.1 shows the Monte Carlo algorithm used in the simulation.

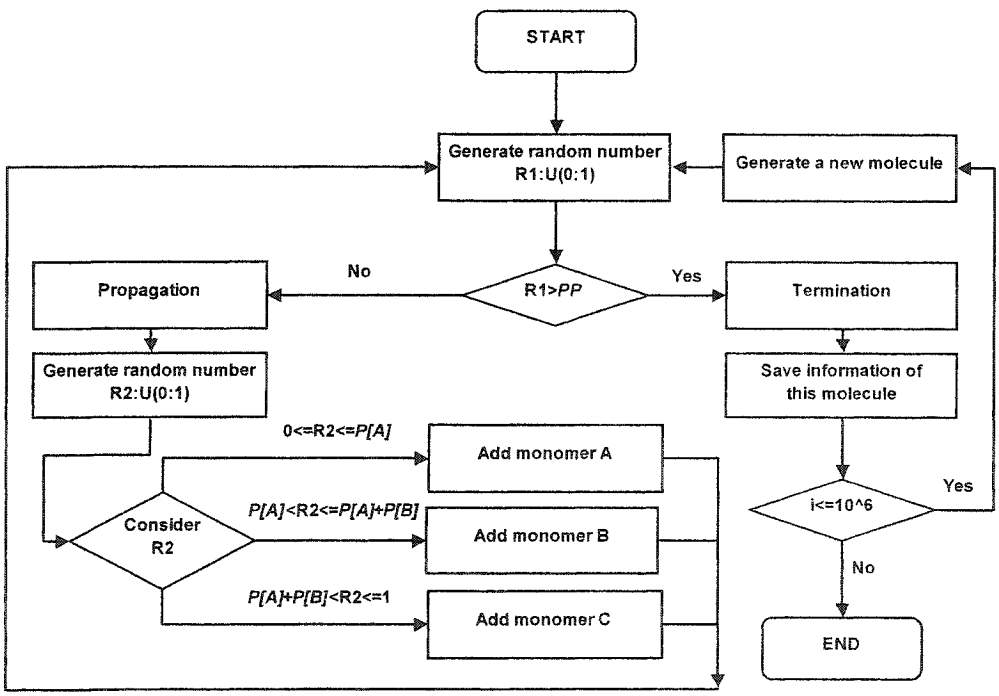


Figure 3.1 Algorithm for Monte Carlo simulation

The kinetic chain length ($r$), molecular weight ($M$), and numbers of each monomer type that are incorporated into each molecule ($N_A$, $N_B$, and $N_C$) are recorded for each chain (note that $N_A+N_B+N_C = r$). The mole fraction of each monomer type can then be calculated. For example, the mole fraction of monomer type A is: $n_A = N_A/r$. The average mole fraction of monomer type A ($\overline{n_A}$) for the whole polymer population is equal to $P[A]$.

$$P[A] = \overline{n_A}, \quad P[B] = \overline{n_B}, \quad P[C] = \overline{n_C} \tag{3.2}$$

The chemical composition distribution can be obtained in terms of number and weight fractions corresponding to $n_A$ and $n_B$. In all simulations, a million polymer molecules are generated to ensure an accurate representation of the statistical properties. The parameters used for the simulations were: $P[A] = 0.3$, $P[B] = 0.4$, $P[C] = 0.3$, $M_A = 28$, $M_B = 42$, $M_C = 104$, and $PP = 0.95$ where $M_A$, $M_B$, and $M_C$ are the molecular weights of monomer types A, B, and C, respectively. The results from the simulation are then used to validate the analytical solution developed in the next section.

## 3.3 DEVELOPMENT OF THEORY FOR BINARY COPOLYMERS

The CCD of random binary copolymers was described by Stockmayer [7]. His expression was later modified to account for the effect of the different molar masses of each monomer type [9]. The resulting function can be reduced to:

$$f_{W,S}(r,n_A) = \frac{r}{\overline{r_N}^2}\cdot exp\left[-\frac{r}{\overline{r_N}}\right]\cdot\frac{1}{\sqrt{2\pi\cdot\overline{n_A}(1-\overline{n_A})/r}}\cdot exp\left[-\frac{(n_A-\overline{n_A})^2}{2\overline{n_A}(1-\overline{n_A})/r}\right] \times\left[1+\frac{(n_A-\overline{n_A})(1-M_B/M_A)}{M_B/M_A+\overline{n_A}(1-M_B/M_A)}\right] \tag{3.3}$$

Recall that this function describes the weight fraction of molecules that have a kinetic chain length of $r$ and a mole fraction A of $n_A$.

Using a statistical approach, Costeux *et al.* [13] obtained a similar bivariate distribution of kinetic chain length and chemical composition. When the effect of the

molar masses of different monomer types is accounted for, their expression can be written as follows (see Appendix A):

$$f_{W,P}(r,n_A) = C^{r}_{r\cdot n_A} \cdot P[A]^{r\cdot n_A} \cdot (1-P[A])^{r\cdot(1-n_A)} \cdot r^2 \cdot (1-PP)^2 \cdot PP^{r-1} \times \left[ \frac{M_A \cdot n_A + M_B \cdot (1-n_A)}{M_A \cdot P[A] + M_B \cdot (1-P[A])} \right] \tag{3.4}$$

where the binomial coefficient ($C^A_B$) is defined as

$$C^A_B \equiv \frac{A!}{(A-B)!\,B!} \tag{3.5}$$

This distribution function was developed using the same strategy used here for the derivation of the CCD of terpolymers, which is described in detail in the following section. To verify the validity of the statistical approach, the results from Equations (3.3) and (3.4) are compared for $PP$ = 0.95, $\overline{n_A}$ = 0.4, $M_A$ = 28, and $M_B$ = 42 (see Figure 3.2). Results from the two approaches are in very good agreement.

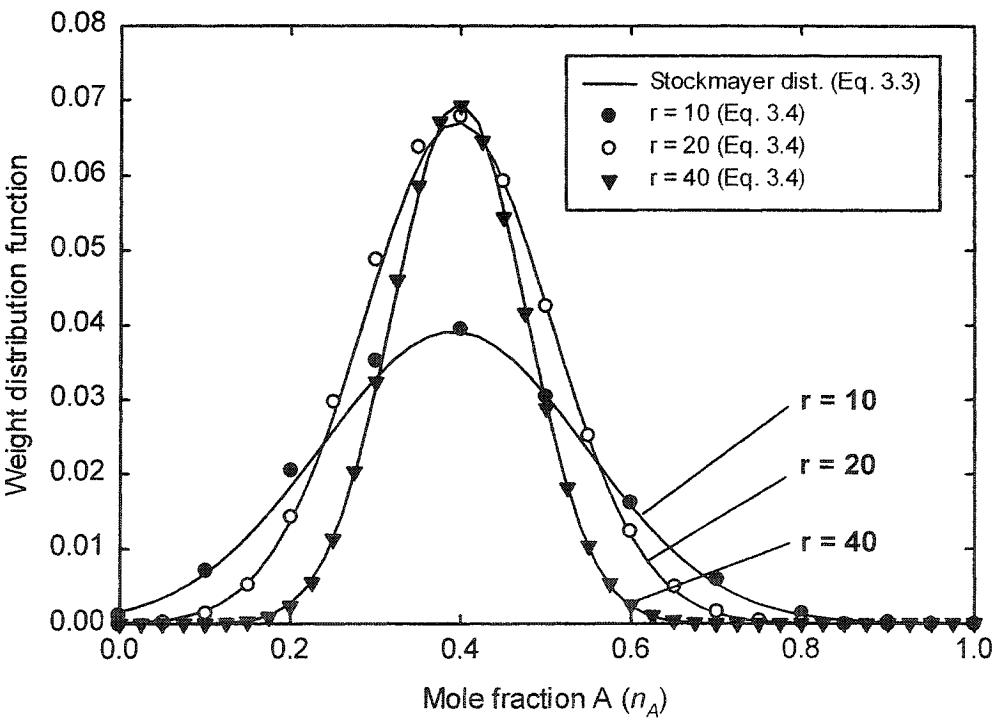


Figure 3.2 Comparison of chemical composition distributions from Stockmayer (Equation (3.3)) and statistical approach (Equation (3.4))

It is important to note that Equation (3.4) is derived in the discrete domain, while approximation functions were used to derive Stockmayer's distribution, which is a continuous function. Therefore, the small discrepancies shown in Figure 3.2 are due to the approximation function used by Stockmayer. The errors in the Stockmayer distribution become more pronounced for short polymer chains.

It is possible to transform Equation (3.4) into the continuous domain by using the Stirling approximation:

$$n! = \sqrt{2\pi} \cdot n^{n+1/2} \cdot exp(-n) \tag{3.6}$$

The combinatory factor can then be evaluated in the continuous domain as follows:

$$C_B^A = \frac{A!}{(A-B)!B!} = \sqrt{\frac{A}{2\pi \cdot B(A-B)}} \cdot \frac{A^A}{B^B (A-B)^{A-B}} \tag{3.7}$$

Using Equation (3.7), Equation (3.4) can be rewritten in the continuous domain as:

$$\begin{aligned} f_{W,P}(r, n_A) = & \sqrt{\frac{1}{2\pi \cdot r \cdot n_A(1-n_A)}} \cdot \left(\frac{P[A]}{n_A}\right)^{r \cdot n_A} \cdot \left(\frac{1-P[A]}{1-n_A}\right)^{r \cdot (1-n_A)} \\ & \times r^2 \cdot (1-PP)^2 \cdot PP^{r-1} \\ & \times \left[\frac{M_A \cdot n_A + M_B \cdot (1-n_A)}{M_A \cdot P[A] + M_B \cdot (1-P[A])}\right] \end{aligned} \tag{3.8}$$

Unlike the model for binary copolymers, the model for terpolymers cannot be easily validated using an existing theory. Further derivations will be compared instead with the results of Monte Carlo simulations.

## 3.4 RANDOM TERPOLYMERS: NUMBER DISTRIBUTION FUNCTION OF CHEMICAL COMPOSITION

It is well known that the number and weight chain length distributions of linear terpolymers synthesized with single-site catalysts follow the most probable distribution:

$$f_N(r) = (1-PP) \cdot PP^{r-1} \tag{3.9}$$

$$f_W(r) = r \cdot (1-PP)^2 \cdot PP^{r-1} \tag{3.10}$$

If a specific kinetic chain length is considered, the number distribution function of chains having $N_A$ units of type A and $N_B$ units of type B can be determined from

$$\begin{aligned} f_N(N_A, N_B \mid r) = C_{N_A}^{r} \cdot C_{N_B}^{r-N_A} \cdot P[A]^{N_A} \cdot P[B]^{N_B} \\ \times (1-P[A]-P[B])^{r-N_A-N_B} \end{aligned} \tag{3.11}$$

Recall that Equation (3.11) gives the fraction of molecules with kinetic chain length $r$ that have $N_A$ and $N_B$ units of type A and B respectively.

The first two binomial coefficients in Equation (3.11) describe all possible arrangements of comonomer units in the chain having a kinetic chain length of $r$, $N_A$ units of A, $N_B$ units of B, and $r$-$N_A$-$N_B$ units of C. The remaining terms describe the probability that a particular molecule can be generated. It is always important to verify that

$$\sum_{N_A=0}^{r} \sum_{N_B=0}^{r-N_A} f_N(N_A, N_B \mid r) = 1 \tag{3.12}$$

A more useful expression for the distribution of $n_A$ and $n_B$ in the continuous domain is obtained by using Stirling's approximation to replace the combinatory factors (Equation 3.13) in Equation (3.11):

$$\begin{aligned} C_{N_A}^{r} C_{N_B}^{r-N_A} &= \frac{r!}{N_A! N_B! (r-N_A-N_B)!} \\ &= \frac{1}{2\pi} \sqrt{\frac{r}{N_A \cdot N_B (r-N_A-N_B)}} \frac{r^r (r-N_A-N_B)^{-(r-N_A-N_B)}}{N_A{}^{N_A} N_B{}^{N_B}} \end{aligned} \tag{3.13}$$

$$\begin{aligned} f_N(n_A, n_B \mid r) = \frac{r}{2\pi} \sqrt{\frac{1}{n_A n_B (1-n_A-n_B)}} \left(\frac{P[A]}{n_A}\right)^{r \cdot n_A} \left(\frac{P[B]}{n_B}\right)^{r \cdot n_B} \\ \times \left(\frac{1-P[A]-P[B]}{1-n_A-n_B}\right)^{r(1-n_A-n_B)} \end{aligned} \tag{3.14}$$

Again, Equation (3.14) is simply a continuous version of Equation (3.11).

A more general form of this distribution function can be obtained for the complete distribution of chain lengths:

$$f_N(r,n_A,n_B) = f_N(n_A,n_B \mid r) \cdot f_N(r) \tag{3.15}$$

where $f_N(r)$ is given by Equation (3.9). Equation 3.15 describes the number fraction of chains that have kinetic chain length $r$, and mole fractions of comonomers A and B, $n_A$ and $n_B$ respectively.

Note that, the above distribution function satisfies the following condition:

$$\int_{r=1}^{\infty} \int_{n_A=0}^{1} \int_{n_B=0}^{1-n_A} f_N(r,n_A,n_B) \cdot dn_B dn_A dr = 1 \tag{3.16}$$

## 3.5 RANDOM TERPOLYMERS: WEIGHT DISTRIBUTION FUNCTION OF CHEMICAL COMPOSITION

The weight distribution function of chemical composition can be calculated from the number distribution function by taking into account the weights of the chains. The weight distribution function of chains of kinetic chain length $r$ with mole fractions of $n_A$ and $n_B$ is given by Equations (3.17) and (3.18).

$$f_W(n_A,n_B \mid r) = f_N(n_A,n_B \mid r) \times \left[ \frac{M_A \cdot n_A + M_B \cdot n_B + M_C(1-n_A-n_B)}{M_A \cdot P[A] + M_B \cdot P[B] + M_C(1-P[A]-P[B])} \right] \tag{3.17}$$

$$f_W(n_A,n_B \mid r) = \frac{r}{2\pi} \sqrt{\frac{1}{n_A n_B (1-n_A-n_B)}} \times \left( \frac{P[A]}{n_A} \right)^{r \cdot n_A} \left( \frac{P[B]}{n_B} \right)^{r \cdot n_B} \left( \frac{1-P[A]-P[B]}{1-n_A-n_B} \right)^{r(1-n_A-n_B)} \times \left[ \frac{M_A \cdot n_A + M_B \cdot n_B + M_C(1-n_A-n_B)}{M_A \cdot P[A] + M_B \cdot P[B] + M_C(1-P[A]-P[B])} \right] \tag{3.18}$$

The validity of Equation (3.18) is demonstrated in Figure 3.3. A more general form of Equation (3.18) can be obtained by considering the weight distribution function of chains having different kinetic chain lengths:

$$f_W(r,n_A,n_B) = f_W(n_A,n_B \mid r) \cdot f_W(r) \tag{3.19}$$

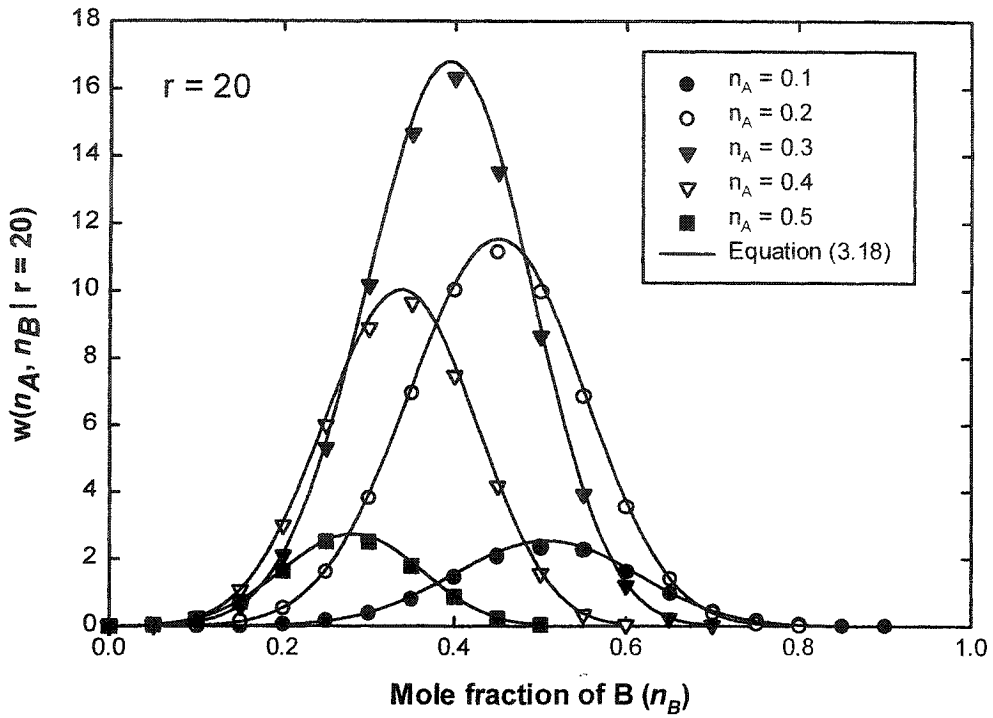


Figure 3.3 Comparison between results from Monte Carlo simulation and Equation (3.18)

One can also calculate the weight distribution function of any particular comonomer type by integrating Equations (3.18) and (3.19) over the other components.

$$f_W(n_A \mid r) = \int_{n_B=0}^{1-n_A} f_W(n_A, n_B \mid r) \cdot dn_B \tag{3.20}$$

Equation (3.21) gives the distribution function of mole fraction of monomer A ($n_A$) for a particular kinetic chain length $r$:

$$f_W(n_A \mid r) = \sqrt{\frac{1}{2\pi \cdot r \cdot n_A(1-n_A)}} \cdot \left(\frac{P[A]}{n_A}\right)^{r \cdot n_A} \cdot \left(\frac{(1-P[A])}{1-n_A}\right)^{r(1-n_A)} \cdot r \times \left[\frac{M_A \cdot n_A + \left[\frac{P[B]}{1-P[A]} \cdot M_B + \frac{1-P[A]-P[B]}{1-P[A]} \cdot M_C\right] \cdot (1-n_A)}{M_A \cdot P[A] + M_B \cdot P[B] + M_C(1-P[A]-P[B])}\right] \tag{3.21}$$

When compared with the results of the Monte Carlo simulation, Equation (3.21) gives very good agreement (see Figure 3.4).

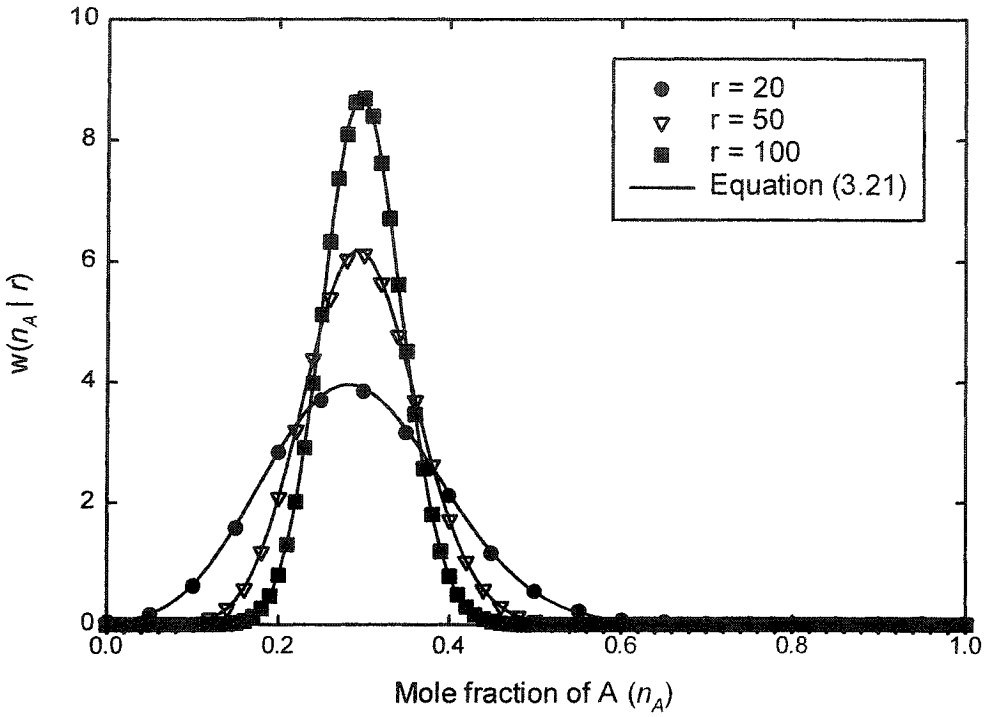


Figure 3.4 Comparison of results of Monte Carlo simulation with Equation (3.21)

Considering different kinetic chain lengths, one can obtain:

$$f_W(r,n_A) = f_W(n_A \mid r) \cdot f_W(r) \tag{3.22}$$

$$\begin{aligned} f_W(r,n_A) = & \sqrt{\frac{1}{2\pi \cdot r \cdot n_A(1-n_A)}} \cdot \left(\frac{P[A]}{n_A}\right)^{r \cdot n_A} \cdot \left(\frac{(1-P[A])}{1-n_A}\right)^{r(1-n_A)} \\ & \times r^2 \cdot (1-PP)^2 \cdot PP^{r-1} \\ & \times \left[\frac{M_A \cdot n_A + \left[\frac{P[B]}{1-P[A]} \cdot M_B + \frac{1-P[A]-P[B]}{1-P[A]} \cdot M_C\right] \cdot (1-n_A)}{M_A \cdot P[A] + M_B \cdot P[B] + M_C(1-P[A]-P[B])}\right] \end{aligned} \tag{3.23}$$

One can clearly see the similarity between Equations (3.8) and (3.23). The difference is only the last term where the molar mass of C comonomer is considered in Equation (3.23). In fact, the coefficient in front of $(1\text{-}n_A)$ in the last term is merely the average

molar masses of monomers B and C. Moreover, Equation (3.23) collapses to Equation (3.8) when 1-*P[A]-P[B]* = 0. This further confirms the validity of our derivation as it correctly reduces to the special case of a binary copolymer.

One can also confirm that Equations (3.18), (3.19), (3.21), and (3.23) satisfy the following conditions:

$$\int_{n_A=0}^{1}\int_{n_B=0}^{1-n_A} f_W(n_A,n_B\,|\,r)\cdot dn_B dn_A = 1 \tag{3.24}$$

$$\int_{r=1}^{\infty}\int_{n_A=0}^{1}\int_{n_B=0}^{1-n_A} f_W(r,n_A,n_B)\cdot dn_B dn_A dr = 1 \tag{3.25}$$

$$\int_{n_A=0}^{1} f_W(n_A\,|\,r)\cdot dn_A = 1 \tag{3.26}$$

$$\int_{r=1}^{\infty}\int_{n_A=0}^{1} f_W(r,n_A)\cdot dn_A dr = 1 \tag{3.27}$$

## 3.6 RANDOM MULTI-COMPONENT COPOLYMERS

Here the more general case where copolymers consist of more than 3 types of monomer is considered. One can develop a general equation similar to the one found in the case of terpolymers using the same strategy. For *m*-component copolymers,

$$f_W(r,n_1,n_2,\ldots,n_{m-1}) = f_W(n_1,n_2,\ldots,n_{m-1}\,|\,r)\cdot f_W(r) \tag{3.28}$$

where,

$$\begin{aligned} f_W(n_1,n_2,\ldots,n_{m-1}\,|\,r) = {} & \sqrt{\frac{r^{m-1}}{(2\pi)^{m-1} n_1\cdot n_2\cdot\ldots\cdot n_{m-1}(1-n_1-n_2\ldots..-n_{m-1})}} \\ & \times\left(\frac{P[1]}{n_1}\right)^{r\cdot n_1}\left(\frac{P[2]}{n_2}\right)^{r\cdot n_2}\ldots\left(\frac{P[m-1]}{n_{m-1}}\right)^{r\cdot n_{m-1}} \\ & \times\left(\frac{1-P[1]-P[2]\ldots-P[m-1]}{1-n_1-n_2\ldots-n_{m-1}}\right)^{r(1-n_1-n_2\ldots-n_{m-1})} \\ & \times\left[\sum_{i=1}^{m}(M_i\cdot n_i)\Big/\sum_{i=1}^{m}(M_i\cdot P[i])\right] \end{aligned} \tag{3.29}$$

By substituting $m$ = 2 and 3 into Equation (3.28), one obtains Equations (3.8) and (3.19), the special cases of binary copolymers and terpolymers, respectively.

## 3.7 CHEMICAL COMPOSITION DISTRIBUTION IN RANDOM TERPOLYMERS

Equation (3.19) is now used to illustrate an interesting aspect of the chemical composition distribution of terpolymers. Similar attributes also exist in the cases of copolymers of more than three components. Figures 3.5, 3.6, and 3.7 show 3D and contour plots of the chemical composition distribution of monomer of type A and B for kinetic chain lengths of 20, 50, and 100, respectively. The parameters used are: $P[A] = 0.3$, $P[B] = 0.4$, $P[C] = 0.3$, $M_A = 28$, $M_B = 42$, $M_C = 104$, and $PP = 0.95$.

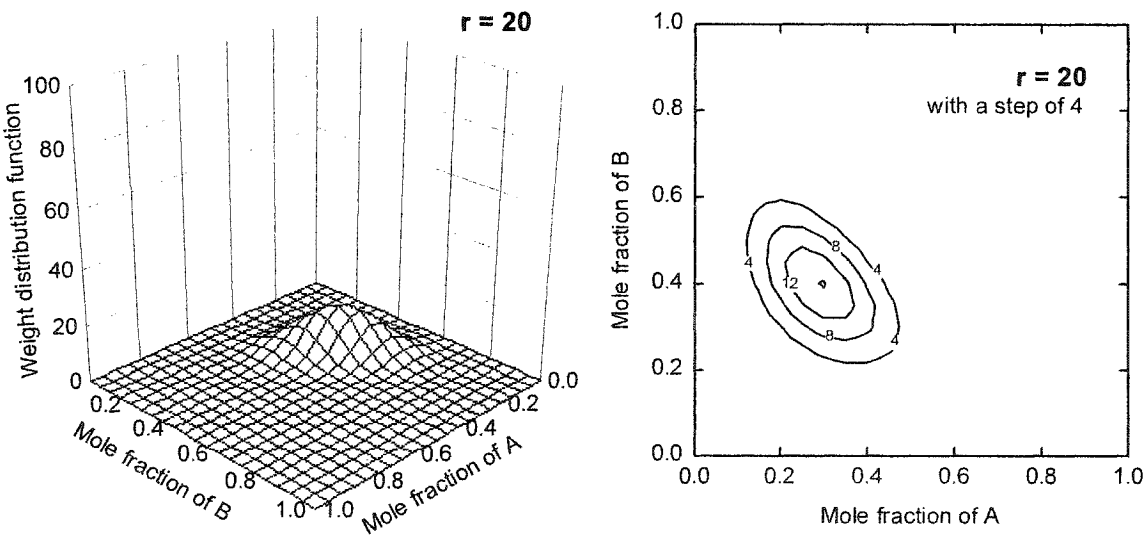


Figure 3.5 Chemical composition distribution in random terpolymers ($r$ = 20)

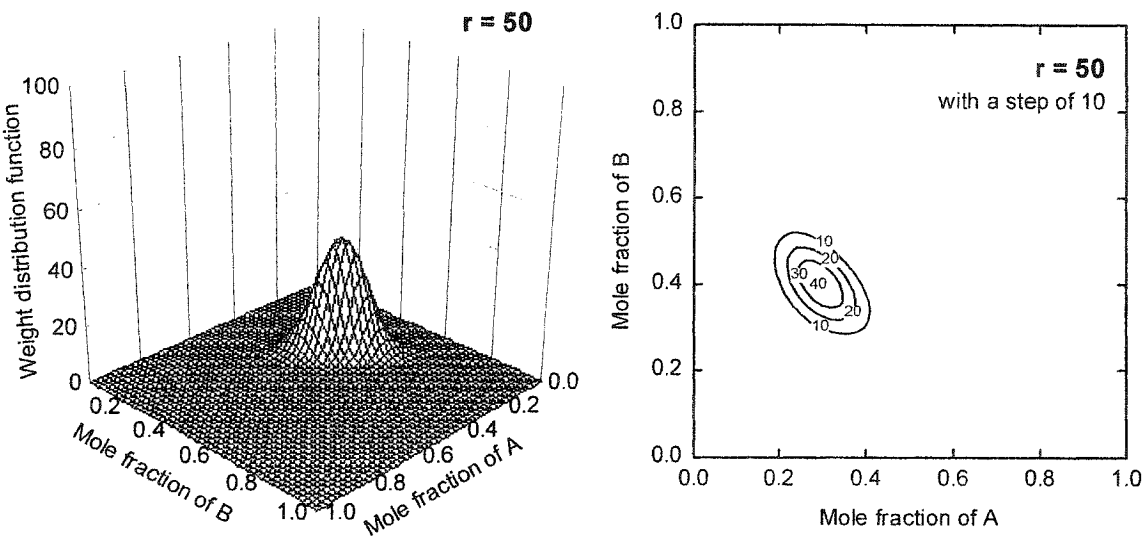


Figure 3.6 Chemical composition distribution in random terpolymers ($r$ = 50)

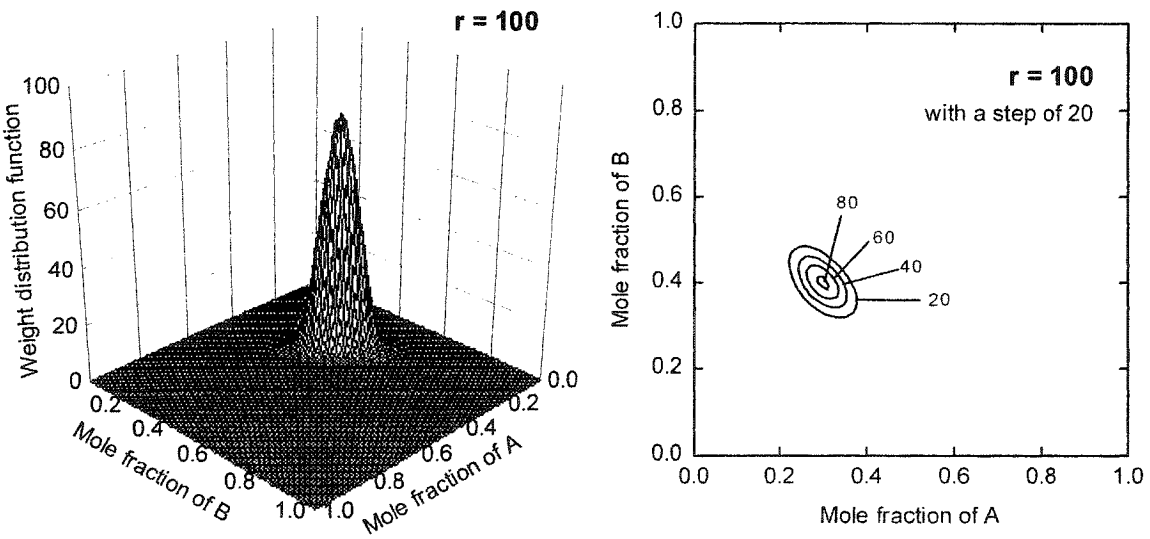


Figure 3.7 Chemical composition distribution in random terpolymers ($r$ = 100)

These figures show that the higher the molecular weight of the chains, the narrower is the chemical composition distribution. Although the breadth of the distribution is altered, the peak position remains the same. The same results are

predicted for random binary copolymers using Stockmayer's bivariate distribution [7].

## 3.8 CLOSING REMARKS

In this chapter, analytical expressions for the chemical composition distribution of random binary copolymers, terpolymers, and multi-component copolymers were developed. The derivations were validated using Stockmayer's distribution in the case of binary copolymers and with Monte Carlo simulations in the case of terpolymers.

For random terpolymers, chemical composition distributions for molecules with different kinetic chain lengths were derived. The results show a broadening of the distribution with decrease in kinetic chain length. For all cases, the peak position, however, is independent of kinetic chain length and located at the position ($\overline{n_A}$, $\overline{n_B}$).

## NOMENCLATURE

| | |
|---|---|
| $i$ | monomer type (e.g., A, B, C, 1, 2, 3) |
| $P[i]$ | probability of incorporating monomer type $i$ into a molecule |
| $PP$ | propagation probability |
| $M_i$ | molecular weight of monomer type $i$ |
| $r$ | kinetic chain length |
| $r_N$ | number average kinetic chain length |
| $M$ | molecular weight of a molecule |
| $N_i$ | number of monomer type $i$ that is incorporated into a molecule |
| $n_A$ | mole fraction of monomer type $i = N_i/r$ |
| $f(r)$ | distribution function of chains having kinetic chain length $r$ |
| $f(r,n_A)$ | distribution function of chains having kinetic chain length $r$ and mole fraction of $n_A$ |
| $f(r,n_A,n_B)$ | distribution function of chains having kinetic chain length $r$ and mole fraction of $n_A$ and $n_B$ |

| | |
|---|---|
| $f(n_A \mid r)$ | distribution function of chains having mole fraction of $n_A$ when only chains having kinetic chain length $r$ are considered |
| $f(n_A, n_B \mid r)$ | distribution function of chains having mole fraction of $n_A$ and $n_B$ when only chains having kinetic chain length $r$ are considered |
| $f(N_A, N_B \mid r)$ | distribution function of chains having number of monomer A = $N_A$ and number of monomer B = $N_B$ when only chains having kinetic chain length $r$ are considered |

Subscripts

| | |
|---|---|
| $N$ | number distribution function |
| $P$ | distribution function derived using statistical approach |
| $S$ | distribution function from Stockmayer distribution |
| $W$ | weight distribution function |

## REFERENCES


1. Koenig J.L., "*Chemical Microstructure of Polymer Chains*", 1st edition, John Wiley&Sons 1980.
2. Soares J.B.P. and Hamielec A.E., "Analyzing TREF Data by Stockmayer's Bivariate Distribution", *Macromolecular Theory and Simulation*, **1995**, *4*, 305.
3. Soares J.B.P., Monrabal B., Nieto J. and Blanco, "Crystallization Analysis Fractionation (CRYSTAF) of Poly(Ethylene-co-1-Octene) Made with Single-Site-Type Catalysts: A Mathematic Model for the Dependence of Composition Distribution on Molecular Weight", *Macromolecular Chemistry and Physics*, **1998**, *199*, 1917.
4. Thomann Y., Sernetz F.G., Thomann R, Kressler J. and Mulhaupt R., "Temperature Rising Elution Fractionation of a Random Ethylene/Styrene Copolymer", *Macromolecular Chemistry and Physics*, **1997**, *198*, 739.

5. Montaudo M.S. and Montaudo G., "Bivariate Distribution in PMMA/PBA Copolymers by Combined SEC/NMR and SEC/MALDI Measurements", *Macromolecules*, **1999**, *32*, 7015.
6. Gordon M., "Universality of the Stockmayer Distribution", *Macromolecules*, **1984**, *17*, 514.
7. Stockmayer W.H., "Distribution of Chain Lengths and Compositions in Copolymers", *Journal of Chemical Physics*, **1945**, *13*, 199.
8. Simha R. and Branson H., "Theory of Chain Copolymerization Reactions", *Journal of Chemical Physics*, **1944**, *12*, 253.
9. Tacx J.C.J.F., Linssen H.N. and German A.L., "Effect of Molar Mass Ratio of Monomers on the Mass Distribution of Chain Lengths and Compositions in Copolymers: Extension of the Stockmayer Theory", *Journal of Polymer Science: Part A: Polymer Chemistry*, **1988**, *26*, 61.
10. Stejskal J., Kratochvil P. and Strakova D., "Study of the Statistical Chemical Heterogeneity of Copolymers by Cross-Fractionation", *Macromolecules*, **1981**, *14*, 150.
11. Stejskal J., Kratochvil P. and Jenkins A.D., "Graft Copolymer Statistics. 2. Application to Graft Copolymers Prepared from Macromonomers", *Macromolecules,* **1987**, *20*, 181.
12. Stejskal J. and Kratochvil P., "Statistical Chemical Heterogeneity of Copolymers. Modification of the Stockmayer Distribution Function of Chemical Composition", *Macromolecules*, **1987**, *20*, 2624.
13. Costeux S., Anantawaraskul S., Wood-Adams P.M. and Soares J.B.P., "Distribution of the Longest Ethylene Sequence in Ethylene/1-Olefin Copolymers Synthesized with Single-Site-Type Catalysts", *Macromolecular Theory and Simulation*, **2002**, *11*, 326.
14. Xu G., "Distribution of Chain Lengths and Composition in Terpolymers", *Journal of Polymer Science: Part A: Polymer Chemistry,* **1997**, *35*, 1161.

CHAPTER 4

# EFFECT OF MOLECULAR WEIGHT AND COMONOMER CONTENT ON CRYSTAF

*Not one thing comes to be randomly,*
*but all things from reason and necessity.*
***Leucippus***

While the measurement of CCD of multicomponent copolymers is not possible, the CCD of binary semi-crystalline copolymers can be estimated using crystallization analysis fractionation (Crystaf). This chapter and the next explain this analytical technique and how polymer chain microstructures and Crystaf operation conditions can influence the results. The chapter first looks at the effect of chain microstructures, specifically the effect of molecular weight and average comonomer content, on Crystaf analyses of ethylene/1-hexene copolymers. Experimental results previously reported in the literature are combined with new data from the present study to test the proposed Monte Carlo Crystaf models.

## 4.1 INTRODUCTION

The chemical composition distribution (CCD) of ethylene/α-olefin copolymers significantly affects the physical and thermal properties of these materials. It is therefore necessary to have quantitative analytical techniques for measuring CCD. Temperature rising elution fractionation (Tref) has been used for several years [1-4],

but is a very tedious technique because of the required two-step procedure described in Chapter 2.

Recently, crystallization analysis fractionation (Crystaf) was developed as an alternative to Tref [5-8]. Requiring shorter analysis times, Crystaf provides results comparable to those of Tref. Crystaf involves a single-step solution crystallization process, in which polymer molecules precipitate at different temperatures according to their crystallizabilities. Crystaf data, which are the amounts of polymer remaining in solution at each crystallization temperature, can be converted to CCD using a calibration curve that relates crystallization temperature to comonomer content. Since Crystaf is still a relatively new technique, a better understanding of the detailed fractionation mechanism and how polymer molecular structure influences fractionation is required. In this chapter, these effects are investigated.

In the case of ethylene/α-olefin copolymers, the average comonomer content and molecular weight are the main structural characteristics that affect their crystallizability and thus their fractionation by Crystaf. Beigzadeh *et al.* [9-10] proposed a Monte Carlo model for Crystaf fractionation based on certain assumptions about the crystallization mechanism and the relationship between lamella thickness and crystallization temperature. The results from the model showed good agreement with their limited experimental data for ethylene/1-octene copolymers.

Later, Costeux *et al.* [11] derived an analytical expression describing the numerical results obtained by Beigzadeh *et al.* [9-10] following statistic arguments. They also explored the predictions of the model for a wider range of parameters from a theoretical point of view but without experimental validation. Recently, Sarzotti *et al.* [12-13] reported experimental results on the effect of comonomer content on Crystaf profiles for ethylene/1-hexene copolymers. In this chapter the extensive experimental data on the effect of comonomer content from Sarzotti *et al.* [12-13] and on the effect of molecular weight determined in the present study are used to evaluate and to propose improvements to the model of Beigzadeh *et al.* [9-10].

## 4.2 EXPERIMENTAL

### 4.2.1 Materials

Ethylene/1-hexene copolymers were used in this investigation. The effect of the number average molecular weight on Crystaf fractionation was studied using fractions of three copolymers with varying 1-hexene content made with metallocene catalysts. These copolymers were fractionated by molecular weight using the preparative fractionation apparatus (PREP) in the solvent/non-solvent mode (PolymerChar, Spain).

In PREP, polymer samples are fractionated by controlling the interaction parameter using successive additions of non-solvent to the polymer solution. In the present study, xylene and diethylene glycol monobuthyl ether were used as the solvent and the non-solvent, respectively. The polymer samples were dissolved at 130°C, before holding at 120°C for stabilization and fractionation. The total volume of solution used in each fractionation step was 180 ml. Table 4.1 shows the volume fraction of solvent in solution used for fractionating each sample.

Table 4.1 Volume fraction of solvent in the solvent/non-solvent mixture for each fraction

| Sample | Volume fraction of solvent in the solvent/non-solvent solution | | | | |
|---|---|---|---|---|---|
| | Fraction 1 | Fraction 2 | Fraction 3 | Fraction 4 | Fraction 5 |
| A | 0.400 | 0.500 | 0.556 | 0.588 | 1.000 |
| B | 0.500 | 0.526 | 0.556 | 0.571 | 1.000 |
| C | 0.500 | 0.526 | 0.556 | 1.000 | ---- |

The fractions of each sample have the same average 1-hexene content but different average molecular weights, as shown in Table 4.2 The molecular weight distribution for each fraction of sample A is displayed in Figure 4.1.

Table 4.2 Properties of fractionated samples for the study of molecular weight effects.

| Sample | Number average molecular weight ($M_n$) | Fractionated sample | Number average molecular weight ($M_n$) | Number average chain length ($r_N$) | Mol percent of 1-hexene ($CPP$)[+] |
|---|---|---|---|---|---|
| A | 36,100 | A1 | 16,700 | 581 | 1.27 |
| | | A2 | 28,400 | 990 | 1.27 |
| | | A3 | 44,900 | 1,564 | 1.27 |
| | | A4 | 73,200 | 2,549 | 1.27 |
| | | A5 | 104,100 | 3,626 | 1.27 |
| B | 35,200 | B1 | 30,900 | 1,055 | 2.3 |
| | | B2 | 51,100 | 1,746 | 2.3 |
| | | B3 | 71,900 | 2,454 | 2.3 |
| | | B4 | 97,300 | 3,323 | 2.3 |
| | | B5 | 151,600 | 5,178 | 2.3 |
| C | 34,300 | C1 | 22,900 | 770 | 3.2 |
| | | C2 | 32,100 | 1,078 | 3.2 |
| | | C3 | 39,500 | 1,325 | 3.2 |
| | | C4 | 67,100 | 2,253 | 3.2 |

[+] The mole fraction of 1-hexene in the fractionated samples is assumed to be equal to the one measured by $C^{13}$ NMR for the parent samples, as the mole fraction of comonomer was reported to be almost constant and independent of chain length for samples synthesized with single site catalyst [14]

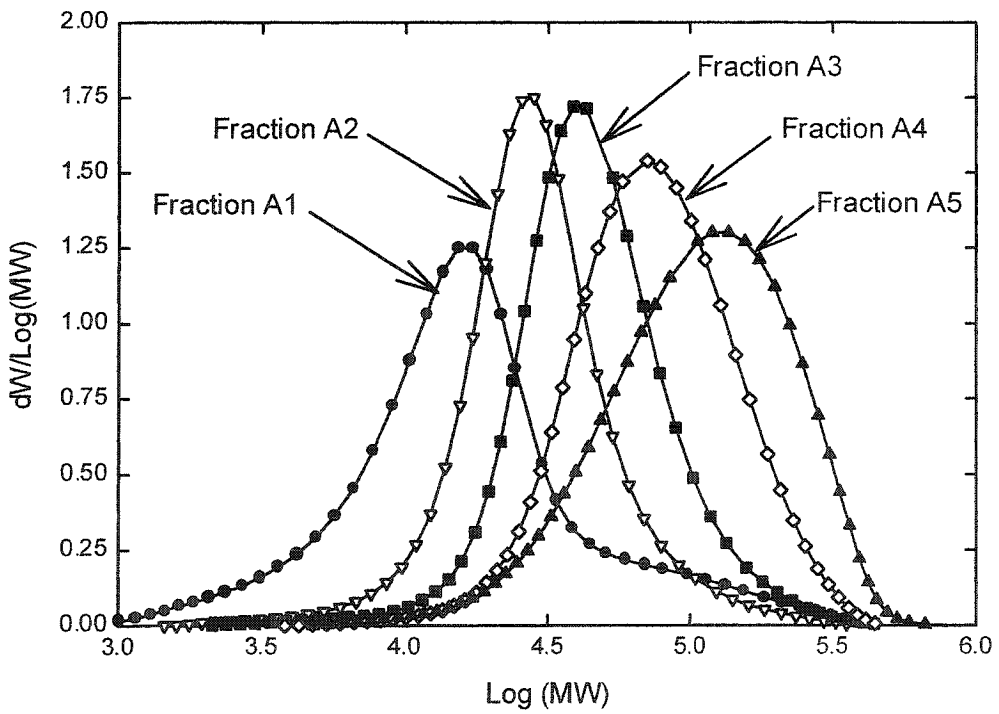


Figure 4.1 MWD of each fraction of sample A

### 4.2.2 Crystaf analysis

In Crystaf analysis, the polymer is dissolved in trichlorobenzene (TCB) at a concentration of 0.1 mg/mL. During the dissolution step, the polymer solution is held at a temperature of 160°C for 60 minutes to ensure complete dissolution. The temperature is then decreased to 95°C and kept at this value for 45 minutes for stabilization before starting the fractionations.

The polymer solution is then cooled at a constant rate of 0.1°C/min to 30°C. Polymer chains with low comonomer content crystallize at higher temperatures inside the vessel. Aliquots of the polymer solution are collected via an in-line filter (to avoid sampling the polymer chains that have already precipitated) and transferred to the in-line infrared detector. The infrared detector monitors the change in polymer concentration in solution with temperature, yielding the integral Crystaf curve. The differential form of the curve, *i.e.* the weight fraction change at each crystallization temperature, is then obtained by numerical differentiation of the integral curve. More details on Crystaf operation procedures are given by Monrabal [5-6].

### 4.2.3 Other Experimental Data

In the second part of this investigation, the data of Sarzotti *et al.* [12-13] were used to validate the Crystaf model. In their work, the effect of comonomer content on Crystaf analysis was studied using a set of ethylene/1-hexene copolymers synthesized using a single-site catalyst. These samples have approximately the same number average molecular weight ($M_n$) of 36,300 (well within the range of ± 10% attributed to experimental error in gel permeation chromatography) but different comonomer contents (varying from 0.68 to 4.2 mol% 1-hexene). Table 4.3 summarizes the properties of these samples.

Table 4.3 Properties of samples for the study of comonomer effects

| Sample | Number average molecular weight ($M_n$) | Number average chain length ($r_N$) | Mol percent of 1-hexene ($CPP$) | PDI |
|---|---|---|---|---|
| 1 | 34,500 | 1,138 | 4.20 | 2.16 |
| 2 | 34,300 | 1,151 | 3.14 | 2.18 |
| 3 | 34,900 | 1,190 | 2.32 | 2.16 |
| 4 | 36,300 | 1,258 | 1.51 | 2.35 |
| 5 | 36,100 | 1,259 | 1.21 | 2.43 |
| 6 | 37,200 | 1,310 | 0.68 | 2.50 |

## 4.3 SIMULATION

### 4.3.1 Chain microstructure

Figure 4.2 is a schematic of an ethylene/α-olefin copolymer chain, which shows the definitions of ethylene sequence (ES), longest ethylene sequence (LES), and average ethylene sequence (AvgES). For a single molecule ES is defined as the number of ethylene units incorporated in a segment of the polymer chain (each segment is separated by one or more comonomer units).

In each copolymer molecule, there is a distribution of ES, as there is generally more than one ethylene segment per molecule. Again considering a single molecule, the LES is defined as the largest ES, and AvgES is the average ES value. These definitions can naturally be extended to any other polymer chain having crystallizable and non-crystallizable segments.

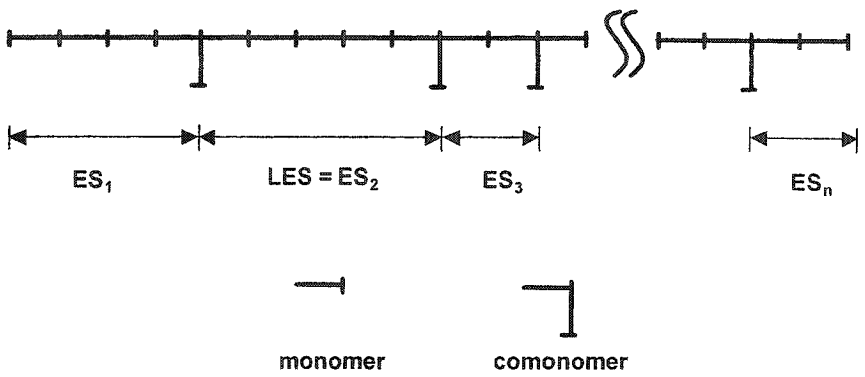


$$AvgES = \frac{\sum_{i=1}^{n} ES_i}{n}$$

Figure 4.2 Illustration of ethylene sequence (ES), longest ethylene sequence (LES), and average ethylene sequence (AvgES) for a LLDPE molecule

### 4.3.2 Monte Carlo Simulation

Monte Carlo simulations were used to generate a population of copolymer molecules having the statistical properties of an ethylene/α-olefin copolymer synthesized with a single-site or metallocene catalyst [9-10]. These simulations depend upon two parameters: an overall propagation probability (*PP*) and a comonomer propagation probability (*CPP*). The parameter *PP* is compared to a randomly generated number to decide whether the chain propagates or terminates. If the chain propagates, the parameter *CPP* is used to choose between the addition of an ethylene or of a 1-olefin molecule. For metallocene-catalyzed copolymers, *PP* can be calculated from the number average chain length ($r_N$) and average comonomer content (*CC*) as follows:

$$r_N = \frac{M_n}{M_{CO} \times CC + M_{MO} \times (1 - CC)} \tag{4.1}$$

$$PP = \frac{r_N - 1}{r_N} \tag{4.2}$$

where $M_n$ is the number average molecular weight, $M_{CO}$ is the molecular weight of comonomer (84 for 1-hexene), and $M_{MO}$ is the molecular weight of monomer (28 for ethylene). As such materials are random copolymers, $CPP$ and $CC$ are equal. This algorithm was used to generate populations representing unfractionated polymer samples (A, B, C and 1 to 6)

In order to simulate the molecular weight-fractionated samples (Samples A1-5, B1-5, and C1-4), the preceding algorithm was modified as shown in Figure 4.3.

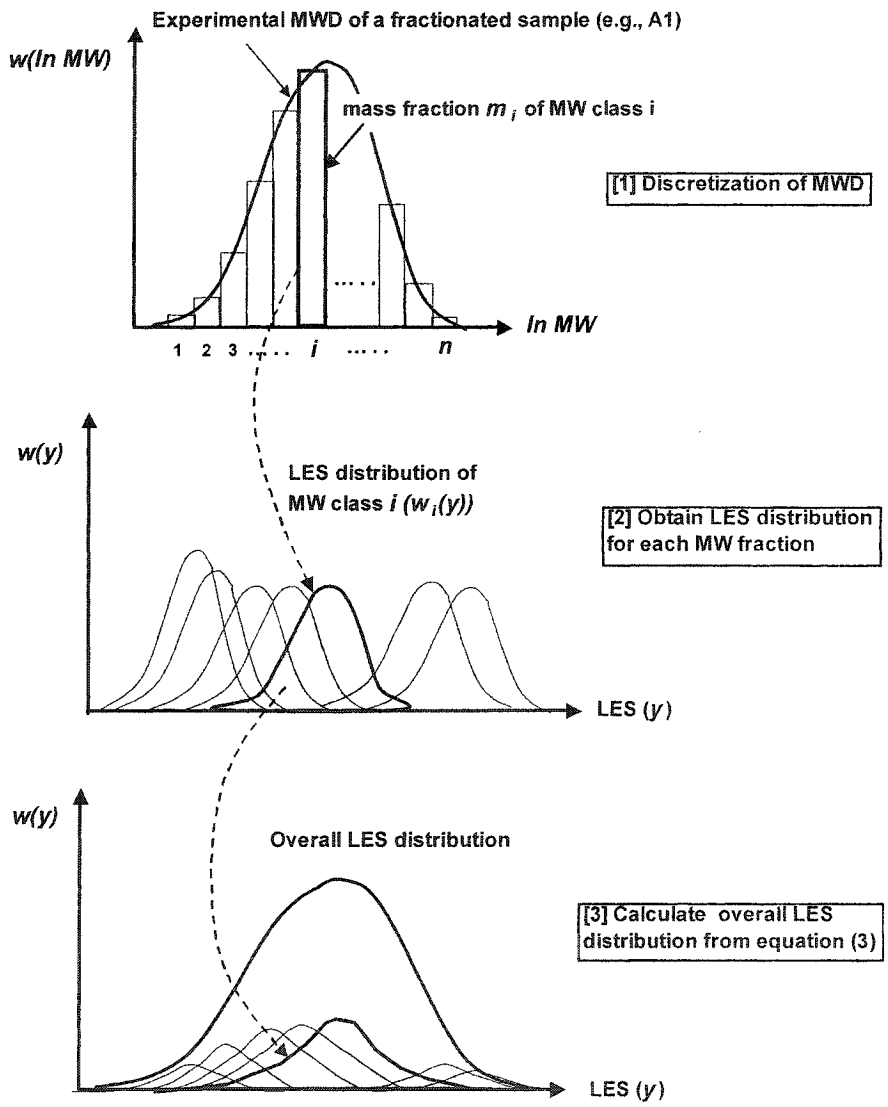


Figure 4.3 Illustration of the computational steps for determining the LES distribution when the MWD is known

First, the experimental MWD of each fractionated sample (*e.g.*, A1) was discretized in $n$ molecular weight classes and the mass fraction ($m_i$) of each molecular weight class was recorded. Secondly, the LES distribution, $w_i(y)$, was calculated via Monte Carlo simulation for each molecular weight class. Finally, the overall LES distribution for the whole polymer fraction, $w(y)$, was obtained by adding up all $w_i(y)$ using the equation:

$$w(y) = \sum_{i=1}^{n} m_i \cdot w_i(y) \tag{4.3}$$

An important assumption made in the second step of the above procedure is that each molecular weight fraction has the same average comonomer content. This hypothesis is valid for polymers made with single-site catalysts under uniform polymerization conditions, such as the ones investigated here. Analysis of metallocene-catalyzed LLDPEs by GPC-FTIR also confirmed that average comonomer content is independent of molecular weight [14].

For the solvent/non-solvent system, the effect of comonomer content and crystallinity on fractionation is negligible, since the fractionation is carried out at a temperature higher than the polymer dissolution temperature. This concept comes from the theoretical treatment of Stockmayer and Fixman and was later confirmed by the experimental work of Tung [15].

### 4.3.3 Crystal thickness and crystallization temperature and their relationship to Crystaf

Polyethylene forms a lamellar crystal structure, as it is crystallized from a dilute solution. The lamella thickness ($\zeta$) is a strong function of the crystallization temperature ($T_C$). This relationship is well described from thermodynamic considerations by the Gibbs-Thompson equation [16]:

$$T_C = \frac{T_S^O(\zeta - \alpha)}{\zeta} - T_S \tag{4.4}$$

Beigzadeh *et al.* [9-10] introduced an additional empirical parameter ($T_S$) to account for supercooling during the crystallization process. In this equation, $T_S^O$ is the equilibrium dissolution temperature, and $\alpha$ is a constant related to the enthalpy of fusion.

In the Crystaf model proposed by Beigzadeh *et al.*, the lamella thickness is assumed to be proportional to the LES. This assumption is based on the hypothesis that comonomer units cannot be part of the lamella lattice. Therefore, the longest ethylene sequence (LES) is the first segment in the chain to crystallize as Crystaf temperature decreases and thus governs the lamella thickness. As soon as the LES crystallizes, the entire molecule precipitates from solution and is no longer detected by the IR detector in Crystaf. Consequently, according to this model, Crystaf profiles are obtained from Equation (4.4) simply by replacing $\zeta$ by the LES distribution and finding values for the parameters $\alpha$, $T_S^O$, and $T_S$ that adequately describe the experimental data.

This is clearly a bold simplification of a rather complex problem, since it ignores chain folding and polymer crystallization kinetic effects. However, it will be shown that this approach leads to a semi-empirical model that better describes the crystallization phenomena taking place in Crystaf. In the present study, the AvgES distribution is also considered as an alternative to the LES distribution for modeling Crystaf profiles.

## 4.4 RESULTS AND DISCUSSION

### 4.4.1 Effect of number average molecular weight ($M_n$)

Molecular weight can affect the crystallizability of polymer chains in two subtle ways. First, a molecule with higher molecular weight has more difficulty folding and fitting into the crystal lattice than another with lower molecular weight and the same crystallizability. Chain movement is certainly more difficult for a molecule with high molecular weight, as the hydrodynamic radius and friction coefficient increase with molecular weight.

Second, molecular weight can affect the crystallization process, because it is related to the LES distribution. Costeux *et al.* [11] showed that LES increases with molecular weight. As the LES can be related to crystallization temperature through the Gibbs-Thomson equation, molecular weight inevitably affects the crystallization process.

Experimental Crystaf profiles for the molecular weight fractions of sample A (recall that each fraction has the same 1-hexene content of 1.27 mol%) are shown in Figure 4.4. Fractions of samples B and C show the same trends. The results demonstrate that as the molecular weight increases, the Crystaf profiles become narrower. This change in the shape of Crystaf profiles is especially pronounced for low molecular weight fractions, with the appearance of a low crystallinity tail. Nieto *et al.* [17] performed Crystaf analysis of a series of ethylene homopolymers of varying molecular weights. They found that the Crystaf profiles of homopolymers changed with molecular weight in a similar way to that shown in Figure 4.4.

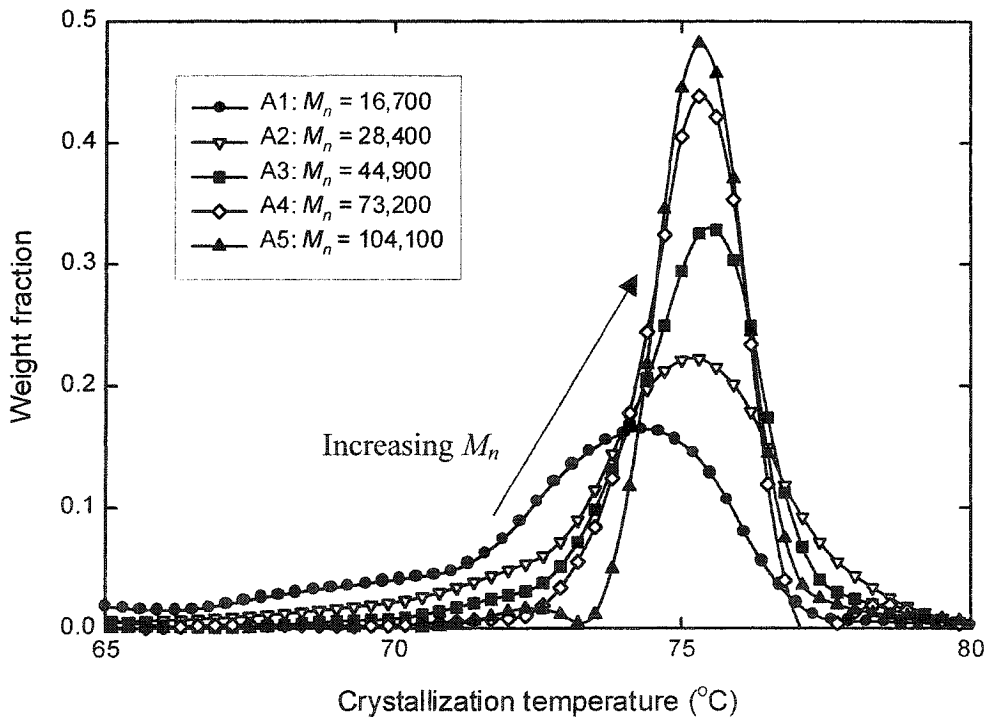


Figure 4.4. Effect of molecular weight on Crystaf profile (Experimental results)

Although a trend of increasing peak temperature with molecular weight is also visible, it is well within the experimental error of ± 1°C observed in Crystaf. Thus,

this effect is practically negligible for this variable. This allows the construction of calibration curves relating comonomer content and peak position that are independent of molecular weight for most polymers of commercial interest. This is a very important conclusion for the use of calibration curves in Crystaf analysis.

However, it is interesting to note that the onset of crystallization takes place at lower temperatures as molecular weight increases for samples A2 through A5. This is probably related to crystallization kinetics effects, since shorter chains can crystallize faster than longer ones and are therefore likely to be closer to the assumed thermodynamic equilibrium. Evidently, if the molecular weight is too small (fraction A1), the LES becomes too short to crystallize at a high temperature, and a decrease in the onset of crystallization temperature is observed.

Figure 4.5 compares experimental and simulated results (based on LES distribution) for these fractions. The computation was done using Equation (4.4) with the two parameters reported by Beigzadeh *et al.* [9-10] ($\alpha$ =10, $T_S^o$ =89°C), while the supercooling temperature $T_S$ was chosen to match the present experimental data. The simulations agree qualitatively with the experimental data. Especially important is the fact that the model can properly describe the low temperature tails for the lower molecular weight fractions. One can, however, observe increasing discrepancies between model and experiments as the molecular weight increases.

Using the LES distribution, the best-fit supercooling temperature ($T_S$) in Equation (4.4) was found to be a function of the number average chain length and comonomer content. Figure 4.6 shows the relationship for each set of fractionated samples (sample A, B, and C). Interestingly, molecular weight and comonomer content (up to a limiting comonomer fraction when the comonomer effect overtakes the influence of molecular weight) synergistically affect the supercooling temperature, as indicated by the steeper slope of the curve for sample C.

### 4.4.2 Effect of comonomer content

The crystallizability of ethylene/α-olefin copolymers is governed primarily by comonomer content. As the amount of comonomer incorporated into the polymer

chains increases, the crystallizability of the chain decreases, and the crystallization temperature is lowered.

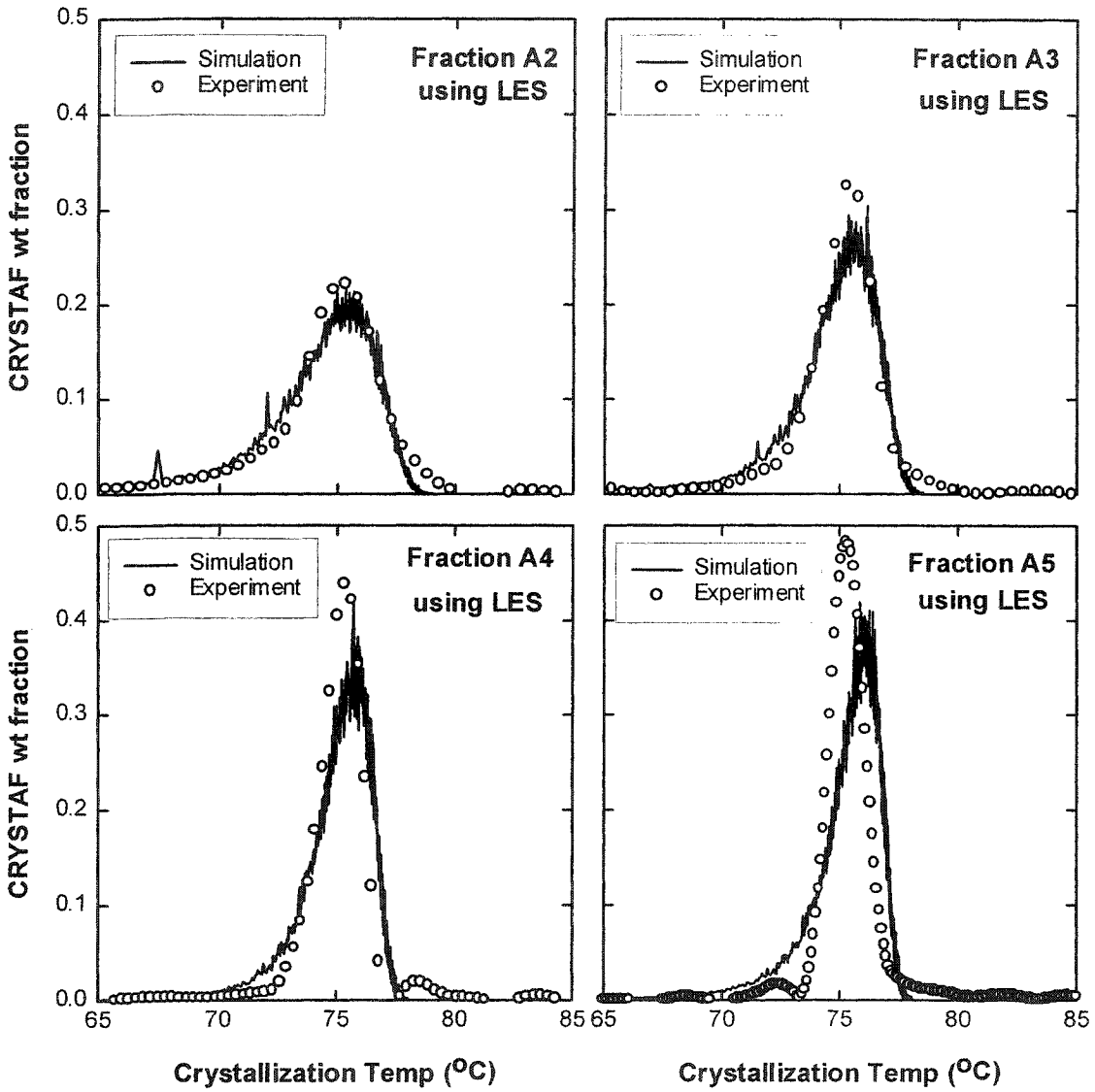


Figure 4.5 Comparison of experimental data with simulation results using LES distribution for various $M_n$ (fractions of sample A, $\alpha$=10, $T_S^o$=89°C)

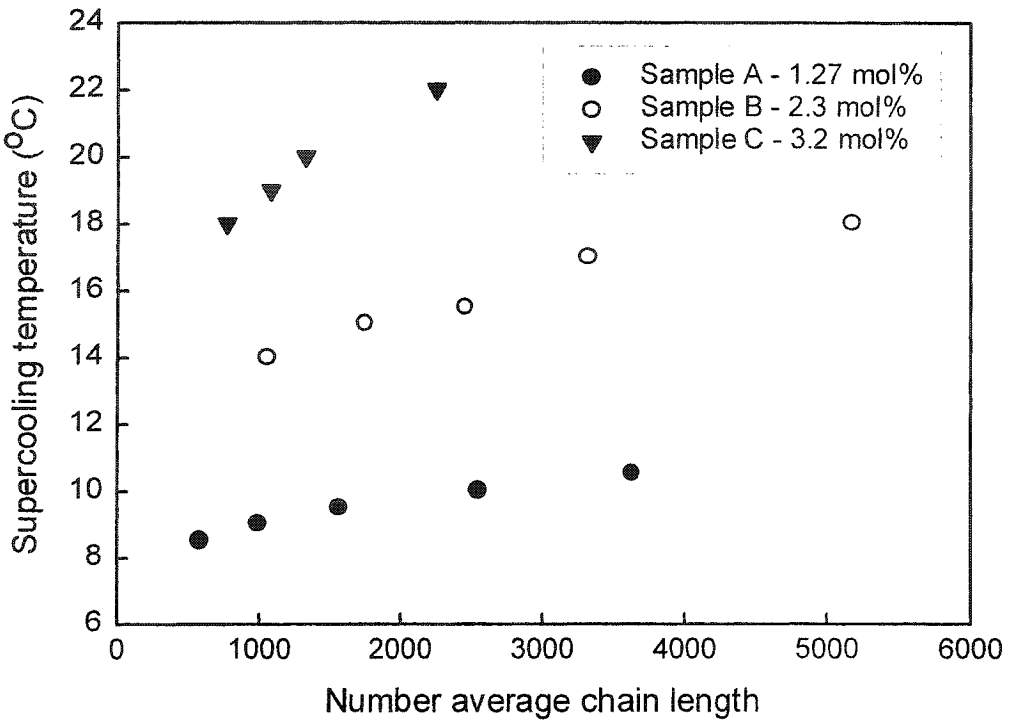


Figure 4.6 Effect of number-average chain length on supercooling temperature for various comonomer content levels

The Crystaf experimental results of Sarzotti *et al.* [12-13] are shown in Figure 4.7. Their results show a significant decrease in Crystaf peak temperature as comonomer content increases. The results also show another significant effect of comonomer: a broadening of the Crystaf distribution as comonomer content increases.

The same features can also be observed in the simulation results (Figure 4.8). The model overestimates the severity of the low temperature tail and underestimates the temperature for the onset of crystallization. The discrepancies increase as comonomer content decreases. This indicates a systematic lack of fit between the LES-based Crystaf model and the experimental data.

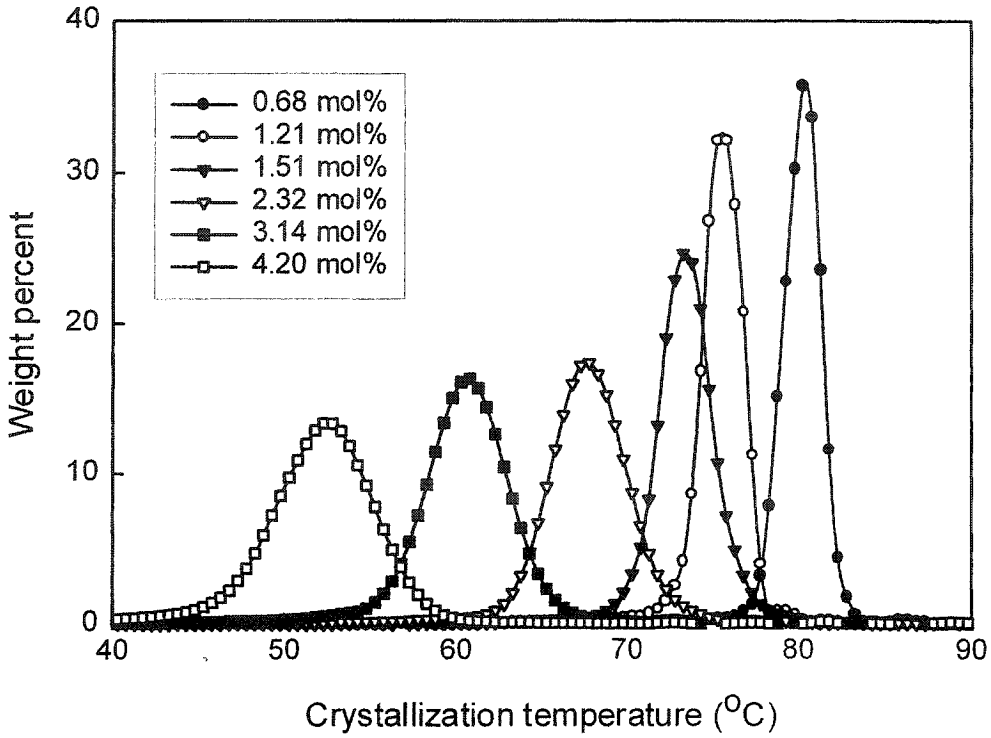


Figure 4.7 Effect of comonomer content on Crystaf profile
(Experimental results from Sarzotti *et al.* [12])

The supercooling temperature, $T_S$, was found to increase linearly with comonomer content, as shown in Figure 4.9. Since it was previously demonstrated that $T_S$ increases linearly with kinetic chain length, least squares regression was used to obtain Equation (4.5) relating the supercooling temperature to comonomer content and molecular weight:

$$T_S = 1.387 + 6.818 \times 10^{-4} \times r_N + 5.689 \times 10^{2} \times CPP \qquad (4.5)$$

All the experimental data for samples A, B and C, and those of Sarzotti *et al.* [12-13] were used to obtain Equation (4.5). Figure 4.10 compares the results predicted using Equation (4.5) with the experimental data. Recall that Equation (4.5) applies to the LES-based model described previously.

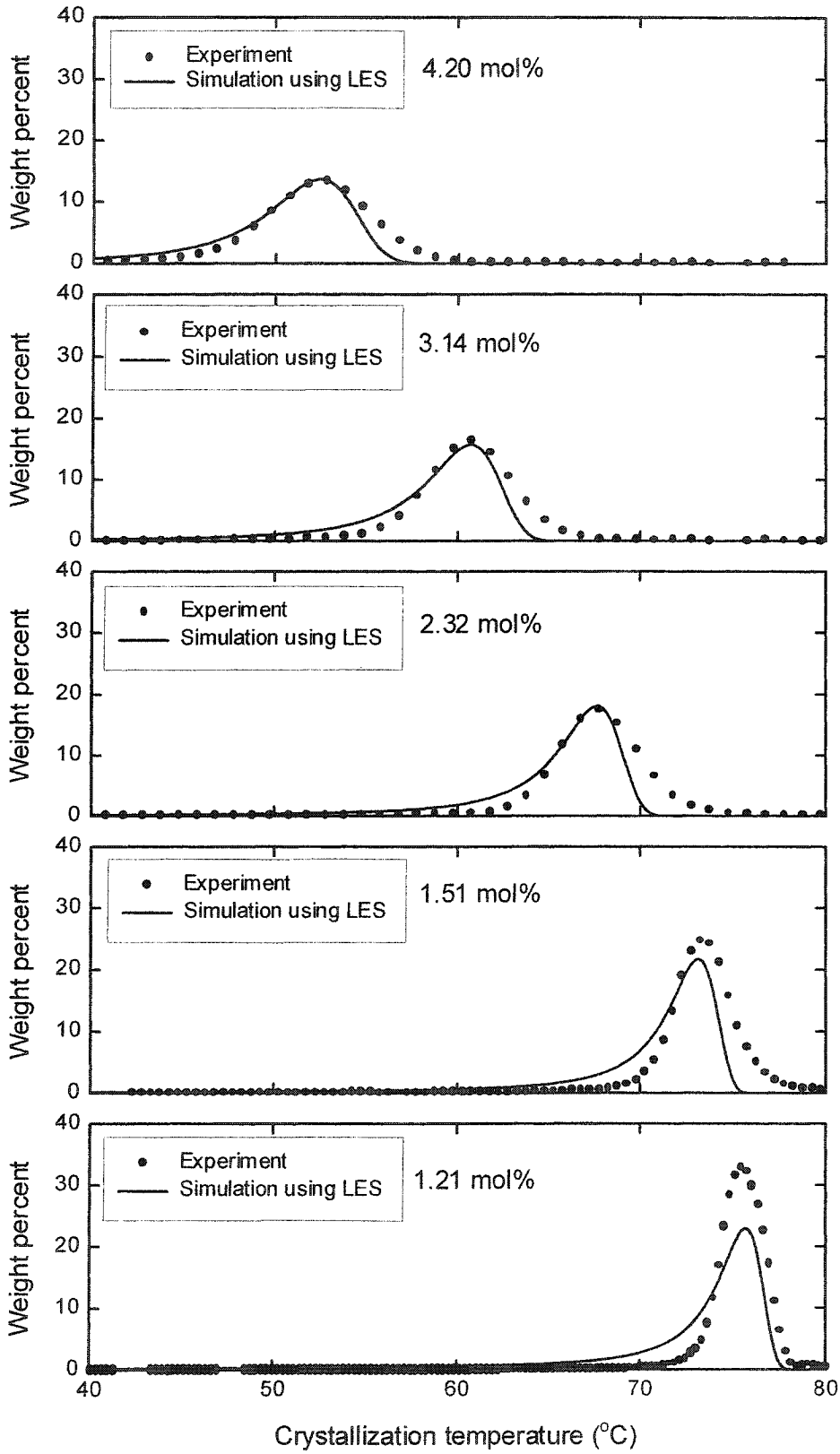


Figure 4.8 Comparison of experimental data with simulation results using LES distribution for various levels of comonomer content ($\alpha$=10, $T_S^o$=89°C)

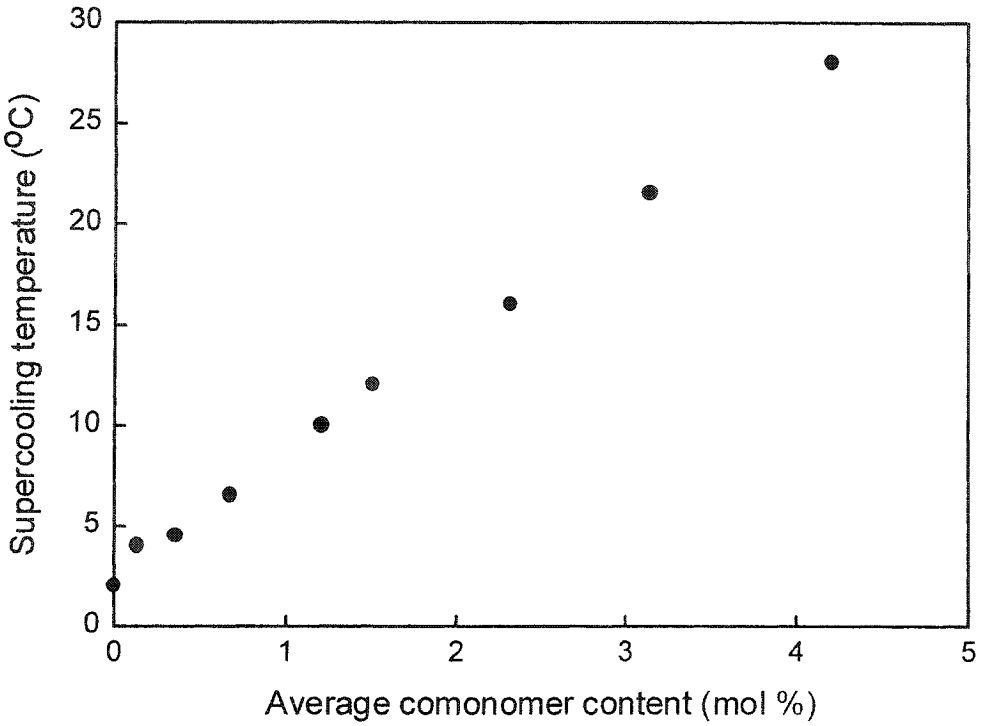


Figure 4.9 Effect of comonomer content on the supercooling temperature for constant $M_n$ ($M_n \approx 35{,}000$)

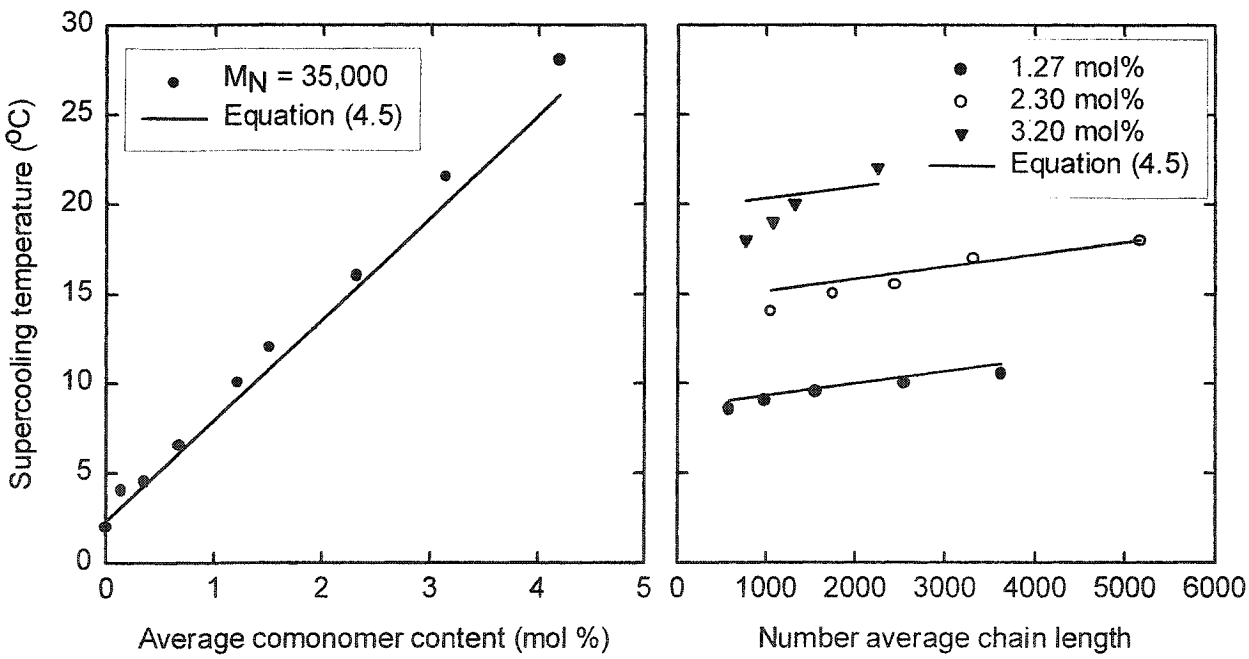


Figure 4.10 Effects of comonomer content and molecular weight on the supercooling temperature (model using LES distribution)

### 4.4.3 Comparison of Crystaf simulations based the LES and AvgES distributions

As demonstrated previously (Figure 4.8), the LES-based model overpredicts the tailing of the distributions and underpredicts the temperature for the onset of crystallization. An alternative model can be developed using the AvgES distribution to replace the LES distribution in Equation (4.4). This method makes use of the numerical procedure described by Beigzadeh *et al.* with the exception that the lamella thickness is now assumed to be determined by the AvgES instead of the LES.

After refitting the parameters $\alpha$ and $T_S$ in Equation (4.4) ($\alpha = 6$, $T_S^o = 89^oC$), the AvgES-based model performs better than the LES-based model. Figures 4.11 and 4.12 compare the AvgES-based simulations of the Crystaf profiles with experimental data for the fractions of sample A and for samples 1 through 5. As compared to the LES-based model, the AvgES-based model slightly improves the fit of the experimental data for the fractionated samples (compare Figures 4.5 and 4.11), but this improvement becomes significant for the samples with different levels of comonomer content (compare Figures 4.8 and 4.12). The improved prediction of the onset of crystallization temperature and low temperature tail argue strongly in favor of using the AvgES distribution instead of the LES distribution for modeling Crystaf fractionation.

One can only speculate as to why the AvgES distribution gives a better fit to the data. The use of the LES distribution assumes that the fractionation process in Crystaf occurs close to thermodynamic equilibrium, thus leading to crystals of maximum achievable size under the experimental conditions used during crystallization. This might not be the case, since it is very likely that kinetic effects interfere with the crystallization process in Crystaf, producing smaller crystallites, as is discussed later in more detail [18]. This might be the reason for the systematic lack of fit when the LES distribution is used to simulate Crystaf profiles. The use of AvgES may indirectly take into account these effects by predicting smaller lamellae than the ones simulated with LES. The AvgEs-based model may thus be less fundamental but more useful as a model of Crystaf fractionation.

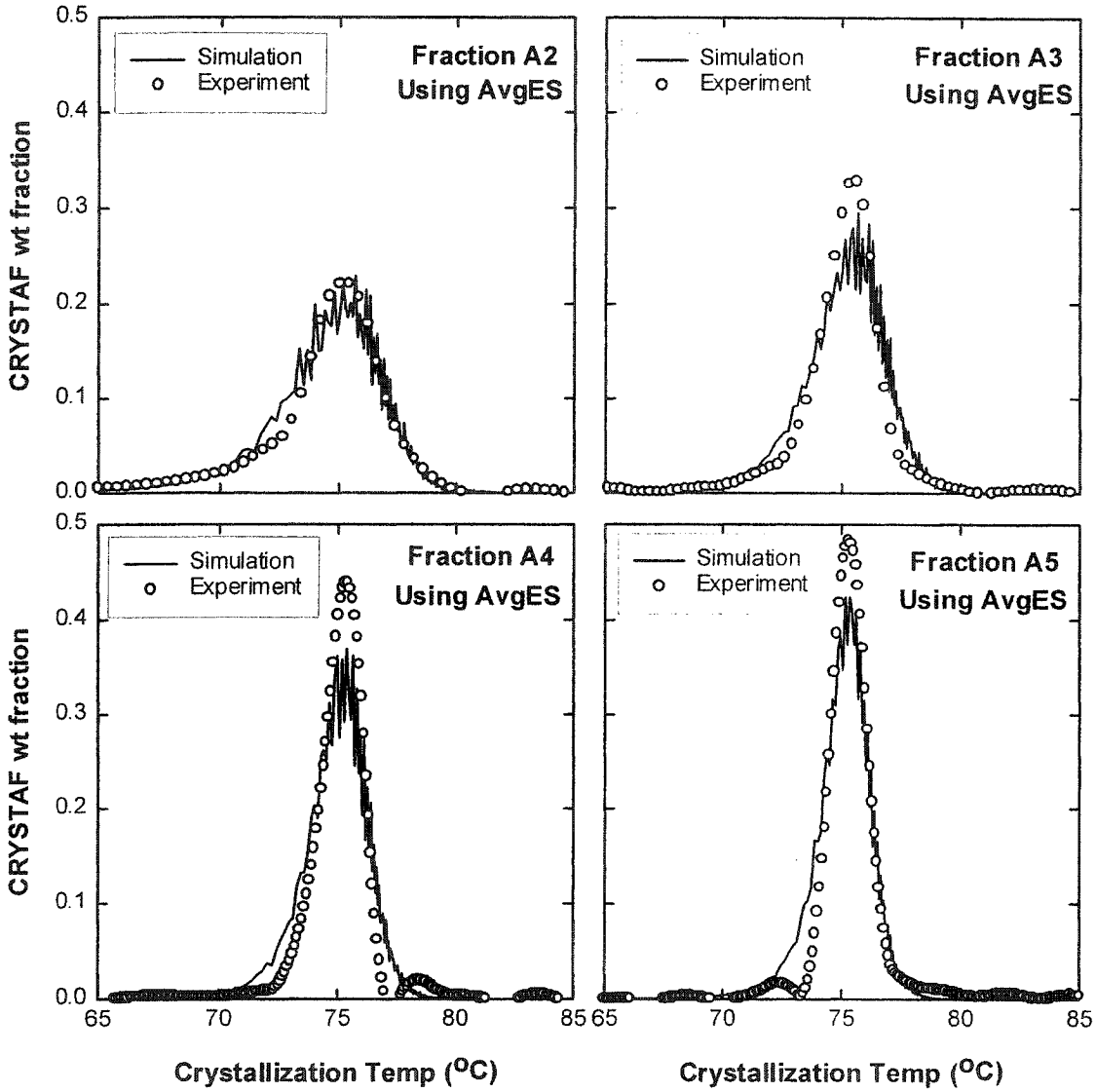


Figure 4.11 Comparison of experimental data with simulation results using the AvgES distribution for various $M_n$ (fractions of sample A, $\alpha$ =6, $T_S^o$ =89°C)

The supercooling temperature was again found to be a function of molecular weight and comonomer content. Equation (4.6) is an empirical equation obtained by least squares fit that relates $T_S$ to $r_N$ and $CPP$ for the AvgES-based model:

$$T_S = 3.0736 + 2.9933 \times 10^{-4} \times r_N + 2.038 \times 10^{2} \times CPP \qquad (4.6)$$

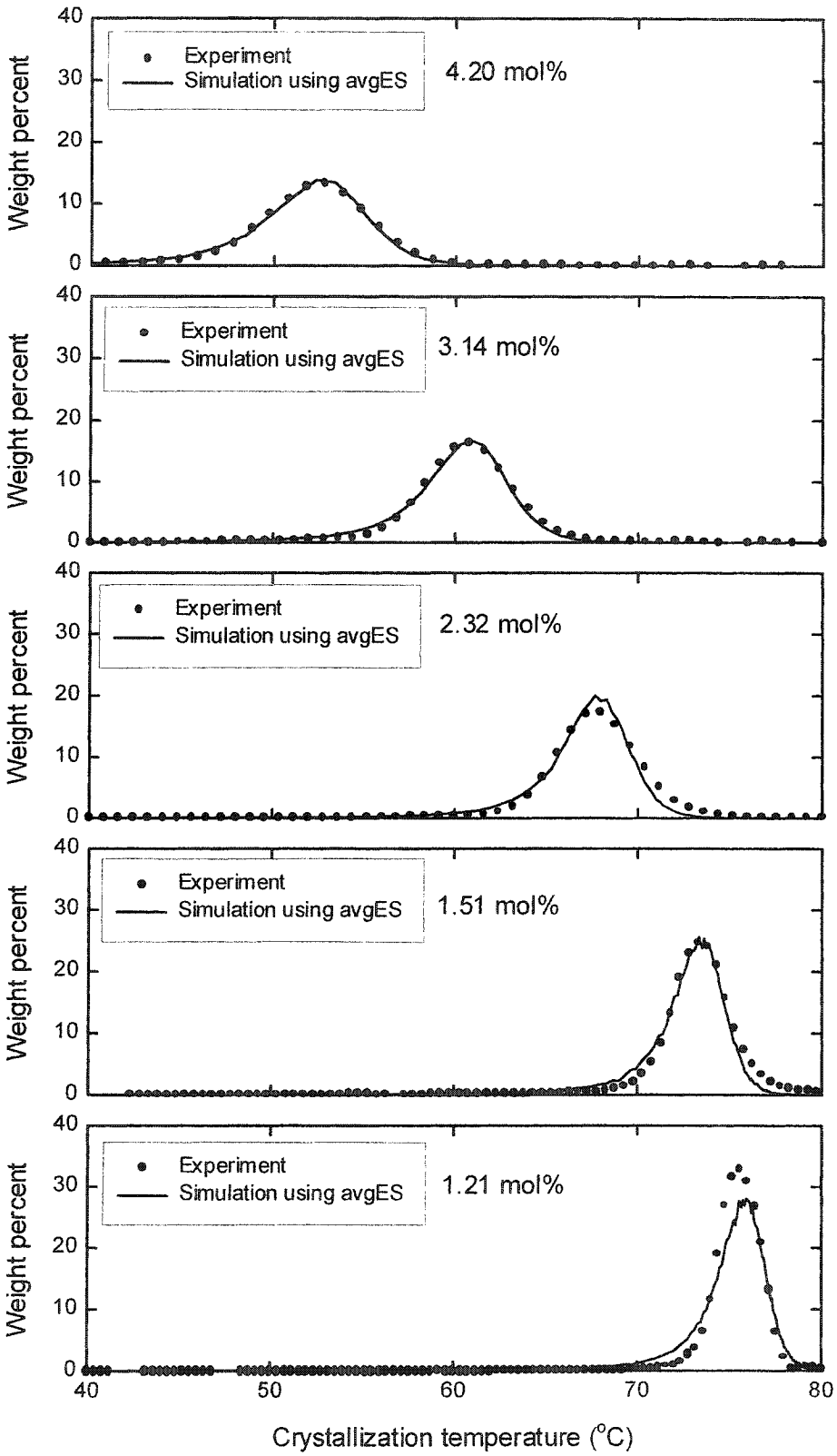


Figure 4.12 Comparison of experimental data with simulation results using avgES distribution for various levels of comonomer content ($\alpha$=6, $T_S^o$=89°C)

Figure 4.13 compares the results from the above equation and the experimental data. This model permits the accurate simulation of Crystaf profiles for ethylene/1-hexene copolymers as a function of molecular weight and comonomer content.

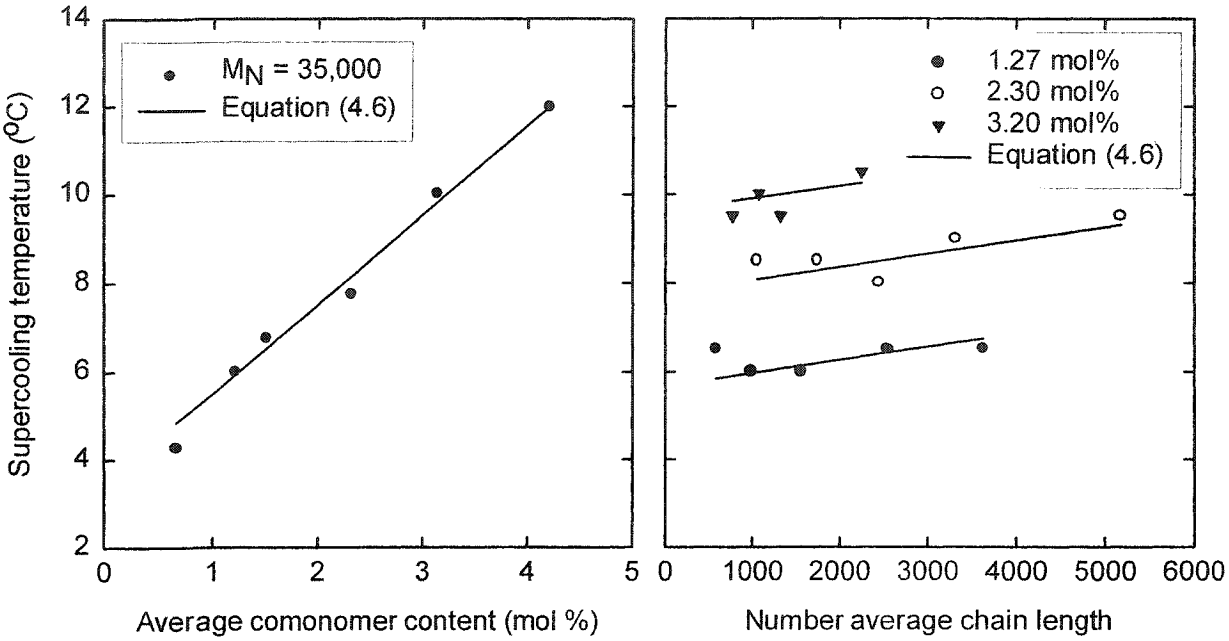


Figure 4.13 Effects of comonomer content and molecular weight on the supercooling temperature (model using avgES distribution)

## 4.5 CLOSING REMARKS

Both molecular weight and comonomer content significantly affect Crystaf profiles. Although Crystaf peak temperatures are practically independent of molecular weight, increased tailing of the Crystaf profile in the low temperature region is observed with decreasing molecular weight. The comonomer content is the most important parameter affecting the location of the Crystaf peak temperature for a given set of operating conditions. Therefore, comonomer content can be quickly estimated using a calibration curve relating peak location and comonomer content. This is the standard procedure in Crystaf analysis, and this investigation proves that it is quantitatively accurate.

The model proposed by Beigzadeh *et al.* [9-10] shows good qualitative agreement with the experimental data, but a systematic lack-of-fit can be observed.

Using the AvgES distribution instead of the LES distribution seems to give a better semi-empirical modeling of Crystaf profiles.

## NOMENCLATURE

*AvgES* average ethylene sequence (see Figure 4.2)

$CC$ average comonomer content

$CPP$ comonomer propagation probability

$ES$ ethylene sequence (see Figure 4.2)

$LES$ longest ethylene sequence (see Figure 4.2)

$M_n$ number average molecular weight

$M_{CO}$ molecular weight of comonomer (hexane = 84)

$M_{MO}$ molecular weight of monomer (ethylene = 28)

$r_N$ number average chain length

$PP$ propagation probability

$T_S$ supercooling temperature

$T_S^0$ equilibrium dissolution temperature

$T_C$ crystallization temperature

$\alpha$ constant in equation (4.4)

$\zeta$ lamella thickness

## REFERENCES


1. Soares J.B.P. and Hamielec A.E., "Temperature Rising Elution Fractionation", in: *Modern Techniques for Polymer Characterization*, R.A. Pethrick, J.V. Dawkins, Eds., John Wiley&Sons, 1999, p. 15-55.
2. Soares J.B.P. and Hamielec A.E., "Temperature Rising Elution Fractionation of Linear Polyolefins", *Polymer*, **1995**, *36*, 1639.
3. Wild L., "Temperature Rising Elution Fractionation", *Advances in Polymer Science*, **1990**, *98*, 1.

4. Wild L. and Blatz C., "Development of High Performance Tref for Polyolefin Analysis", in: *New Advances in Polyolefins*, T.C. Chung, Eds, Plenum Press 1993, p. 147-157.
5. Monrabal B., "Crystallization Analysis Fractionation: A New Technique for the Analysis of Branching Distribution in Polyolefins", *Journal of Applied Polymer Science,* **1994**, *52*, 491.
6. Monrabal B., "CRYSTAF: Crystallization Analysis Fractionation. A New Approach to the Composition Analysis of Semicrystalline Polymers", *Macromolecular Symposia,* **1996**, *110*, 81.
7. Monrabal B., Blanco J., Nieto J. and Soares J.B.P, "Characterization of Homogeneous Ethylene/1-Octene Copolymers Made with a Single-Site Catalyst. CRYSTAF Analysis and Calibration", *Journal of Polymer Science: Part A: Polymer Chemistry*, **1999**, *37*, 89.
8. Britto L.J.D., Soares J.B.P., Penlidis A. and Monrabal B., "Polyolefin Analysis by Single-Step Crystallization Fractionation", *Journal of Polymer Science: Part B: Polymer Physics*, **1999**, *37*, 539.
9. Beigzadeh D., Soares J.B.P. and Duever T.A., "Modeling of Fractionation in CRYSTAF Using Monte Carlo Simulation of Crystallizable Sequence Lengths: Ethylene/1-Octene Copolymers Synthesized with Single-Site-Type Catalysts", *Journal of Applied Polymer Science*, **2001**, *80*, 2200.
10. Beigzadeh D., "Long Chain Branching in Ethylene Polymerization Using Combined Metallocene Catalyst Systems", *PhD thesis*, University of Waterloo, Canada, 2000.
11. Costeux S., Anantawaraskul S., Wood-Adams P.M. and Soares J.B.P., "Distribution of the Longest Ethylene Sequence in Ethylene/1-Olefin Copolymers Synthesized with Single-Site-Type Catalysts", *Macromolecular Theory and Simulation*, **2002**, *11*, 326.
12. Sarzotti D.M., "Heterogeneous Metallocene Catalysts for Olefin Polymerization: Effects of Support Material on Microstructure", *Master Thesis*, University of Waterloo, Canada, 2001.

13. Sarzotti D.M., Soares J.B.P. and Penlidis A., "Ethylene/1-Hexene Copolymers Synthesized with a Single-Site Catalyst: Crystallization Analysis Fractionation, Modeling, and Reactivity Ratio Estimation", *Journal of Polymer Science: Part B: Polymer Physics*, **2002**, *40*, 2595.
14. Faldi A. and Soares J.B.P., "Characterization of the Combined Molecular Weight and Composition Distribution of Industrial Ethylene/1-Olefin Copolymers", *Polymer,* **2001**, *42*, 3057.
15. Tung L.H., "Fractionation of Polyethylene", *Journal of Polymer Science*, **1956**, *20*, 495.
16. Mandelkern L., "Thermodynamic and Physical Properties of Polymer Crystals Formed from Dilute Solution", *Progress in Polymer Science*, **1970**, *2,* 165.
17. Nieto J., Oswald T., Blanco F., Soares J.B.P. and Monrabal B., "Crystallizability of Ethylene Homopolymers by Crystallization Analysis Fractionation", *Journal of Polymer Science: Part B: Polymer Physics*, **2001**, *39*, 1616.
18. Hosoda S., Nomura H., Gotoh Y. and Kihara H., "Degree of Branch Inclusion into the Lamellar Crystal for Various Ethylene/1-Olefin Copolymers", *Polymer*, **1990**, *31*, 1999.

CHAPTER 5

# EFFECT OF OPERATION PARAMETERS ON TREF AND CRYSTAF

*Simplicity is the key to effective scientific inquiry.*

***Stanley Milgram***

In the last chapter, the effects of chain microstructure on Crystaf were examined. This chapter explores the effect of operation parameters on both Tref and Crystaf analyses using a series of ethylene/α-olefin copolymers and their blends. The operating parameters investigated are the cooling, heating, and solvent flow rates. Therefore, this chapter focuses mainly on the role of crystallization kinetics in the fractionation processes of both techniques. The possibility of cocrystallization is also discussed in this chapter.

## 5.1 INTRODUCTION

Temperature rising elution fractionation (Tref) and crystallization analysis fractionation (Crystaf) are techniques widely used for the qualitative estimation of chemical composition distribution (CCD) of semi-crystalline copolymers, specifically ethylene/α-olefin copolymers. Both techniques can fractionate polymer chains of different crystallizabilities via crystallization from dilute solution.

Tref is a two-step process consisting of precipitation and elution [1-4]. In the first step, polymer chains are crystallized and precipitated from a dilute solution at a

constant cooling rate in a column loaded with inert support. In the second step, solvent flows through the column while the temperature is increased, thus eluting the polymer precipitated in the first step. The concentration of polymer eluted at each elution temperature is monitored with a mass-sensitive detector.

Crystaf [5-8] is based on a single, polymer-solution crystallization step at a constant cooling rate. The change in concentration of the polymer solution is monitored during the crystallization period, leading to a cumulative concentration profile. The derivative of the cumulative concentration profile indicates the fraction of polymer crystallized at each temperature, thus providing the same information obtained using Tref in a shorter time.

The preferred condition for fractioning polymer chains of different crystallizabilities is close to thermodynamic equilibrium, where crystallization kinetic effects should be negligible. Ideally, this allows each polymer chain to crystallize and precipitate separately at its crystallization temperature. Practically this condition is very difficult if not impossible to achieve, as very long analysis times would be required. In practice, a low cooling rate, in the range of 0.1-0.3°C/min is used.

This chapter investigates the effect of crystallization kinetics on Tref and Crystaf and explains the optimum compromise between analysis time, accuracy, and resolution of the fractionation. This chapter also looks at cocrystallization effects during polymer crystallization from dilute solution. Cocrystallization is the phenomenon whereby chains with different crystallizabilities crystallize at the same temperature. For the specific case of ethylene/α-olefin copolymers, this leads to the simultaneous crystallization of chains with different α-olefin content, which is highly undesirable when one is trying to estimate the chemical composition of these copolymers. Blends of well-defined ethylene/α-olefin copolymers were used in this investigation.

Most recent studies on crystallization kinetics for both isothermal and non-isothermal conditions have focused on crystallization from the melt state using differential scanning calorimetry (DSC) [9-11]. Similarly, although the crystallization of blends of linear and branched polyethylenes has been studied for decades, most investigations focused on crystallization from the melt state to understand miscibility

and to improve the processability and specific properties of products [12-13]. The present study focuses on crystallization kinetics and the cocrystallization of polymers from dilute solutions as determined using blends of samples having the same molecular weight but different comonomer fractions.

## 5.2 EXPERIMENTAL

### 5.2.1 Materials

Three ethylene/1-hexene copolymers and one ethylene/1-octene copolymer were used in this investigation. All samples were produced using single-site type catalysts; hence, the chemical composition distribution is expected to be narrow and unimodal for each sample and the polydispersity indices are close to 2.0. Blends of ethylene/1-hexene copolymers were also used to investigate the effect of cocrystallization. As all the ethylene/1-hexene copolymers have approximately the same molecular weight (within ±10%), the only difference in chain crystallizability is caused by different comonomer contents. Thus, blends of these samples are ideally suited to investigate the effect of comonomer distribution alone on cocrystallization. Table 5.1 summarizes the properties of the samples used in this investigation.

Table 5.1 Summary of the samples used in this investigation

| Sample | Comonomer type | Molecular weight ($M_N$) | Comonomer content (mol%) |
|---|---|---|---|
| A | Hexene | 37,200 | 0.68 |
| B | Hexene | 36,300 | 1.51 |
| C | Hexene | 34,300 | 3.14 |
| D | Octene | 40,700 | 2.19 |

| Sample | Weight ratio A:B:C |
|---|---|
| B1 | 30:40:30 |
| B2 | 0:50:50 |

### 5.2.2 Crystallization Analysis Fractionation (Crystaf)

Crystaf analysis was performed using a CRYSTAF model 200 manufactured by PolymerChar S.A. (Valencia, Spain). Crystallization is carried out in 60 mL stirred stainless steel vessels. The polymer sample is dissolved in 1,2,4 trichlorobenzene (TCB) at a concentration of 0.4 mg/mL, and the solution is held at 160°C for one hour to ensure complete dissolution. Then the temperature of the polymer solution is decreased to 95°C and allowed to stabilize for 45 minutes before starting the fractionation. A stirring rate of 200 rpm is used in the dissolution and stabilization steps, and 100 rpm is used during crystallization.

During crystallization, the temperature is decreased to 30°C at a constant cooling rate (0.0033-2.0°C/min). The change of polymer concentration in solution is monitored with an on-line infrared detector and plotted as a function of crystallization temperature to give the integral Crystaf profile. The amount of polymer that crystallizes at each temperature is determined by differentiating the integral Crystaf profile to give the derivative Crystaf profile at that temperature. More details of the data analysis procedures of Crystaf are given by Monrabal [5-6].

### 5.2.3 Temperature Rising Elution Fractionation (Tref)

Tref analysis was carried out using a CRYSTAF-TREF-V-LS apparatus manufactured by PolymerChar S.A. (Valencia, Spain). In the dissolution step, the polymer sample is dissolved in 1,2,4 Trichlorobenzene (TCB) in one of the Crystaf vessels at a concentration of 1 mg/mL at 160°C for one hour. The sample is then loaded into the Tref column packed with inert support and held at 95°C for 45 minutes for stabilization.

The polymer sample is crystallized and precipitated on the support inside the Tref column by slowly decreasing the temperature to 30°C at a constant cooling rate between 0.05 and 0.5°C/min. The column temperature is kept at 30°C for 45 minutes for stabilization before the elution step starts. In the elution step, solvent (TCB) flows through the column at a constant flow rate of 0.2 mL/min while the temperature in the

column is slowly increased to 100°C at a constant heating rate between 0.1 and 1°C/min. The concentration of polymer being eluted is measured with an infrared detector and plotted as a function of elution temperature to give the Tref profile. Additional information on Tref operation can be found in the literature [1-4].

## 5.3 CRYSTAF: RESULTS AND DISCUSSION

### 5.3.1 Effect of polymer concentration

It is well known that the crystallization temperature of a polymer solution depends on its concentration as indicated by Flory's equation [5] (see Section 2.4). During the crystallization period of Crystaf, the concentration of polymer in solution decreases as the molecules crystallize and precipitate from solution. It is generally believed, however, that this concentration change does not significantly affect Crystaf results.

In order to ensure that results from Crystaf analyses were not affected by changes in polymer concentration, a series of experiments was carried out at a cooling rate of 0.1°C/min with solutions having concentrations varying from 0.2 to 1.0 mg/ml (Figure 5.1). An experiment with a concentration lower than 0.2 mg/ml is not possible, as the signal-to-noise ratio of the on-line infrared detector is too low to obtain a reliable Crystaf profile. A very slight shift of the crystallization peak temperature can be observed only for an initial polymer concentration of 0.2 mg/ml, but this difference is well within the experimental error of Crystaf.

During Crystaf analysis, the concentration decreases from the initial polymer concentration to the concentration of polymer that is still soluble at the end of the analysis. From Figure 5.1, the independence of Crystaf profiles on polymer concentration implies that this effect is not of major significance.

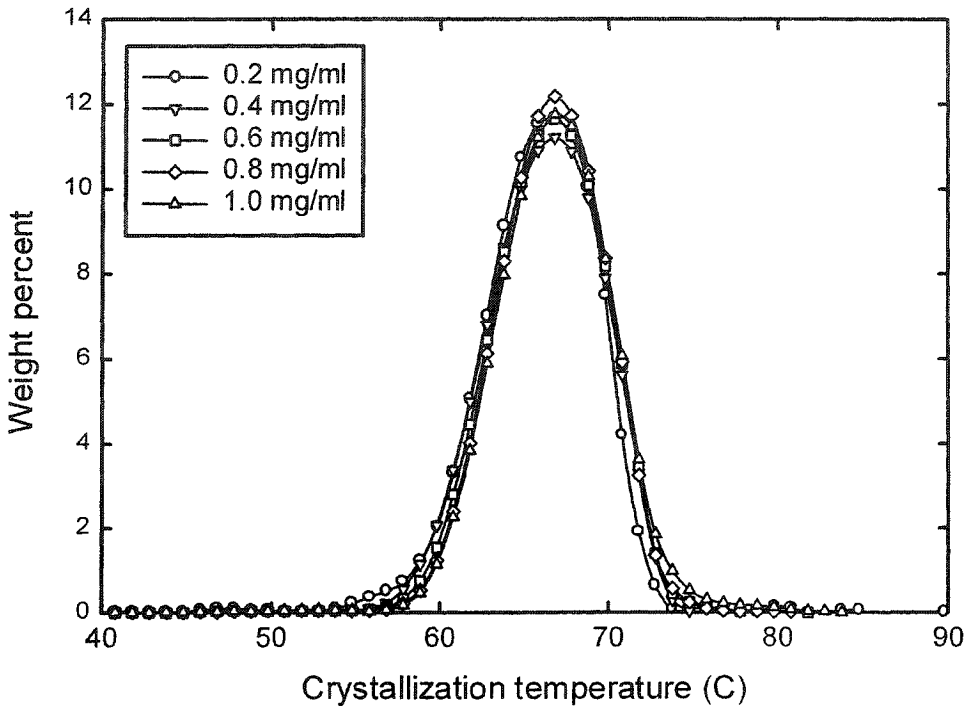


Figure 5.1 Effect of polymer concentration on Crystaf profile (sample D)

### 5.3.2 Temperature lag during the analysis

In routine Crystaf analysis, the oven temperature is taken to be the crystallization temperature. As the present study involved much faster cooling rates, the actual temperature inside the crystallization vessel had to be determined as a function of the cooling rate to avoid errors arising from the temperature lag of the system.

A series of experiments were carried out to measure the temperature lag between the oven and the five crystallization vessels in the Crystaf apparatus. A preliminary set of experiments indicated that temperature differences among the five crystallization vessels were negligible, and one vessel was therefore selected at random for this study.

To avoid crystallization of polymer on the thermocouples, pure solvent was used. (The change of heat capacity of the solvent due to polymer is negligible, since the solutions used in Crystaf are very dilute.) Other than the absence of polymer and the location of temperature measurement, the experiments were carried out at the same conditions as normal Crystaf analysis. Figure 5.2 shows how the temperature lag varies as a function of temperature for various cooling rates.

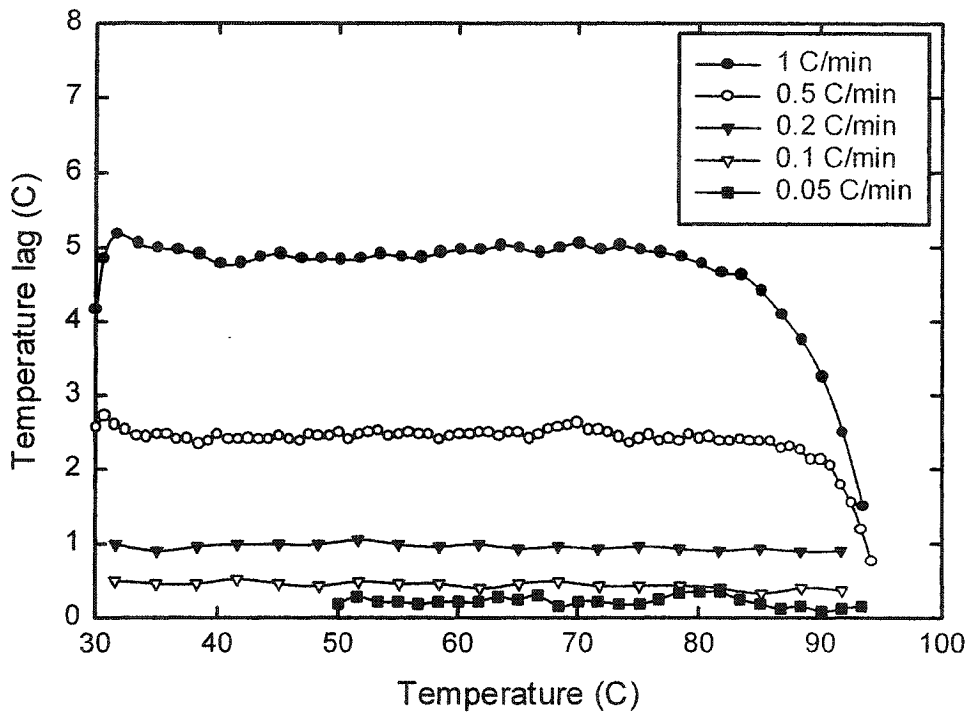


Figure 5.2 Lag between oven temperature and temperature inside a crystallization vessel at various cooling rates

Since all our polymer samples crystallize below 85°C, the transient regime in Figure 5.2 was discarded, and the average temperature lag in the steady state regime was used to correct the Crystaf profiles. Figure 5.3 shows the average temperature lag as a function of cooling rate, which can be expressed by the simple linear relationship,

$$T_{lag} = 5.02 \times (CR) - 0.05 \qquad (5.1)$$

where $T_{lag}$ is an average temperature lag in °C and $CR$ is the cooling rate in °C/min. It is important to note that this relationship may be system-dependent, *e.g.* it likely varies from one Crystaf unit to another.

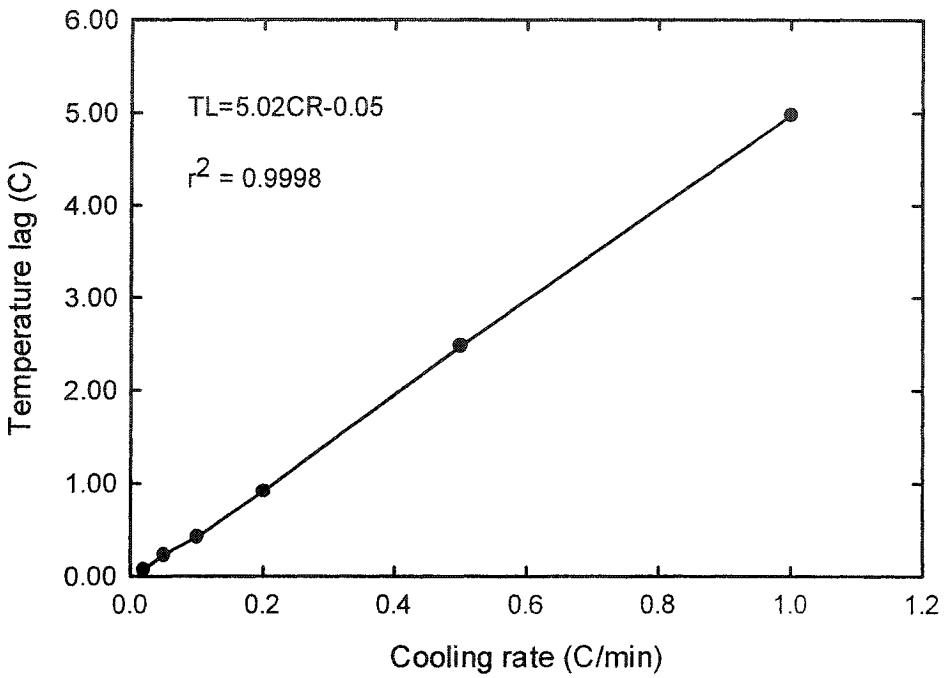


Figure 5.3 Average temperature lag as a function of cooling rate

### 5.3.3 Effect of cooling rate on Crystaf profiles

Figures 5.4 and 5.5 show the effect of cooling rate on the integral and derivative Crystaf profiles, respectively. These profiles were corrected to account for the temperature lag in the system, and the observed differences are thus related solely to crystallization kinetic effects.

A slow cooling rate permits the polymer molecules to crystallize at higher temperatures. This results in a shift of the Crystaf profiles to higher temperatures for slower cooling rates as shown in Figures 5.4 and 5.5. It is interesting to note that the cooling rate of 0.1°C/min that is commonly used is in fact very far from equilibrium. This is contrary to the generally held belief that the fractionation process in Crystaf occurs close to thermodynamic equilibrium [14-16].

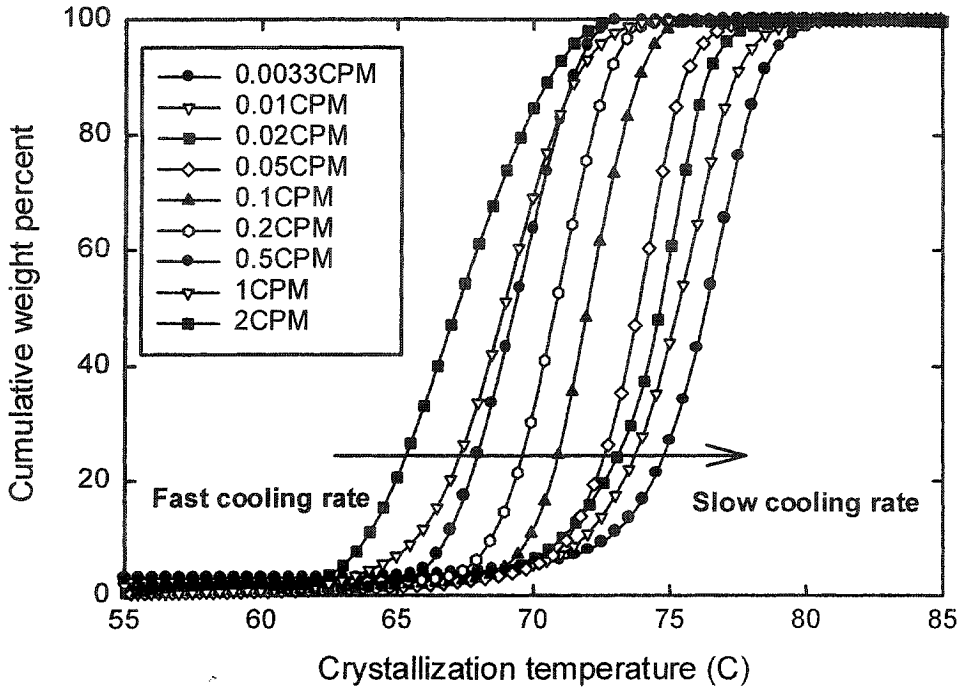


Figure 5.4 Integral Crystaf curves for sample B at various cooling rates.

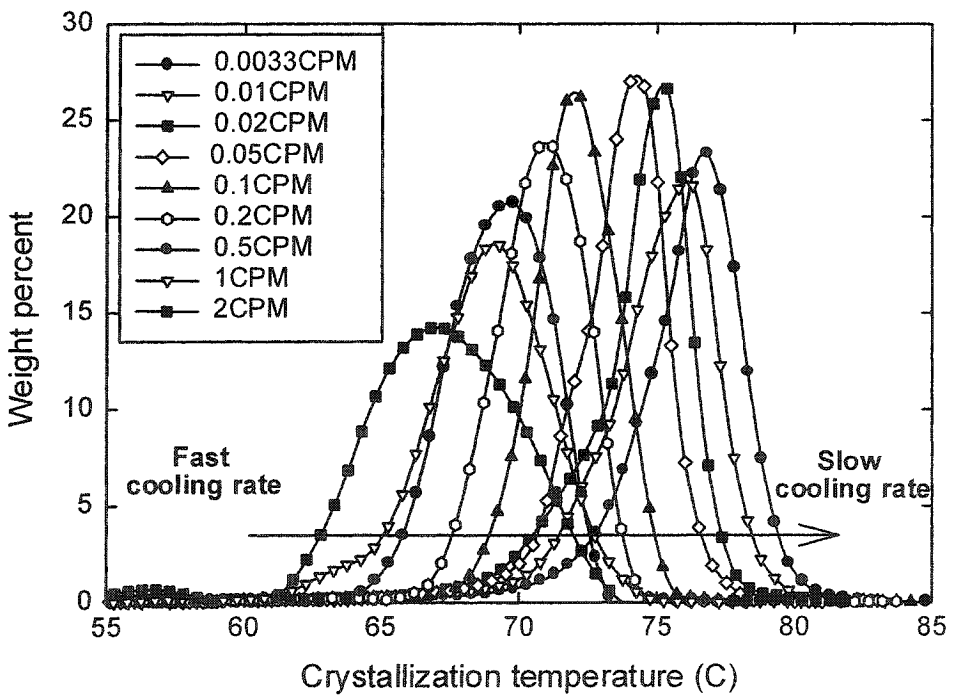


Figure 5.5 Derivative Crystaf curves for sample B at various cooling rates

Experiments were also carried out to determine whether there was a change of molecular weight distribution (MWD) during Crystaf analysis due to polymer degradation. This is particularly important when the slowest cooling rates were used, as these involved analysis times of up to 2 weeks. Figure 5.6 compares the MWD (measured by high temperature gel permeation chromatography) of polymers before and after Crystaf analysis at a cooling rate of 0.01°C/min. It is clear that the MWD varies with analysis time, indicating that the polymer has likely degraded and/or formed cross-links during the Crystaf analysis. This might also explain the change of shape of Crystaf profiles when a very slow cooling rate is used.

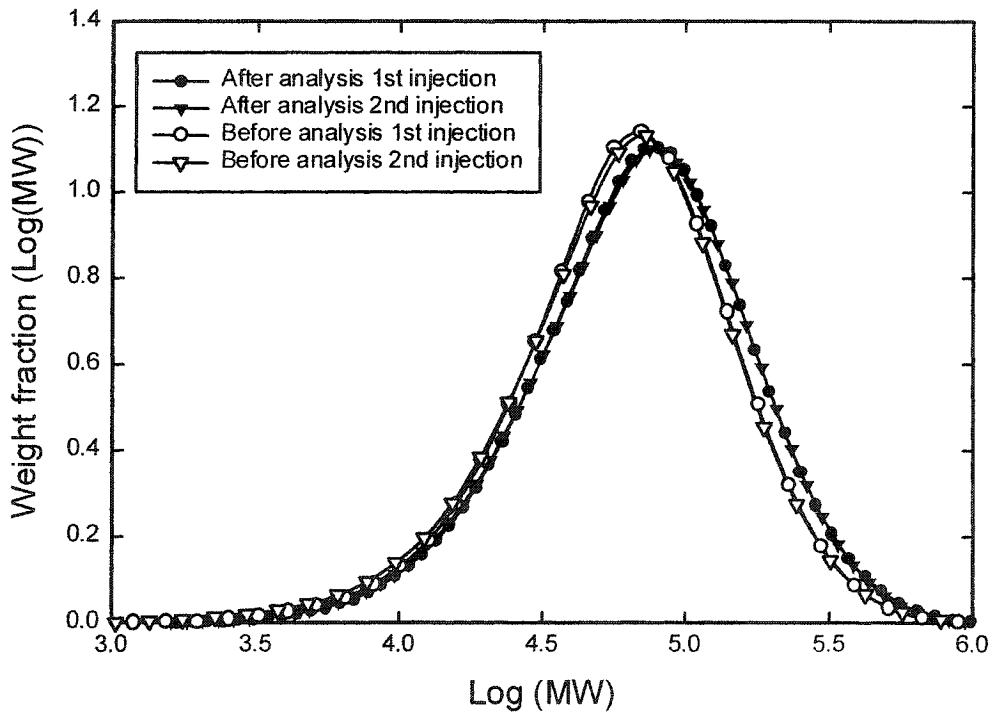


Figure 5.6 Comparison of molecular weight distribution before and after Crystaf analysis (cooling rate = 0.01°C/min)

The position of the Crystaf peaks is plotted as a function of cooling rate for several samples in Figure 5.7. An empirical linear relationship exists between the Crystaf peak temperature ($T_P$) and the natural logarithmic of the cooling rate ($CR$):

$$T_P = a \times ln(CR) + b \tag{5.2}$$

The parameters of this empirical relation depend on the average comonomer content of the sample. Values of these parameters are given in Figure 5.7.

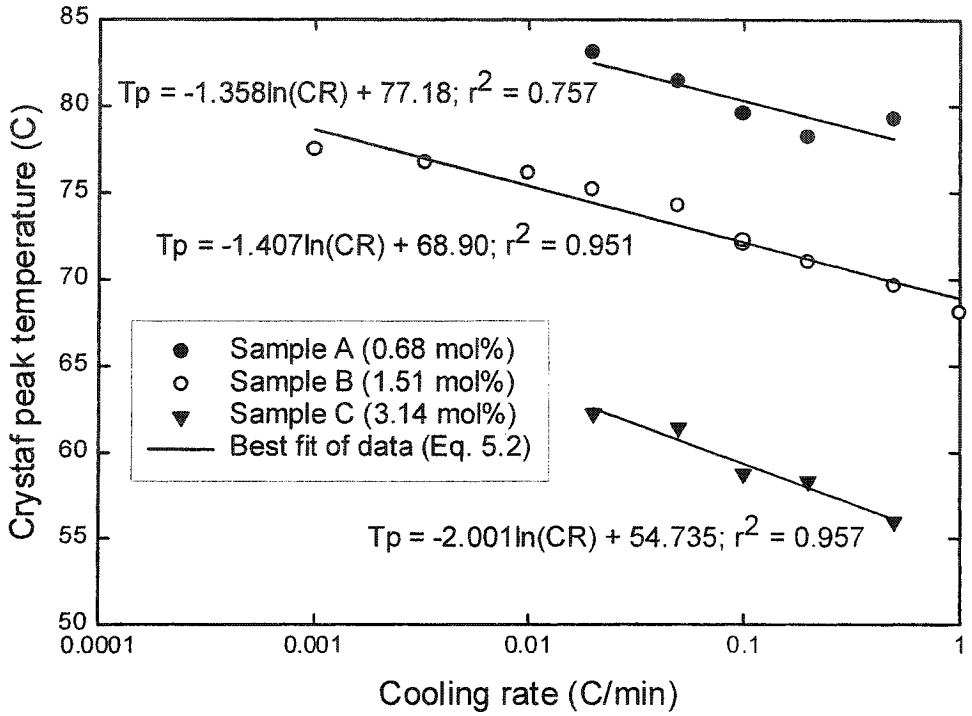


Figure 5.7 Crystaf peak temperatures as a function of cooling rate

The average comonomer content of polymer samples is usually estimated from the results of Crystaf by use of a linear calibration curve relating comonomer content to peak temperature [7, 17-19]. Clearly, Crystaf calibration curves also depend on the cooling rate used during the analysis.

Using the experimental data of the present study together with the results from Sarzotti *et al.* [20-21], a generalized calibration curve for ethylene/1-hexene copolymers was constructed as shown in Figure 5.8 and is described by in Equation (5.3),

$$CC = 10.0 - 0.1216 \times T_P - 0.1653 \times ln(CR) \qquad (5.3)$$

where $CC$ is the average comonomer content in mol percent, $T_P$ is the Crystaf peak temperature in °C, and $CR$ is the cooling rate in °C/min. This equation provides a

better approximation of average comonomer content when a calibration curve for the cooling rate used is not available.

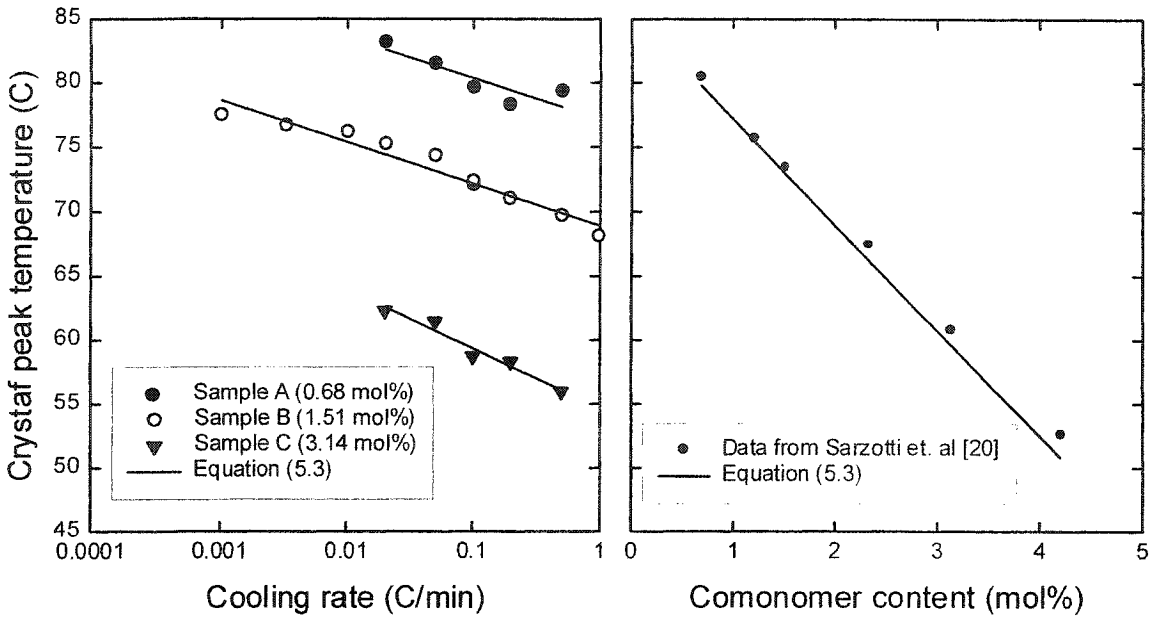


Figure 5.8 Validation of the generalized calibration curve equation (5-3) for ethylene/1-hexene copolymers

### 5.3.4 Effect of cocrystallization on Crystaf profiles

Two blends of ethylene/1-hexene samples were used to investigate the effect of cocrystallization on Crystaf profiles. Since the molecular weight of the individual samples was similar, the effect of comonomer content on cocrystallization could be studied without the complication of the additional effects of molecular weight differences.

Cocrystallization was investigated by comparing the experimental Crystaf profiles of the blends with their estimated Crystaf profiles, assuming a total absence of cocrystallization. The Crystaf profiles of the blends in the absence of cocrystallization were estimated by summing the Crystaf profiles of the parent samples, each measured alone, multiplied by their weight fractions in the blend. Comparisons of calculated and experimental Crystaf profiles of each blend for various cooling rates are shown in Figures 5.9 and 5.10.

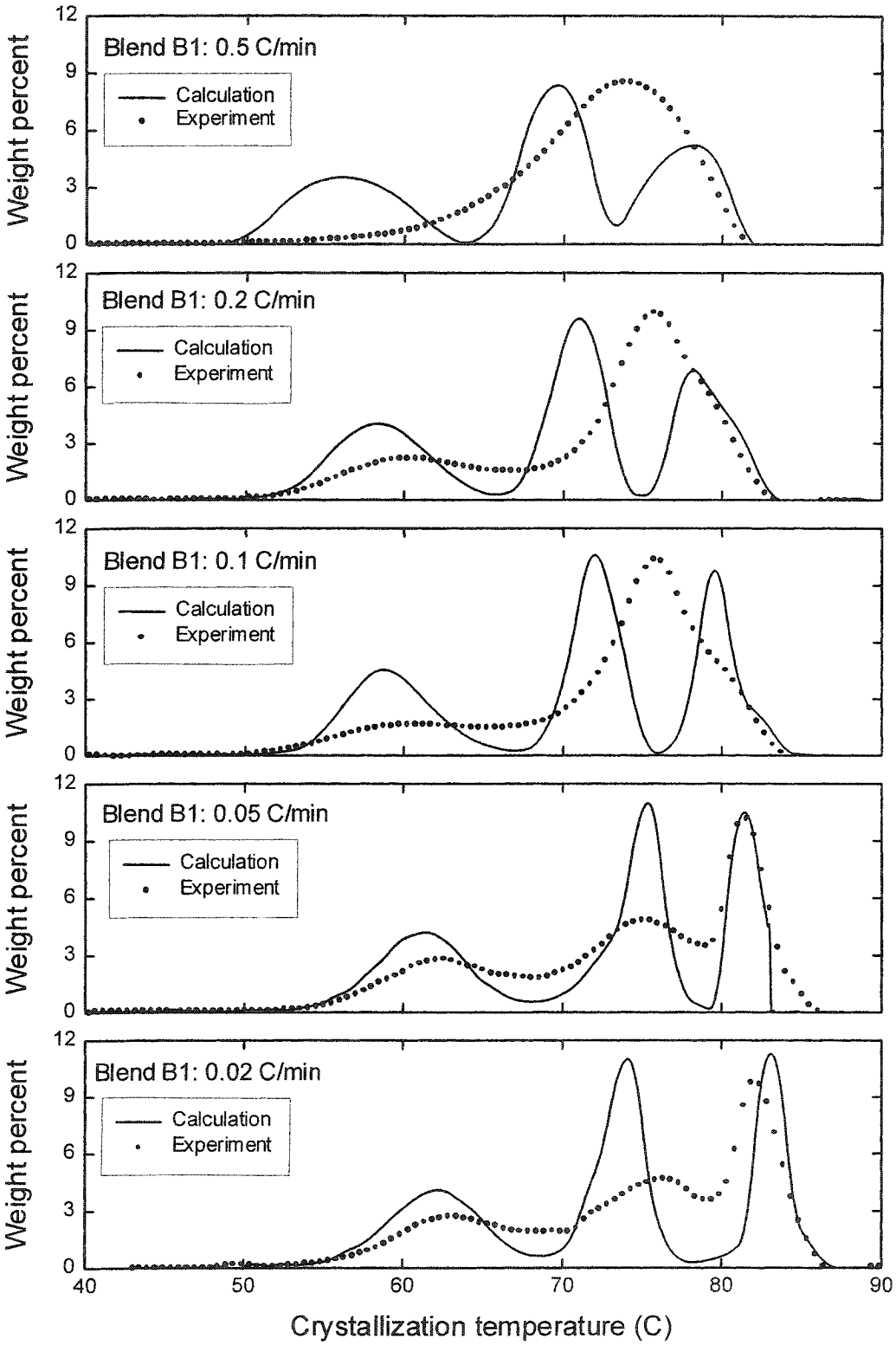


Figure 5.9 Comparisons of calculated and experimental Crystaf profiles for blend B1 at various cooling rates

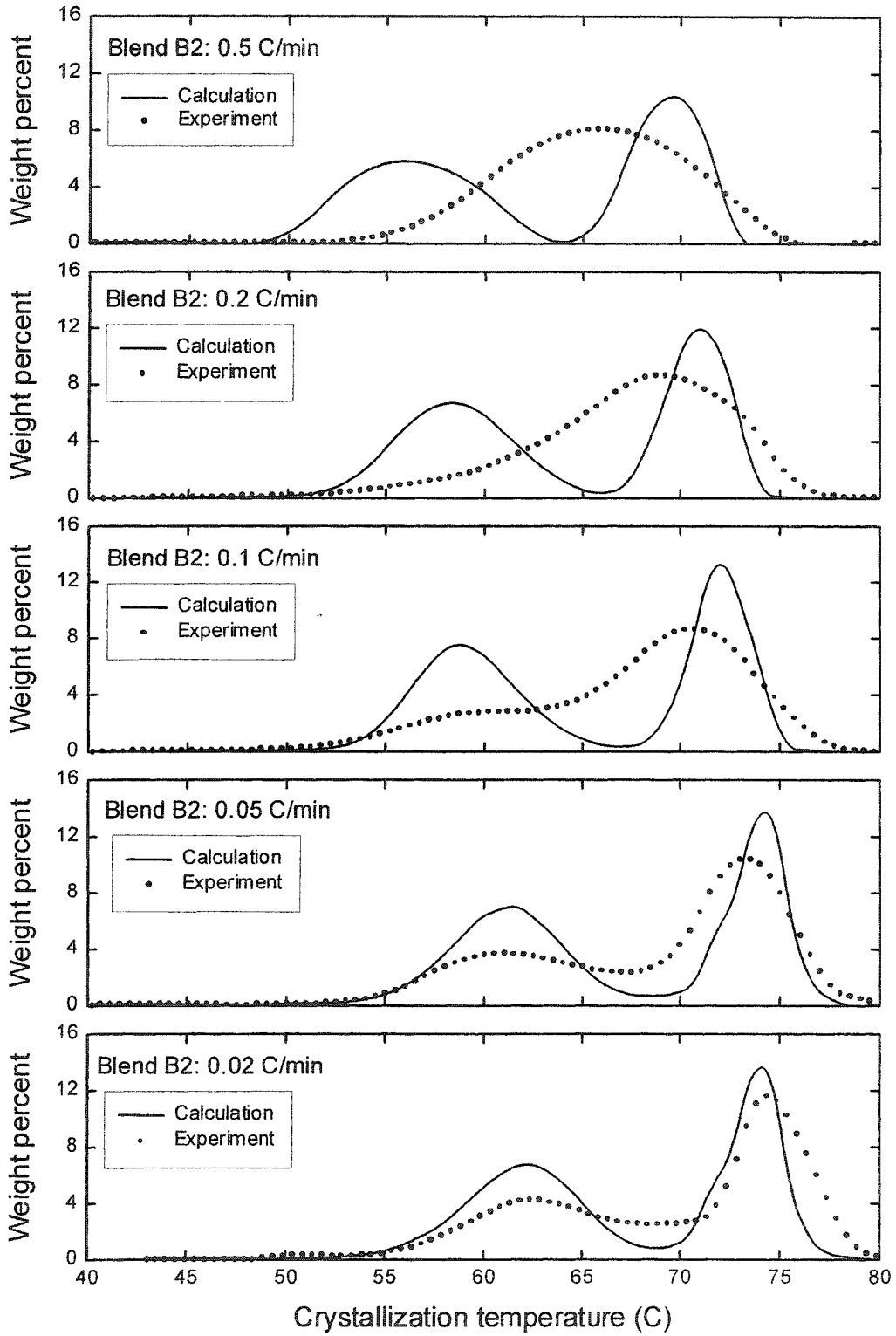


Figure 5.10 Comparisons of calculated and experimental Crystaf profiles for blend B2 at various cooling rates

The results were surprising. Figure 5.9 clearly indicates that cocrystallization has an important effect on Crystaf, especially when fast cooling rates are used. At a cooling rate of 0.5°C/min the cocrystallization effect is so strong that a unimodal peak is generated, which is in sharp contrast to the expected Crystaf profile. When slower cooling rates of 0.2 and 0.1°C/min were used, bimodal distributions with a shoulder at high crystallization temperatures were produced. Trimodal Crystaf profiles were obtained only at cooling rates of 0.05 and 0.02°C/min.

Figure 5.10 shows the results of a similar study for blend B2. In this case, bimodal profiles were detected at a cooling rate of 0.1°C/min. Better peak resolution was observed, as expected, at the lower cooling rates of 0.05 and 0.02°C/min.

In general, cocrystallization during Crystaf decreases with decreasing cooling rate. Nonetheless, some cocrystallization is still present even at a cooling rate of 0.02°C/min. It is also important to note that a cooling rate of 0.1°C/min, which is normally used in Crystaf, is not adequate for fractionating blends of polyolefins that have similar crystallization temperatures.

The implications of this result for the analysis of polyolefins made using multiple-site catalysts are significant. It is believed that a polymer synthesized using Ziegler-Natta catalysts contains a mixture of chains produced at different catalyst sites. These samples generally have very broad distributions of molecular weight and chemical composition. If one views a sample synthesized using Ziegler-Natta catalysts as a complex blend of various polymer populations, it is clear that the typically used cooling rate of 0.1°C/min will not give adequate resolution of the several components of the sample. In order to measure CCD more accurately understand the nature of these catalysts, a more time consuming Crystaf analysis at a very slow cooling rate is unavoidable.

## 5.4 TREF: RESULTS AND DISCUSSION

### 5.4.1 Effect of polymer concentration on Tref profiles

To ensure that Tref analysis is independent of polymer concentration, a set of experiments were carried out using sample D at concentrations ranging from 1 to 4 mg/ml. The analyses were carried out using a cooling rate of 0.2°C/min, a heating rate of 1°C/min, and a solvent flow rate of 0.5 ml/min. The results are shown in Figure 5.11.

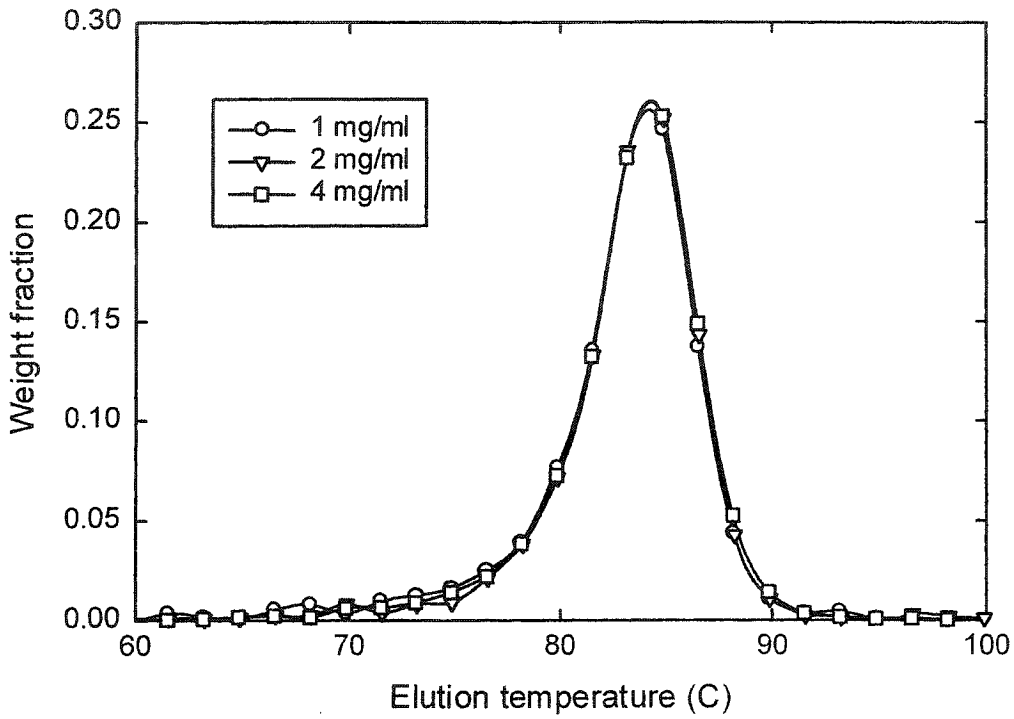


Figure 5.11 Effect of polymer concentration on Tref profile (sample D)

The results indicate that the Tref profile is independent of polymer concentration within the range investigated in this study. It should be noted that although Tref profiles are independent of polymer concentration, a low polymer concentration reduces the detector signal-to-noise ratio and lead to a loss of precision.

### 5.4.2 Effect of cooling rate on Tref profiles

Figure 5.12 shows the effect of cooling rate during the crystallization step on Tref. The heating rate and solvent flow rate were fixed at 0.2°C/min and 0.2 ml/min,

respectively. Tref profiles become broader when the cooling rate is lowered. This might be due to the fact that slow cooling rates provide more time for polymer molecules to rearrange and crystallize close to their equilibrium crystallization temperature.

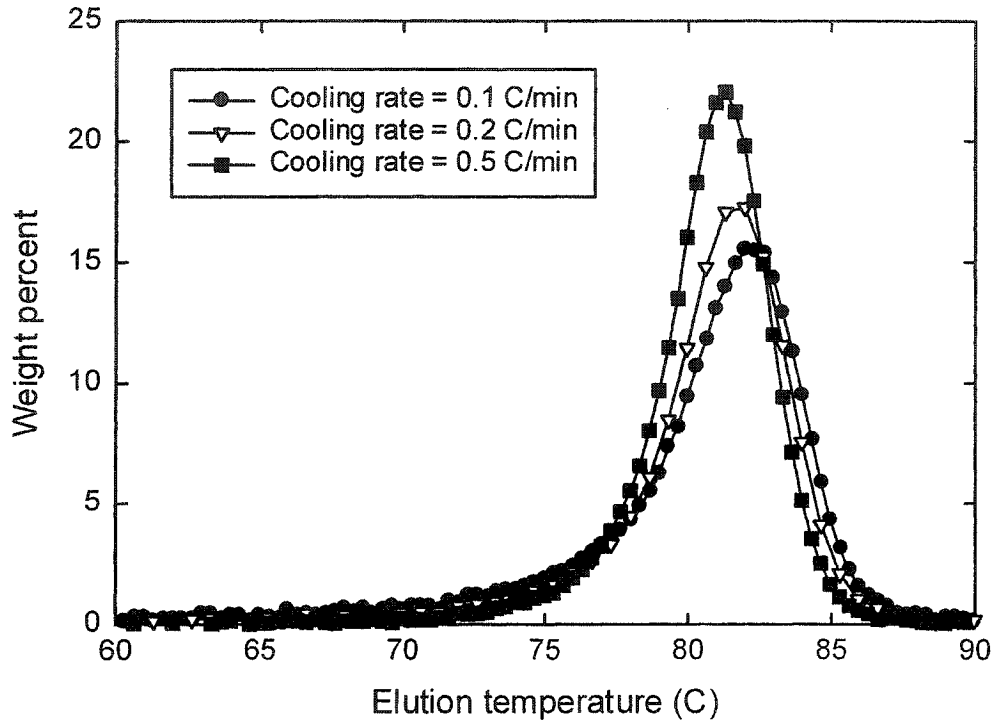


Figure 5.12 Effect of cooling rate on Tref profiles (sample D)

As opposed to Crystaf, the location of Tref peaks is not a strong function of cooling rate (compare, for instance, Figures 5.5 and 5.12). It might be speculated that the support present in the Tref column provides nucleating centers during the crystallization step, making this technique less sensitive to cooling rate than Crystaf. In Crystaf, there is no inert support, and the crystallization therefore begins with a nucleation process that depends on the crystallization temperature.

Another possible reason for these differences between Crystaf and Tref is that after the crystallization step in Tref, the column is normally held at a constant temperature (stabilization period) for about one hour, followed by the elution step when the temperature is increased slowly. During this period, chain re-crystallization may occur with the formation of larger, better-formed crystallites. Therefore, the

elution step in Tref "reinforces" the fractionation that took place in the crystallization step and may lead to a more robust fractionation process, at the cost of a longer analysis time.

### 5.4.3 Effect of solvent flow rate on Tref profiles

The effect of the solvent flow rate used during the Tref elution step is shown in Figure 5.13. A cooling rate of 0.2°C/min and a heating rate of 0.2°C/min were used for this set of experiments.

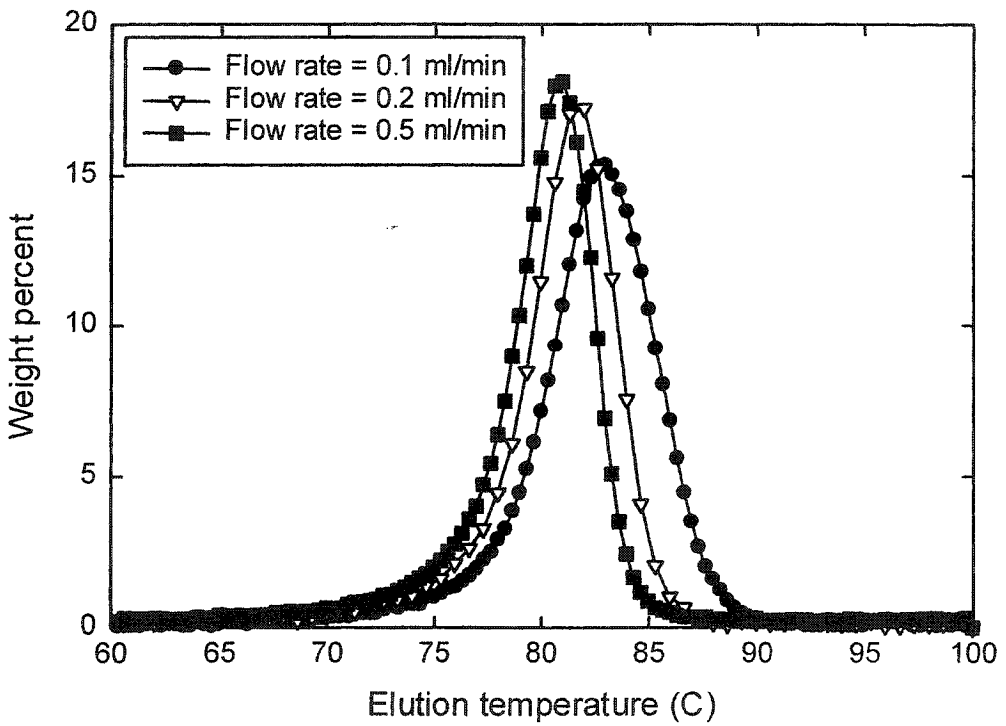


Figure 5.13 Effect of solvent flow rate on Tref profile (sample D)

Tref profiles become broader at lower solvent flow rates. This might be due to axial dispersion in the Tref column. Perhaps more importantly, solvent residence time in the column increases at lower flow rates, and broader ranges of polymer molecules are consequently eluted per pass of solvent at lower flow rates. Tref peak temperatures increase with decreasing flow rates, which is probably also related to the

solvent residence time in the column: high residence times in the column imply that the polymer solution will reach the detector at later times (or at higher temperatures).

Although the solvent flow rate can affect Tref peak temperature and shape, one does not normally have much freedom in selecting this parameter. A higher solvent flow rate reduces axial dispersion in the column but also reduces the signal to noise ratio. One should try to keep the ratio between heating rate and solvent flow rate constant so that each fraction will contain polymer molecules eluted over the same temperature range. For instance, consider the situation when solvent flow rates are 0.1 and 0.2 ml/min and the ratio of heating rate to solvent flow rate is 1. Assuming that the volume of the Tref column is 2.0 ml, the solvent will have different residence times in the column; 20 and 10 minutes, respectively. However, in both cases the solvent will elute polymer over the same temperature range of 2°C before it flows out of the column. Therefore, the signal to noise ratio can be kept the same, even though the flow rate has changed.

The above strategy was tested by doing a series of Tref analyses of sample B with constant ratios of cooling rate (CR): heating rate (HR): solvent flow rate (FR) =1:1:1. Figure 5.14 shows Tref profiles for several rates (with constant ratios) indicating that the proposed concept is valid, as is easily seen by comparison of Figures 5.13 and 5.14.

### 5.4.4 Effect of heating rate on Tref profiles

The effect of heating rate during the elution step on Tref profiles is shown in Figure 5.15. For this set of experiments, a cooling rate of 0.2°C/min and a solvent flow rate of 0.2 ml/min were used.

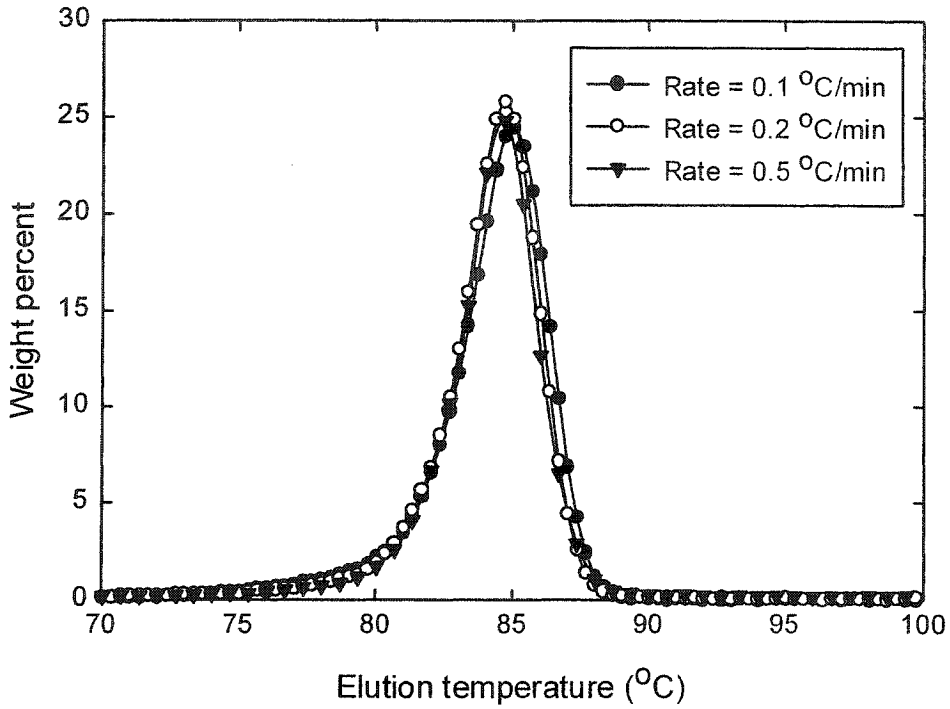


Figure 5.14 Comparison of Tref profiles for sample B when the ratios of cooling rate (CR): heating rate (HR): solvent flow rate (FR) are 1:1:1.

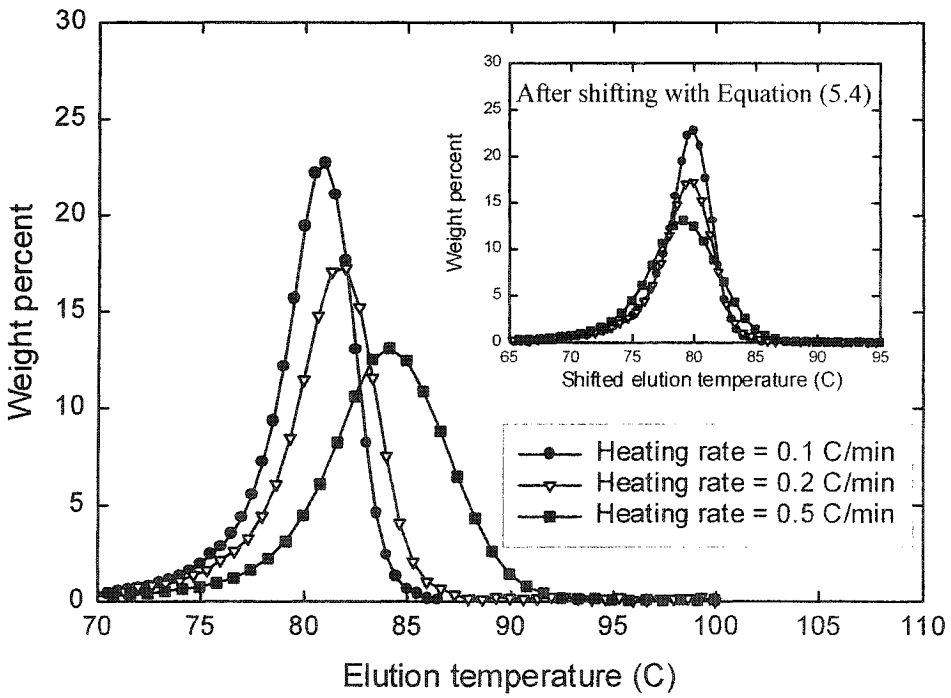


Figure 5.15 Effect of heating rate on Tref profiles (sample D)

Tref profiles become broader as the heating rate increases, likely because at the same solvent flow rate, solvent will elute polymer over a wider range of crystallinities when high heating rates are used. For example, consider the heating rates of 0.1 and 1°C/min. The solvent residence in the column is 10 minutes, assuming a column volume of 2 ml. Over this period of time, solvent will elute polymer in the temperature range of 1°C for a heating rate of 0.1°C/min, while it will elute polymer in the temperature range of 10°C at a heating rate of 1°C/min.

Figure 5.15 also shows that the Tref peak location shifts to higher temperatures with increasing heating rate, because the elution temperature recorded by the time solvent has reached the end of column is higher when higher heating rates are used. To explain this, consider heating rates of 0.1 and 1°C/min. Assuming that the solvent enters the column at 75°C, by the time the solvent reaches the end of the column the elution temperature will be recorded as 76°C for the case of a heating rate of 0.1°C/min, while the elution temperature will be recorded as 85°C for a heating rate of 1.0°C/min.

The Tref peak location can be corrected using the approach described above with the following equation:

$$T_{e,correct} = T_e - \frac{Column \quad volume}{Solvent \quad flow \quad rate} \times Heating \quad rate \tag{5.4}$$

As shown in Figure 5.15, the Tref profiles for different heating rates shifted using Equation (5.4) have about the same peak temperature. Evidently, profiles measured at higher heating rates are broader due to the faster dissolution of the polymer chains.

### 5.4.5 Effect of cocrystallization on Tref profiles

The effect of cocrystallization on Tref profiles were investigated using the blends described in Table 5.1. Tref analysis of each parent sample present in the blends was carried out at various cooling rates in order to calculate Tref profiles for the blends in the case of no cocrystallization.

Comparisons of calculated and experimental Tref profiles of blend B1 at various cooling rates are shown in Figure 5.16. Significant cocrystallization is evident, especially at fast cooling rates. As in the case of Crystaf analysis, a better-resolved profile was obtained when slower cooling rates were used.

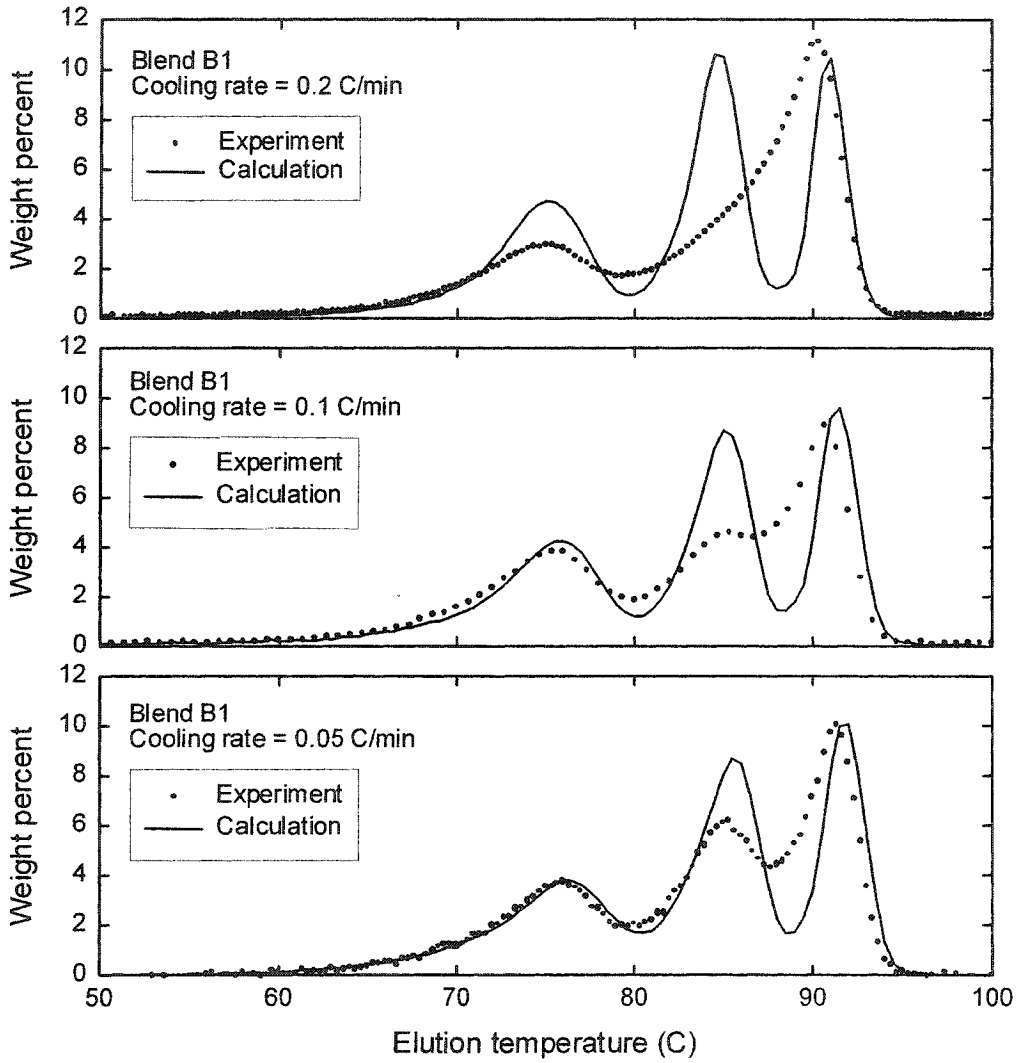


Figure 5.16 Comparisons between experimental and calculated Tref profiles for blend B1 at various cooling rates

At a cooling rate of 0.2°C/min, the Tref profile is bimodal with strong cocrystallization for the two parent samples with low comonomer content. As the cooling rate is lowered to 0.1°C/min, the single peak at high temperature starts to

separate into two peaks. At the cooling rate of 0.05°C/min, the Tref profile is clearly trimodal with each peak corresponding that of the parent sample.

Unlike Crystaf, where the peak location of the blend components shifts significantly with cooling rate (Figure 5.9 and 5.10), the locations of Tref peaks are relatively insensitive to cooling rate (Figure 5.16).

## 5.5 COMPARISON BETWEEN CRYSTAF AND TREF ANALYSIS

Figure 5.17 compares the results of Crystaf and Tref of blends B1 and B2 at the same cooling rate. It is obvious that Tref provides better resolution of the blend components than Crystaf when the same cooling rate is used.

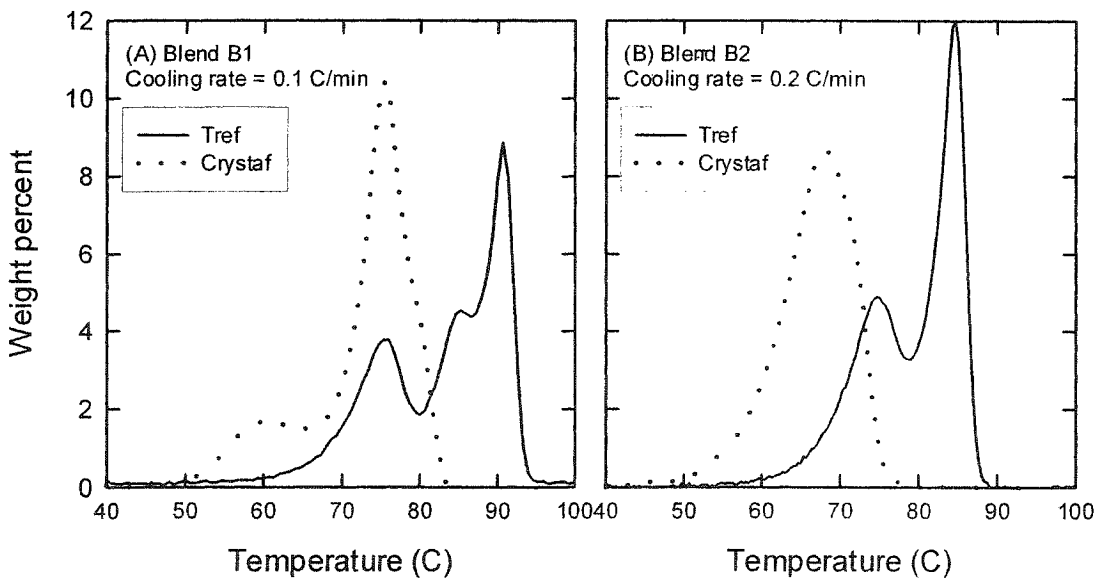


Figure 5.17. Comparison of Crystaf and Tref profiles at the same cooling rate

It is clear that copolymers that have complex CCD, *e.g.* copolymers synthesized with multiple-site-type catalyst, will require slow cooling rates in both Crystaf and Tref. For this type of copolymer, the time required by the elution step of Tref is generally not very long compared to that needed for the crystallization step, but it is important to allow sufficient time for the elution step, since this leads to

better peak resolution (Figure 5.15). In order to obtain results comparable to Tref, Crystaf has to be carried out at lower cooling rates, thus lengthening the analysis time. In fact, for low cooling rates, this additional time in Crystaf may exceed the time required in the elution step of Tref. Table 5.2 shows the approximate time required for Crystaf and Tref analyses for various cooling and heating rates (heating rate applies to Tref only). Therefore, Tref may be a better choice for analyzing samples with complex CCD, if excellent peak resolution is required.

Table 5.2 Comparison of approximate Crystaf and Tref analysis times per run

| Cooling rate (°C/min) | Crystaf analysis time (min) | Tref analysis time for several heating rates | | |
|---|---|---|---|---|
| | | 0.5°C/min | 0.2°C/min | 0.1°C/min |
| 0.5 | 235 | 425 | 620 | 945 |
| 0.2 | 430 | 620 | 815 | 1140 |
| 0.1 | 755 | 945 | 1140 | 1465 |
| 0.05 | 1405 | 1595 | 1790 | 2115 |
| 0.02 | 3355 | 3545 | 3740 | 4065 |
| 0.01 | 6605 | 6795 | 6990 | 7315 |

When the CCD is unimodal and narrow, relatively faster cooling rates can be used to estimate average comonomer content. The Crystaf profiles for single-site ethylene/1-hexene copolymers over a wide range of cooling rates (Figure 5.5) show that no significant additional information is obtained with very slow cooling rates. For fast cooling rates, the time required for the elution step in Tref can be significant, and the time required for Tref analysis can therefore be considerably longer than the time required for Crystaf analysis (See Table 5.2). For most routine applications, Crystaf analysis with the usual cooling rate of 0.1°C/min is sufficient to estimate average comonomer contents and CCDs of copolymers with unimodal distributions.

Another advantage of Crystaf analysis is that it can be used to analyze up to 5 samples at the same time. One might argue that Tref can be used for analyzing more than one sample at a time as well, provided that several columns are used in parallel. Although this is true, a much more complicated experimental apparatus, involving

several solvent pumps, would be required, and there is thus no doubt that Crystaf is the best option for the parallel analysis of samples.

## 5.6 CLOSING REMARKS

The effects of cooling rate and cocrystallization on Crystaf and Tref were investigated using ethylene/α-olefin copolymers synthesized by single-site catalysts and their blends. It was shown that the typical cooling rates used with both techniques result in crystallization far from the thermodynamic equilibrium, and crystallization kinetics strongly influences the results obtained with Crystaf and Tref.

Strong cocrystallization takes place during the analysis of polyolefin blends, especially at high cooling rates, and impacts the way Crystaf and Tref profiles should be interpreted. In general, Tref is more useful for analyzing samples with complex CCDs, as it provides better peak resolution. However, Crystaf is better for most routine measurements due to its easy operation, relatively short analysis time, and the ability to analyze up to five samples simultaneously.

## REFERENCES


1. Soares J.B.P. and Hamielec A.E., "Temperature Rising Elution Fractionation of Linear Polyolefins", *Polymer*, **1995**, *36*, 1639.
2. Wild L., "Temperature Rising Elution Fractionation", *Advances in Polymer Science*, **1990**, *98*, 1.
3. Wild L. and Blatz C., "Development of High Performance Tref for Polyolefin Analysis", in: *New Advances in Polyolefins*, T.C. Chung, Eds, Plenum Press 1993, p. 147-157.
4. Soares J.B.P. and Hamielec A.E., "Temperature Rising Elution Fractionation", in: *Modern Techniques for Polymer Characterization*, R.A. Pethrick, J.V. Dawkins, Eds., John Wiley&Sons, 1999, p. 15-55.

5. Monrabal B., "Crystallization Analysis Fractionation: A New Technique for the Analysis of Branching Distribution in Polyolefins", *Journal of Applied Polymer Science,* **1994**, *52*, 491.
6. Monrabal B., "CRYSTAF: Crystallization Analysis Fractionation. A New Approach to the Composition Analysis of Semicrystalline Polymers", *Macromolecular Symposia,* **1996**, *110*, 81.
7. Monrabal B., Blanco J., Nieto J. and Soares J.B.P, "Characterization of Homogeneous Ethylene/1-Octene Copolymers Made with a Single-Site Catalyst. CRYSTAF Analysis and Calibration", *Journal of Polymer Science: Part A: Polymer Chemistry*, **1999**, *37*, 89.
8. Britto L.J.D., Soares J.B.P., Penlidis A. and Monrabal B., "Polyolefin Analysis by Single-Step Crystallization Fractionation", *Journal of Polymer Science: Part B: Polymer Physics*, **1999**, *37*, 539.
9. Kim M.-H. and Phillips P.J., "Nonisothermal Melting and Crystallization Studies of Homogeneous Ethylene/1-Olefin Random Copolymers", *Journal of Applied Polymer Science,* **1998**, *70*, 1893.
10. Wasiak A., Sajkiewicz P. and Wozniak A., "Effects of Cooling Rate on Crystallinity of i-Polypropylene and Polyethylene Terephthalate Crystallized in Nonisothermal Conditions", *Journal of Polymer Science: Part B: Polymer Physics*, **1999**, *37*, 2821.
11. Chiu F-C., Fu Q., Peng Y., Shih H-H., "Crystallization Kinetics and Melting Behavior of Metallocene Short-Chain Branched Polyethylene Fractions", *Journal of Polymer Science: Part B: Polymer Physics,* **2002**, *40*, 325.
12. Galante M.J., Mandelkern L. and Alamo R.G., "The Crystallization of Blends of Different Types of Polyethylene: The Role of Crystallization Conditions", *Polymer*, **1998**, *39*, 5105.
13. Rana S.K., "Effect of Cocrystallization on Kinetic Parameters of High-Density Polyethylene/Linear Low-Density Polyethylene Blend", *Journal of Applied Polymer Science*, **1996**, *61*, 951.
14. Beigzadeh D., Soares J.B.P. and Duever T.A., "Modeling of Fractionation in CRYSTAF Using Monte Carlo Simulation of Crystallizable Sequence

Lengths: Ethylene/1-Octene Copolymers Synthesized with Single-Site-Type Catalysts", *Journal of Applied Polymer Science*, **2001**, *80*, 2200.

15. Beigzadeh D., "Long Chain Branching in Ethylene Polymerization Using Combined Metallocene Catalyst Systems", *PhD thesis*, University of Waterloo, Canada, 2000.
16. Costeux S., Anantawaraskul S., Wood-Adams P.M. and Soares J.B.P., "Distribution of the Longest Ethylene Sequence in Ethylene/1-Olefin Copolymers Synthesized with Single-Site-Type Catalysts", *Macromolecular Theory and Simulation*, **2002**, *11*, 326.
17. Faldi A. and Soares J.B.P., "Characterization of the Combined Molecular Weight and Composition Distribution of Industrial Ethylene/1-Olefin Copolymers", *Polymer*, **2001**, *42*, 3057.
18. Brull R., Pasch H., Ruaubenheimer H.G., Sanderson R., van Reenen A.J. and Wahner U.M., "Investigation of the Melting and Crystallization Behavior of Random Propane/1-Olefin Copolymers by DSC and CRYSTAF", *Macromolecular Chemistry and Physics*, **2001**, *202*, 1281.
19. Graef S.M., Brull R., Pasch H. and Wahner U.M., "Monitoring the Chemical Heterogeneity of Metallocene-Catalysed Copolymers of Ethylene and Higher 1-Olefins using CRYSTAF and SEC-FTIR", *e-Polymers*, **2003**, no 005.
20. Sarzotti D.M., Soares J.B.P. and Penlidis A., "Ethylene/1-Hexene Copolymers Synthesized with a Single-Site Catalyst: Crystallization Analysis Fractionation, Modeling, and Reactivity Ratio Estimation", *Journal of Polymer Science: Part B: Polymer Physics*, **2002**, *40*, 2595.
21. Sarzotti D.M., "Heterogeneous Metallocene Catalysts for Olefin Polymerization: Effects of Support Material on Microstructure", *Master Thesis*, University of Waterloo, Canada, 2001.

CHAPTER 6

# COCRYSTALLIZATION PHENOMENA IN CRYSTAF

*The researches of many commentators have already thrown*
*much darkness on this subject, and it is probable that,*
*if they continue, we shall soon know nothing about it at all.*
***Mark Twain***

As shown in the last chapter, cocrystallization may happen during Crystaf analysis, affecting Crystaf profiles and interfering with the interpretation of the CCD. This chapter investigates this phenomenon in more detail and establishes the main factors causing cocrystallization by analyzing a series of ethylene/α-olefin copolymers. Three factors are considered: (1) comonomer type, (2) cooling rate, and (3) similarity of chain crystallizability.

## 6.1 INTRODUCTION

The properties of copolymers are influenced not only by their average comonomer content, but also by their chemical composition distribution (CCD) [1-4]. The relationship between the CCD of ethylene/α-olefin copolymers and their mechanical and thermal properties is not yet clearly established for polyolefins.

In order to develop structure-property relationships for copolymers, one needs an analytical technique that can accurately determine the CCD. In the case of semi-crystalline copolymers, two analytical techniques are used: temperature rising elution fractionation (Tref) [5-8], and crystallization analysis fractionation (Crystaf) [9-12].

Both techniques fractionate polymer chains according to their crystallizabilities via crystallization from dilute solution. Details of the operations of both techniques have been discussed extensively in the literature [5-12]. Although both techniques produce very similar results, Tref is more complex and time-consuming than Crystaf.

To use any characterization technique quantitatively, it is important to know the key factors that can affect its results, and it is crucial to know what factors might lead to the misinterpretation of analytical data. Although the possibility of cocrystallization during Crystaf analysis has been considered before by many researchers [9-10, 13-14], it was not found to be a significant factor, because previous studies involved only blends of different polymers (PP/HDPE/LDPE blends) or blends of polymers having very distinct crystallizabilities.

In the last chapter, Crystaf was used to analyze blends of ethylene/1-hexene copolymers having similar crystallizabilities. Surprisingly, very strong cocrystallization effects were found. In fact, for some operating conditions this effect was so strong that the Crystaf profiles were altered from the true multimodal or bimodal distributions to apparent unimodal distributions. Therefore, it is critical to understand cocrystallization in order to avoid it when blend resolution is an issue.

In this chapter, the key factors leading to cocrystallization during the Crystaf analysis of ethylene/α-olefin blends are investigated. Both operation parameters and microstructural properties of the blends can cause cocrystallization. The three factors considered were: (1) the comonomer type in the ethylene/α-olefin copolymer blends, (2) the similarity of the chain crystallizabilities of the parent samples in the blend, and (3) the cooling rate used in the analysis.

## 6.2 EXPERIMENTAL

### 6.2.1 Materials

All the ethylene/α-olefin copolymers were synthesized in semi-batch mode using a 300 ml Parr autoclave reactor. Four comonomers were used: propylene, 1-hexene, 1-octene, and 1-dodecene. The polymerizations were performed at 60°C and 100 psi (6.8 atm) ethylene partial pressure. Approximately 0.25 μmol of Zr in form of rac-

ethylene bis(indenyl)zirconium dichloride (rac-Et(Ind)$_2$ZrCl$_2$) was used in each reaction with methylaluminoxane (MAO) at an Al/Zr ratio of 2,000. More details on the polymerization process used have been given by previous researchers [15].

As all samples were synthesized using a single-site catalyst, narrow and unimodal CCDs were expected. In order to eliminate the effect of molecular weight, all samples were produced with similar number average molecular weights ($M_N$ same within ±10 %). The properties of these samples are summarized in Table 6.1. The last letter in the sample identification code indicates the comonomer used: P for propylene, H for 1-hexene, O for 1-octene, and D for 1-dodecene.

Table 6.1 Average properties of ethylene/α-olefin copolymers used

| Sample | Comonomer type | Crystaf peak temp (0.1°C/min) | Number avg MW ($M_N$) | Weight avg MW ($M_W$) |
|---|---|---|---|---|
| PEP64 | Propylene | 78.3 | 39,700 | 143,600 |
| PEP384 | Propylene | 64.5 | 40,900 | 90,700 |
| PEP387 | Propylene | 71.6 | 35,400 | 91,600 |
| PEP637 | Propylene | 58.3 | 45,300 | 96,100 |
| PEH23c | 1-Hexene | 79.1 | 37,200 | 92,800 |
| PEH65c | 1-Hexene | 71.6 | 36,300 | 85,300 |
| PEH100d | 1-Hexene | 67.3 | 34,900 | 75,200 |
| PEH150e | 1-Hexene | 58.3 | 34,300 | 74,600 |
| PEH200a | 1-Hexene | 52.5 | 34,500 | 74,500 |
| PEO2 | 1-Octene | 79.8 | 34,600 | 83,400 |
| PEO3 | 1-Octene | 49.1 | 35,900 | 89,800 |
| PEO5 | 1-Octene | 69.3 | 35,900 | 100,000 |
| PED10c | 1-Dodecene | 82.8 | 35,500 | 90,900 |
| PED50 | 1-Dodecene | 77.9 | 36,100 | 80,100 |
| PED150b | 1-Dodecene | 71.4 | 36,500 | 83,000 |
| PED200 | 1-Dodecene | 61.0 | 36,400 | 82,100 |

Blends of the parent samples (50/50 weight %) were used to investigate cocrystallization during Crystaf analysis. Table 6.2 shows the compositions of the blends. The components of each blend may differ in comonomer type, but all have

similar crystallization temperatures. This allows us to compare blends having the same range of crystallization temperature and to focus on the role of comonomer in cocrystallization.

Table 6.2. Composition of ethylene/α-olefin copolymer blends

| Blend sample | 1st component (50% by weight) | 2nd component (50% by weight) | Difference between Crystaf peak temperatures ($\Delta T_C$) |
|---|---|---|---|
| BPEP1 | PEP64 | PEP384 | 13.8 |
| BPEP2 | PEP64 | PEP387 | 6.7 |
| BPEP3 | PEP64 | PEP637 | 20.0 |
| BPEH2 | PEH65c | PEH150e | 13.3 |
| BPEH4 | PEH23c | PEH100d | 11.8 |
| BPEH5 | PEH65c | PEH100d | 4.3 |
| BPEH6 | PEH65c | PEH200a | 19.1 |
| BPEO1 | PEO2 | PEO5 | 10.5 |
| BPED1 | PED10c | PED150b | 11.4 |
| BPED3 | PED10c | PED50 | 4.9 |
| BPED4 | PED10c | PED220 | 21.8 |
| BPEX1 | PEP64 | PEH100d | 11.0 |
| BPEX2 | PED10c | PEP387 | 11.2 |

### 6.2.2 Crystaf

Crystaf analysis was performed using a CRYSTAF model 200 manufactured by PolymerChar S.A. (Valencia, Spain). In the analysis, the polymer is dissolved in 1,2,4 trichlorobenzene (TCB) in a 60 ml stirred vessel at a concentration of 0.2 mg/ml. The polymer solution is held at 160°C for 60 min to ensure complete dissolution of the polymer sample. The temperature of the solution is then decreased to 95°C for 45 min for stabilization before starting the fractionation.

During the crystallization period, the temperature of the column is reduced to 30°C at a slow, constant cooling rate (0.1 – 0.5°C/min). The decrease in polymer concentration in solution with temperature is monitored using an in-line infrared

detector (cumulative profile). The amount of polymer crystallized at each temperature is obtained by numerical differentiation of the cumulative profile.

## 6.3 RESULTS AND DISCUSSION

Cocrystallization was investigated by comparing the experimental Crystaf profiles of the blends with their estimated Crystaf profiles, assuming a total absence of cocrystallization. The Crystaf profiles of the blends in the absence of cocrystallization were estimated by summing the Crystaf profiles of the parent samples, each measured alone, multiplied by their weight fractions in the blend. For a binary blend, this is:

$$\hat{\chi}(T_c) = w_1\chi_1(T_c) + (1 - w_1)\chi_2(T_c) \tag{6.1}$$

where $\hat{\chi}(T_c)$ is the estimated Crystaf profile for the blend (a function of crystallization temperature, $T_c$), $\chi_1(T_c)$ and $\chi_2(T_c)$ are the measured Crystaf profiles for the blend components, and $w_1$ is the weight fraction of component 1.

Deviations from the estimated profile indicate that cocrystallization is occurring during the analysis.

### 6.3.1 Effect of comonomer type

The role of comonomer type on the melting and crystallization of copolymer chains has been the subject of many investigations over several decades [16-20]. Comonomer type has been reported to affect the density [18], crystallinity [18], and dissolution temperature [19] of copolymers. This is due to the fact that comonomer type can significantly affect the degree of comonomer inclusion into the crystal unit [21].

A series of ethylene/α-olefin samples and their blends were analyzed using Crystaf to investigate the effect of comonomer type on cocrystallization. In order to make a fair comparison between blends of polymers with different comonomer types, samples of each comonomer type were chosen in such a way that the blends had a similar range of crystallization temperatures and that the crystallization temperatures of the blend components was as close as possible, as illustrated in Figure 6.1.

Figure 6.1 shows the Crystaf profiles of blends involving four comonomers (BPEP1, BPEH4, BPEO1, and BPED1) measured at the same cooling rate of 0.1°C/min. Notice that the melting range and the peak positions of all blends is similar, the main difference being the comonomer. Table 6.1 also shows that the molecular weights of all the samples are about the same, so that molecular weight effects should not be a concern in this investigation. Figure 6.1 shows that, for these blends, comonomer type does not significantly affect the cocrystallization process, as the difference between the calculated and experimental profiles is very small in all cases.

Each of the blends in Figure 6.1 involves components having the same comonomer. In Figure 6.2, blends of copolymers of different comonomer are listed. Blends BPEP1 (Figure 6.1) and BPEX1 share one of the parent samples (PEP64, an ethylene/propylene copolymer) but differ in the other. The second component of BPEP1 (PEP384) is an ethylene/propylene copolymer, while the second component of BPEX1 (PEH100d) is an ethylene/1-hexene copolymer. Since only slight cocrystallization occurs in both cases, there is no significant impact from the difference of comonomer types. A similar conclusion can be drawn from the comparison of blends BPED1 (Figure 6.1) and BPEX2 (Figure 6.2).

### 6.3.2 Effect of cooling rate

In the previous chapter, it was showed that fractionation in Crystaf is governed by crystallization kinetics and that a change in the cooling rate can significantly affect Crystaf profiles. In this chapter, blends are analyzed at the faster cooling rate of 0.5°C/min to determine the impact of this variable on cocrystallization.

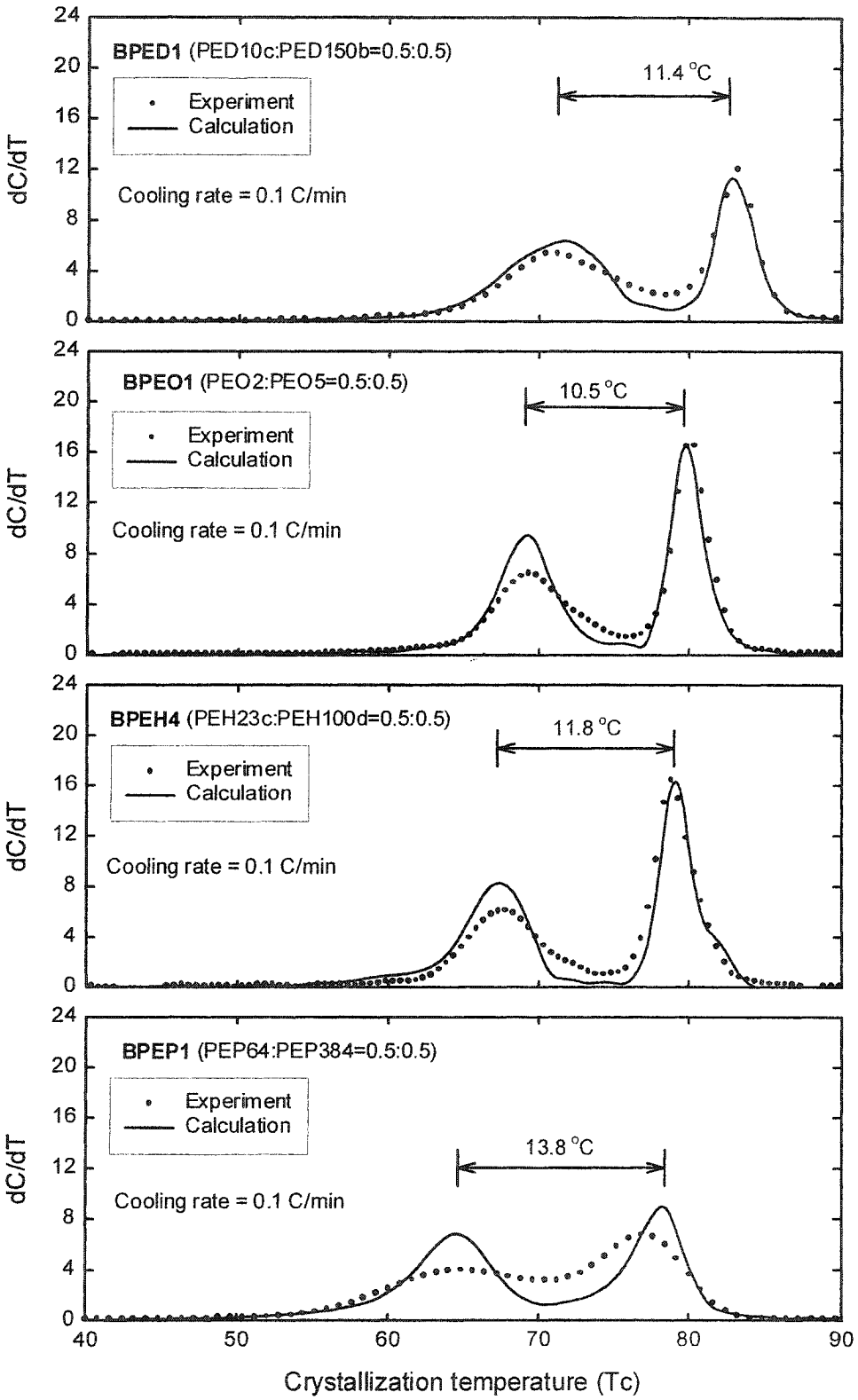


Figure 6.1 Effect of comonomer type on cocrystallization at a cooling rate of 0.1°C/min for blends involving a single comonomer

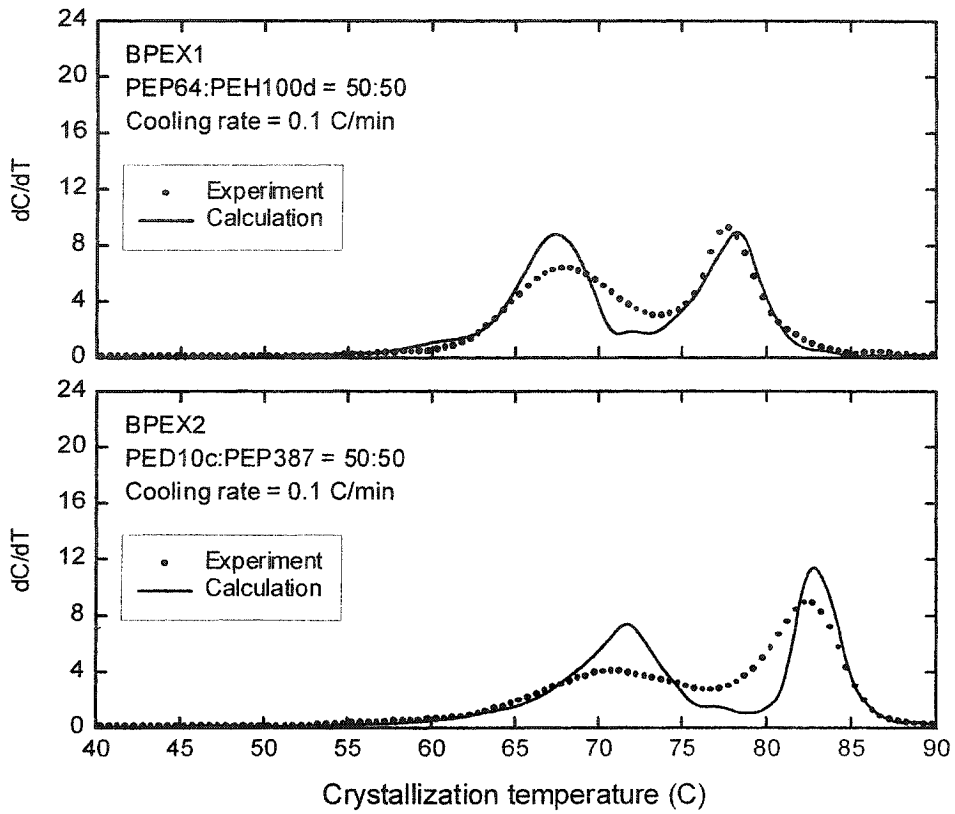


Figure 6.2 Crystaf analyses of blends of copolymers involving different comonomers at a cooling rate of 0.1°C/min

The comparison of Figures 6.3 and 6.4 with Figures 6.1 and 6.2 shows that the cooling rate has a dramatic effect on cocrystallization. At a cooling rate of 0.5°C/min, cocrystallization is so strong that only unimodal distributions are observed. This is very different from the bimodal distribution shown in Figures 6.1 and 6.2 for the same blends. As fractionation conditions move further from thermodynamic equilibrium, cocrystallization during the analysis becomes more important.

Since cocrystallization can lead to the misinterpretation of the CCD, it is important that Crystaf analysis be carried out at a slow cooling rate to obtain good peak resolution. This is especially important when information on the CCD of a copolymer with complex CCD (*e.g.*, multimodal distributions, such as those that arise from the use of heterogeneous Ziegler-Natta catalysts) is required.

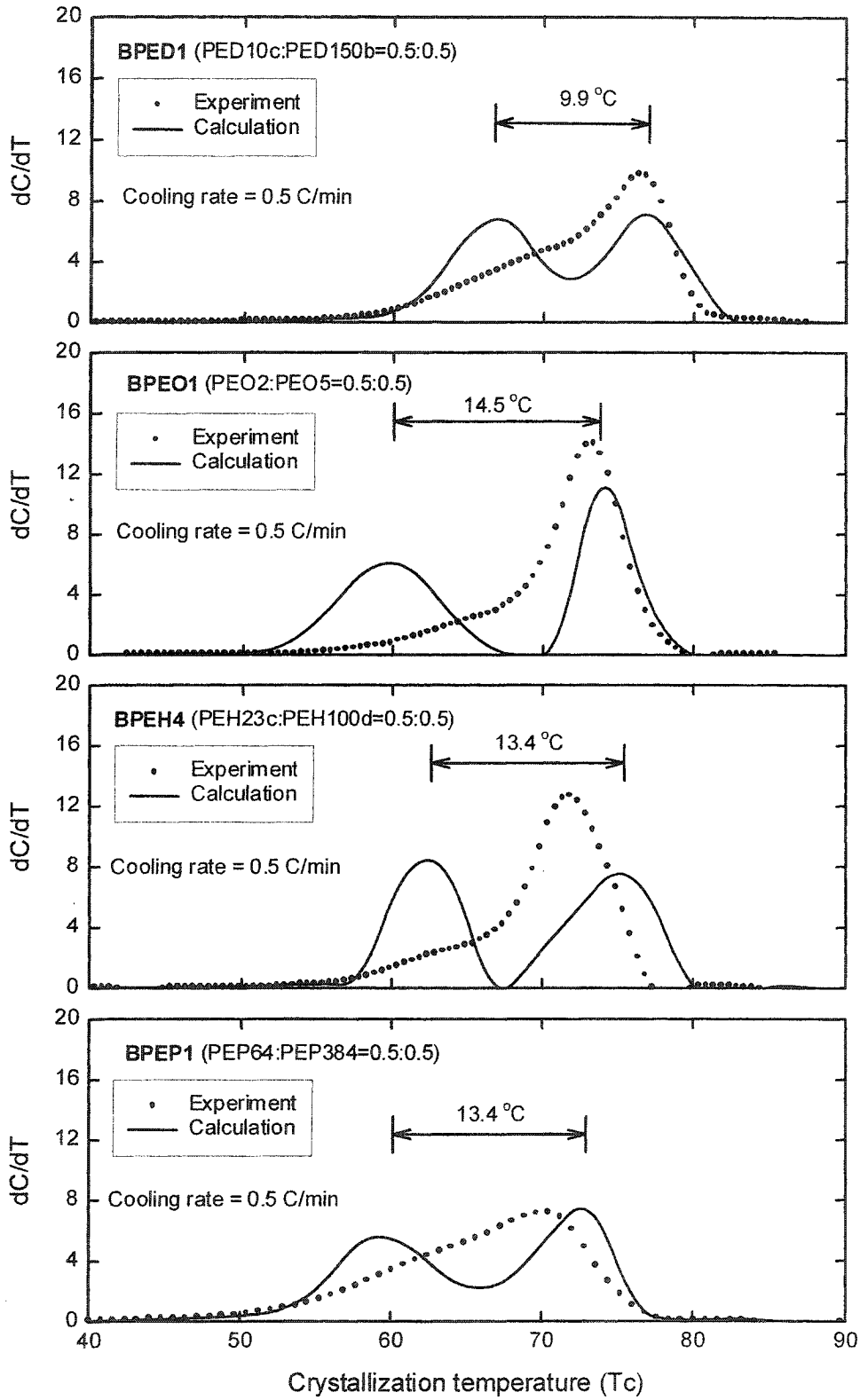


Figure 6.3 Effect of comonomer on cocrystallization at a cooling rate of 0.5°C/min for blends involving the same comonomer

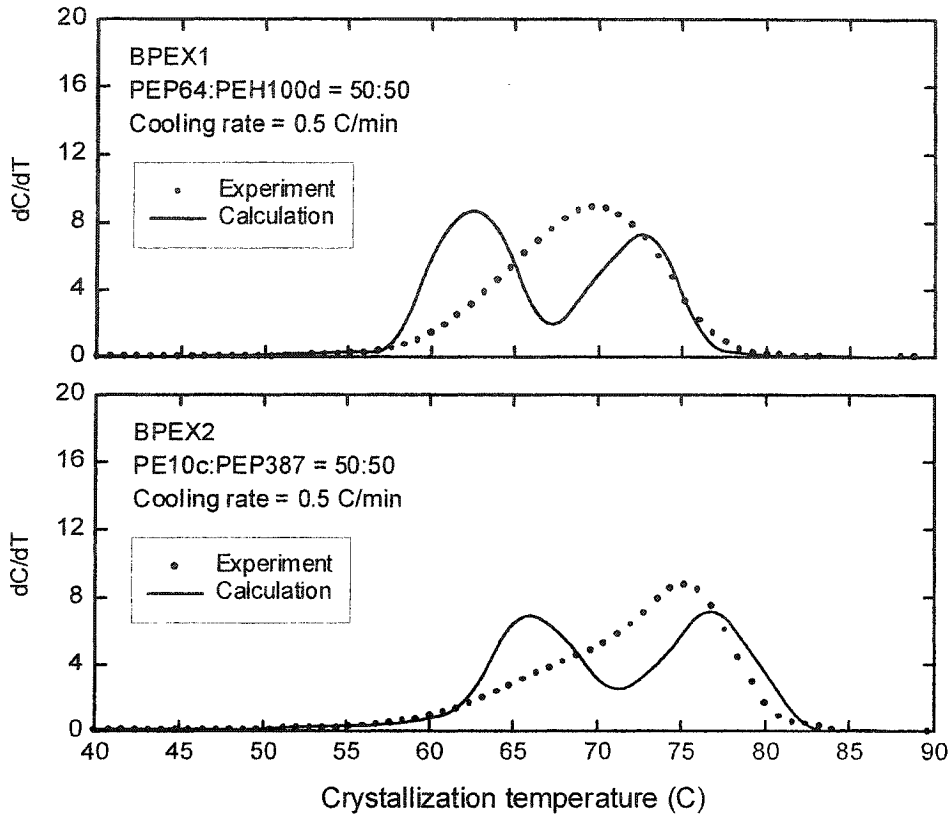


Figure 6.4 Crystaf analyses of blends of copolymers involving different comonomers at a cooling rate of 0.5°C/min

### 6.3.3 Effect of similarity of chain crystallizabilities

To see how the similarity of chain crystallizability affects cocrystallization during Crystaf analysis, a series of binary blends in which one of the components was the same, but the other had increasingly different crystallization temperatures, were investigated. For example, consider the binary blends of ethylene/1-dodecene copolymers BPED3, BPED1, and BPED4 (Figure 6.5). All of the blends in this series combine PED10c with another component of increasingly lower crystallization temperature. This is quantified by the difference between the Crystaf peak temperatures of the two parent samples, $\Delta T_C$. A small $\Delta T_C$ indicates that both chain populations crystallize over relatively the same range of temperature and thus have similar chain crystallizabilities.

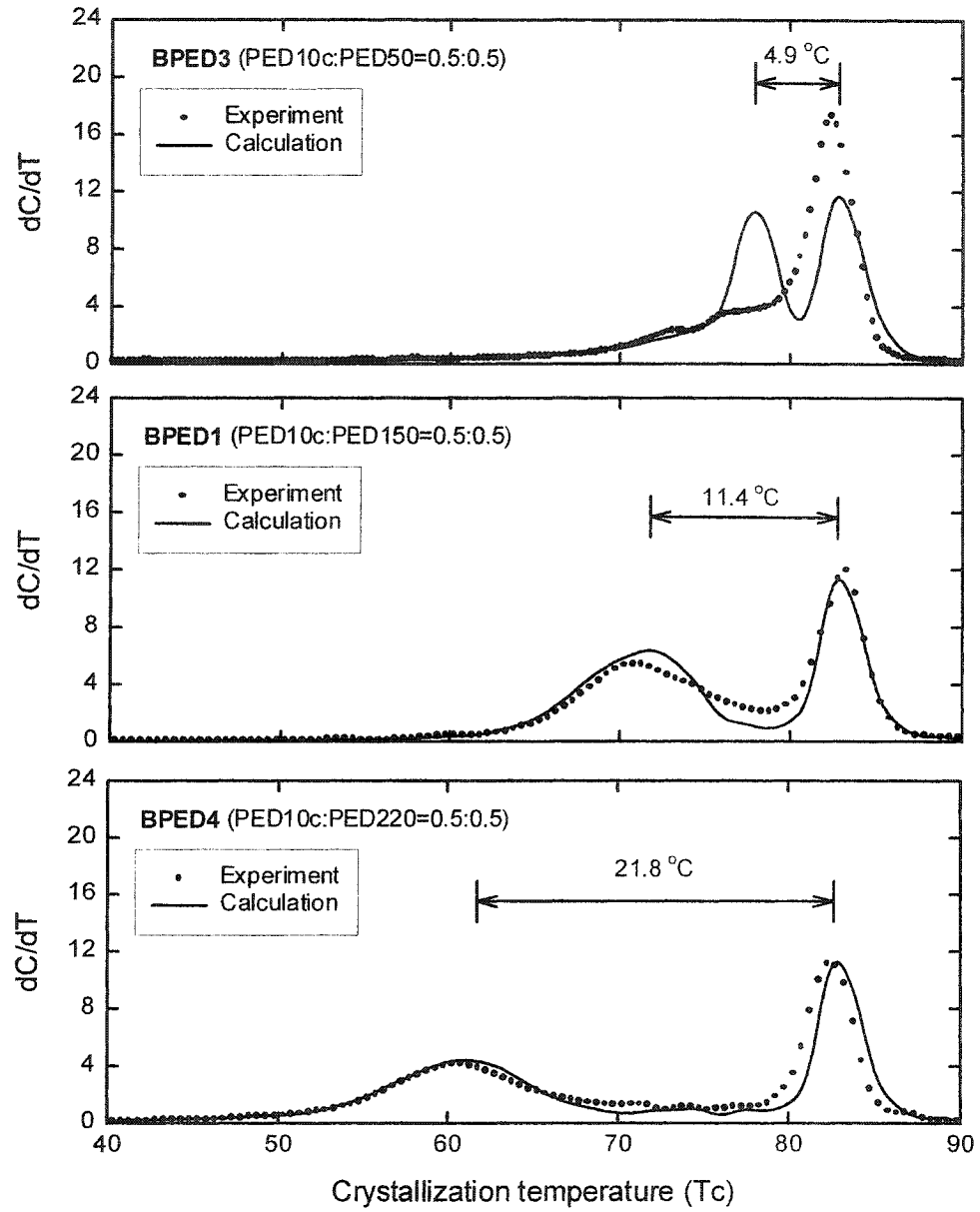


Figure 6.5 Effect of $\Delta T_C$ on cocrystallization during Crystaf analysis at a cooling rate of 0.1°C/min (blends of ethylene/1-dodecene copolymers)

By varying $\Delta T_C$, one sees a significant change in cocrystallization behavior (Figure 6.5). Similarity of chain crystallizabilities clearly induces cocrystallization during the analysis. At the smallest $\Delta T_C$ considered, cocrystallization has such a dramatic impact that Crystaf produces a unimodal distribution instead of the true binary distribution calculated from the Crystaf profiles of the parent samples. The

similar findings for blends of ethtylene/1-hexene and ethylene/propylene copolymers, (Figures 6.6 and 6.7), were obtained. This indicates that this phenomenon depends exclusively on $\Delta T_C$ and not on comonomer type. It should be pointed out that this phenomenon arises even when the standard Crystaf cooling rate of 0.1°C/min is used.

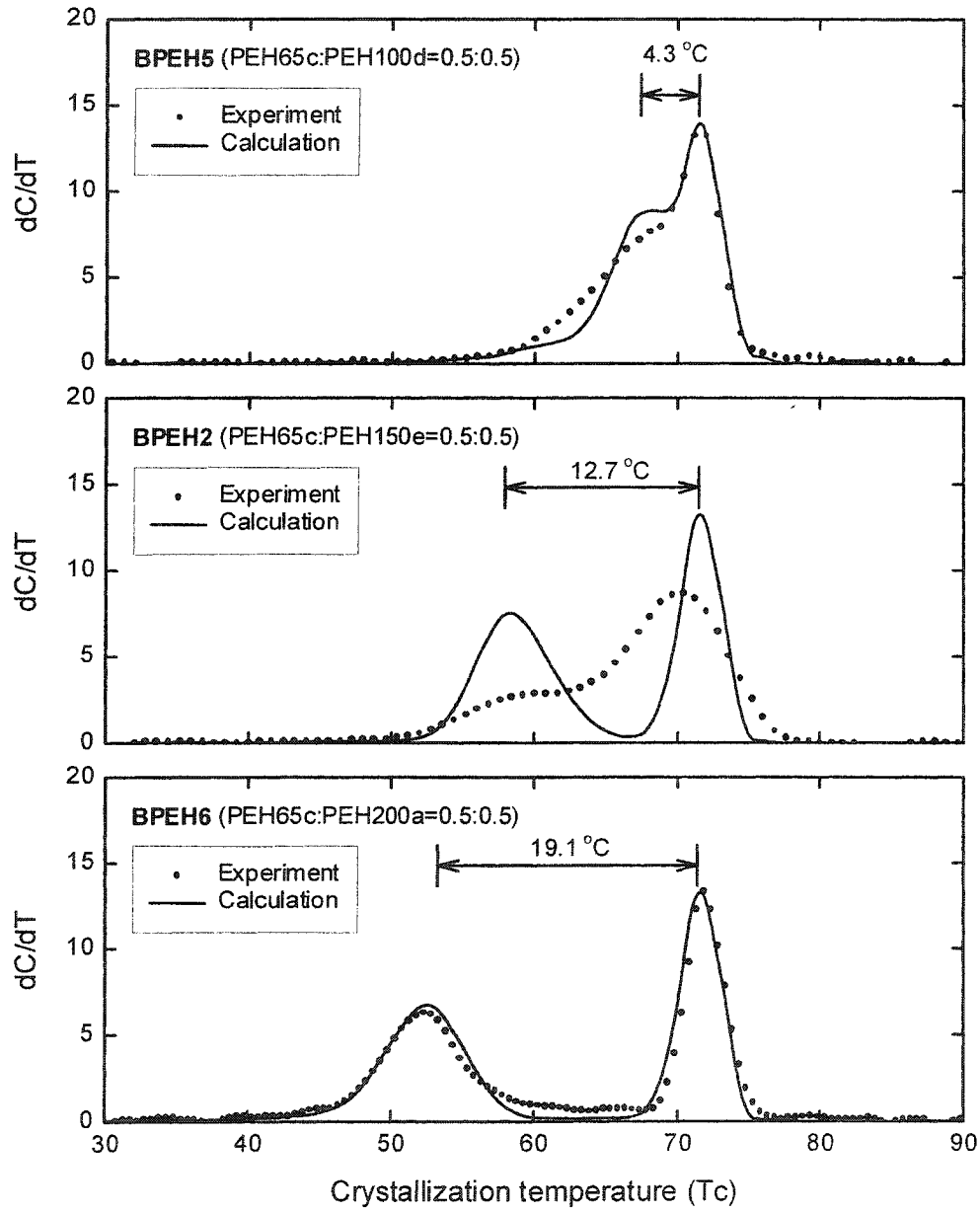


Figure 6.6 Effect of $\Delta T_C$ on cocrystallization during Crystaf analysis at a cooling rate of 0.1°C/min (blends of ethylene/1-hexene copolymers)

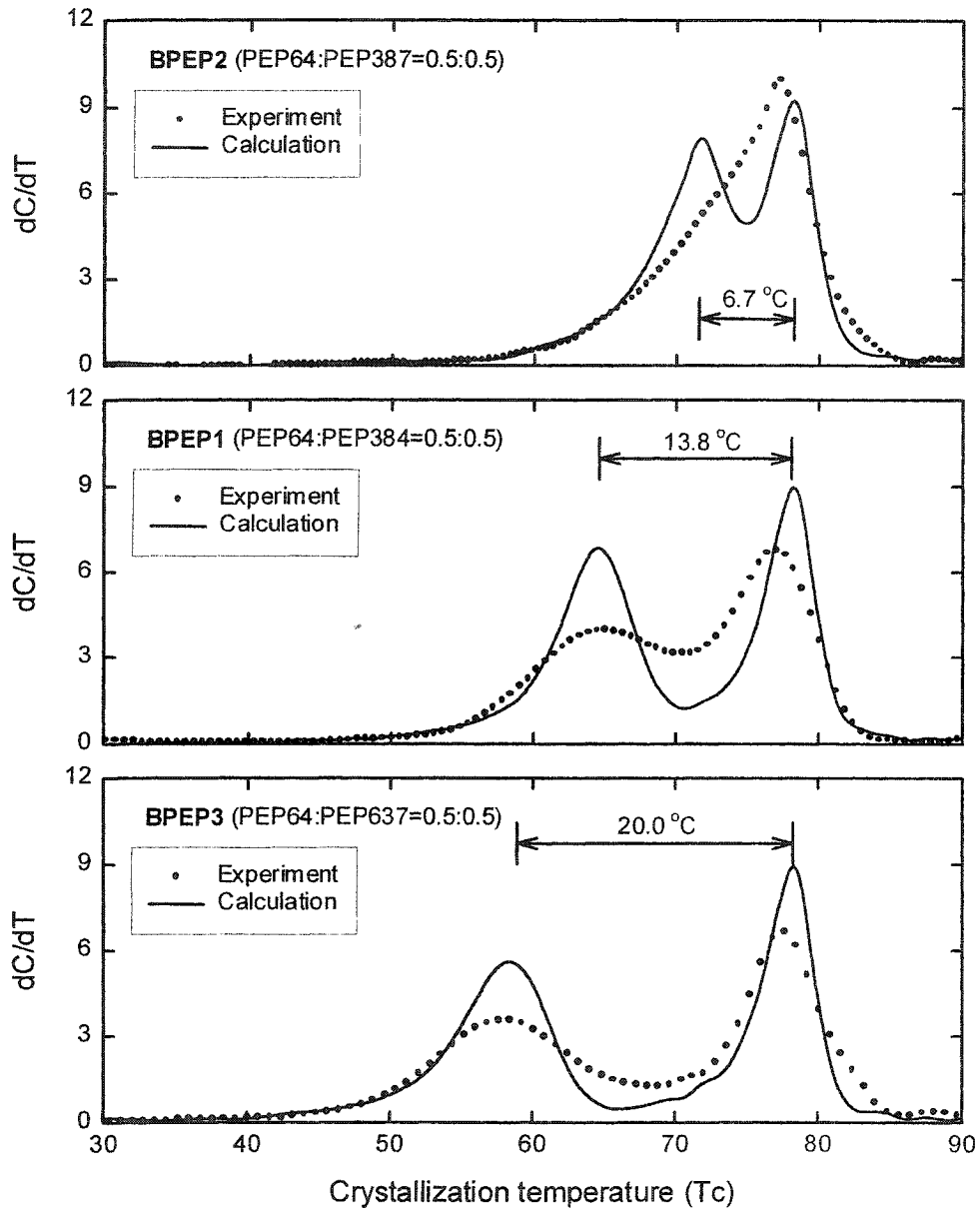


Figure 6.7 Effect of $\Delta T_C$ on cocrystallization during Crystaf analysis at a cooling rate of 0.1°C/min (blends of ethylene/propylene copolymers)

At first glance, when $\Delta T_C$ is small, it appears that cocrystallization occurs because, after crystallized, chains with high crystallizabilities may act as nuclei for chains having lower crystallizabilities and thus promote the crystallization of chains

with low crystallizabilities. Therefore, chains with low crystallizabilities start to crystallize at higher temperatures than they would if present alone, as they can grow on the existing nuclei without having to undergo the nucleation process.

A careful examination of the situation when $\Delta T_C$ is larger, however, shows that the above explanation is not correct, as the crystallization of chains with less crystallizability is not necessarily affected by the existence of the nuclei from chains with high crystallizabilities. This is revealed by the fact that, in the case of high $\Delta T_C$, there is no shift of the low temperature Crystaf peak, and experimental and calculated Crystaf profiles are almost identical.

These results imply that cocrystallization in fact occurs during the nucleation process, as the cocrystallization is most pronounced only when a small $\Delta T_C$ is involved. Consequently, conucleation seems to be a prerequisite condition for a measurable cocrystallization effect in Crystaf.

## 6.4 CLOSING REMARKS

In this chapter, cocrystallization of ethylene/α-olefin copolymers during Crystaf analysis was discussed. By using four blends of copolymers with different comonomers (propylene, 1-hexene, 1-octene, and 1-dodecene), it was shown that comonomer type does not affect cocrystallization in Crystaf. The cooling rate, however, is found to have an important effect on cocrystallization, as a fast cooling rate strongly promotes cocrystallization. The use of a slow cooling rate is recommended if information on CCD of copolymers with complex CCDs is required.

The similarity of chain crystallizabilities, as indicated by the difference in the Crystaf peak temperatures of the parent samples ($\Delta T_C$), is another very important factor that strongly affects cocrystallization. A small $\Delta T_C$, which indicates that the chain crystallizabilities of the blend components are very similar, induces cocrystallization even at the standard Crystaf crystallization rate of $0.1^{\circ}$C/min.

## REFERENCES


1. Gownder M., "Branching of LLDPE as Studied by Crystallization Analysis Fractionation and Its Effect on Mechanical Properties of Films", *Journal of Plastic Film and Sheeting*, **2001**, *17*, 53.
2. Cady L.D., "LLDPE Properties Tied to Branch Distribution", *Plastics Engineering*, **1987**, 25.
3. Simon L.C., de Souza R.F., Soares J.B.P. and Mauler R.S., "Effect of Molecular Structure on Dynamic Mechanical Properties of Polyethylene Obtained with Nickel-Diimine Catalysts", *Polymer*, **2001**, *42*, 4885.
4. Soares J.B.P., Abbott R.F. and Kim J.D., "Environmental Stress Cracking Resistance of Polyethylene: the Use of CRYSTAF and SEC to Establish Structure-Property Relationships", *Journal of Polymer Science: Part B: Polymer Physics*, **2000**, *38*, 1267.
5. Wild L., "Temperature Rising Elution Fractionation", *Advances in Polymer Science*, **1990**, *98*, 1.
6. Soares J.B.P. and Hamielec A.E., "Temperature Rising Elution Fractionation of Linear Polyolefins", *Polymer*, **1995**, *36*, 1639.
7. Soares J.B.P. and Hamielec A.E., "Temperature Rising Elution Fractionation", in: *Modern Techniques for Polymer Characterization*, R.A. Pethrick, J.V. Dawkins, Eds., John Wiley&Sons, 1999, p. 15-55.
8. Wild L. and Blatz C., "Development of High Performance Tref for Polyolefin Analysis", in: *New Advances in Polyolefins*, T.C. Chung, Eds, Plenum Press 1993, p. 147-157.
9. Monrabal B., "Crystallization Analysis Fractionation: A New Technique for the Analysis of Branching Distribution in Polyolefins", *Journal of Applied Polymer Science,* **1994**, *52*, 491.
10. Monrabal B., "CRYSTAF: Crystallization Analysis Fractionation. A New Approach to the Composition Analysis of Semicrystalline Polymers", *Macromolecular Symposia,* **1996**, *110*, 81.

11. Monrabal B., Blanco J., Nieto J. and Soares J.B.P, "Characterization of Homogeneous Ethylene/1-Octene Copolymers Made with a Single-Site Catalyst. CRYSTAF Analysis and Calibration", *Journal of Polymer Science: Part A: Polymer Chemistry*, **1999**, *37*, 89.
12. Britto L.J.D., Soares J.B.P., Penlidis A. and Monrabal B., "Polyolefin Analysis by Single-Step Crystallization Fractionation", *Journal of Polymer Science: Part B: Polymer Physics*, **1999**, *37*, 539.
13. Pasch H., Brull R., Wahner U. and Monrabal B., "Analysis of Polyolefins by Crystallization Analysis Fractionation", *Macromolecular Materials and Engineering*, **2000**, *279*, 46.
14. Brull R., Grumel V., Pasch H., Raubenheimer H.G., Sanderson R. and Wahner U.M., "Analysis of Polyolefin Blends by CRYSTAF", *Macromolecule Symposium*, **2002**, *178*, 81.
15. Sarzotti D.M., Soares J.B.P. and Penlidis A., "Ethylene/1-Hexene Copolymers Synthesized with a Single-Site Catalyst: Crystallization Analysis Fractionation, Modeling, and Reactivity Ratio Estimation", *Journal of Polymer Science: Part B: Polymer Physics*, **2002**, *40*, 2595.
16. Burfield D.R. and Kashiwa N., "DSC Studies of Linear Low Density Polyethylene. Insights into the Disrupting Effect of Different Comonomers and the Minimum Fold Chain Length of the Polyethylene Lamellae", *Makromolecule Chemistry*, **1985**, *186*, 2657.
17. Brull R., Pasch H., Ruaubenheimer H.G., Sanderson R., van Reenen A.J. and Wahner U.M., "Investigation of the Melting and Crystallization Behavior of Random Propane/1-Olefin Copolymers by DSC and CRYSTAF", *Macromolecular Chemistry and Physics*, **2001**, *202*, 1281.
18. Shirayama K., Kita S.-I. And Watabe H., "Effects of Branching on Some Properties of Ethylene/1-Olefin Copolymers", *Die. Makromolekilare Chemie,* **1972**, *151*, 97.
19. Savitski E.P., Caflisch G.B., Killian C.M., Meadows M., Merkley J.H. and Huff B.J., "Influence of the Short-Chain Branch Length on the Calibration of

Temperature Rising Elution Fractionation Systems", *Journal of Applied Polymer Science*, **2003**, *90*, 722.

20. Graef S.M., Brull R., Pasch H. and Wahner U.M., "Monitoring the Chemical Heterogeneity of Metallocene-Catalysed Copolymers of Ethylene and Higher 1-Olefins using CRYSTAF and SEC-FTIR", *e-Polymers*, **2003**, no 005.
21. Hosoda S., Nomura H., Gotoh Y. and Kihara H., "Degree of Branch Inclusion into the Lamellar Crystal for Various Ethylene/1-Olefin Copolymers", *Polymer*, **1990**, *31*, 1999.

CHAPTER 7

# CONCLUSIONS AND ORIGINAL CONTRIBUTIONS

*With as much as we think we know, there is much to learn.*

***Anonymous***

## 7.1 CONCLUSIONS

The following conclusions are made based on this study.

1. Analytical expressions describing the CCD of random binary copolymers, terpolymers, and multicomponent copolymers were developed using the statistical approach. The new analytical solutions agree with the ones from Monte Carlo simulation and provide a much more elegant representation of the CCD of multicomponent random copolymers.
2. In the case of random terpolymers, examination of CCDs for molecules with different kinetic chain lengths showed that the distribution broadens with decreasing kinetic chain length. The peak position was found to be independent of kinetic chain length.
3. Both molecular weight and comonomer content affect the shape of Crystaf profiles, but Crystaf peak temperatures are practically independent of molecular weight. Increased tailing of the Crystaf profile in the low temperature region with decreasing molecular weight was clearly observed.

4. For a given set of operating conditions, the comonomer content is the key parameter affecting the Crystaf peak temperature. Therefore, comonomer content can be quickly and reliably estimated using a calibration curve relating peak temperature to comonomer content.
5. A Crystaf model based on the average ethylene sequence distribution was proposed. The new model agrees well with experimental data over a wide range of molecular weight and comonomer content. Compared to a previous model based on the longest ethylene sequence distribution, the new model gives a better fit to data and improves the prediction of the onset of the crystallization temperature.
6. The typical operating conditions used in Tref and Crystaf analyses are far from thermodynamic equilibrium, and crystallization kinetics strongly influence the CCD of copolymers as estimated using Tref and Crystaf.
7. Strong cocrystallization can take place during the analysis of polyolefin blends and can distort the CCD obtained from Tref and Crystaf. It appears that Tref is more appropriate for analyzing samples with complex CCDs, as it provides better peak resolution for the same cooling rate. Crystaf, however, is better for most routine measurements due to its simpler and faster operation.
8. The cooling rate was found to play an important role in cocrystallization, as a fast cooling rate strongly promotes cocrystallization. Therefore, use of a slow cooling rate is essential when high-resolution information on the CCD of a copolymer with a complex CCD is required.
9. The similarity of chain crystallizabilities can also significantly affect cocrystallization. A small difference between Crystaf peak temperatures of parent samples induces cocrystallization even at a typical Crystaf cooling rate of $0.1^{\circ}C$/min.
10. By studying four blends of copolymers with different comonomer types (propylene, 1-hexene, 1-octene, and 1-dodecene), it was found that comonomer type does not affect cocrystallization in Crystaf.

## 7.2 CONTRIBUTIONS TO KNOWLEDGE

1. While terpolymers and multicomponent copolymers have a number of commercial applications, the structure-property relationships of these materials are not yet understood. The results of the present study are a crucial step toward this understanding. For the first time convenient analytical expressions are developed that describe the chemical composition distribution of multicomponent random copolymers, the key microstructural feature that governs many physical properties of copolymers.
2. This study quantifies the effect of chain microstructural characteristics, specifically average molecular weight and comonomer content, on Crystaf profiles. It is demonstrated that Crystaf peak temperature is governed mainly by comonomer content and is almost independent of molecular weight for several polyolefins. This finding confirms that comonomer content can be quickly estimated from Crystaf peak temperature by means of a calibration curve, since the influence of molecular weight is negligible.
3. The present study also proposed a Crystaf model based on the distribution of average ethylene sequences. The model describes experimental data better than previous Crystaf models.
4. It is generally believed that the fractionation process during Tref and Crystaf analyses occurs at conditions near thermodynamic equilibrium. This investigation is the first to show that this assumption is incorrect, and it systematically describes the role of crystallization kinetics in Tref and Crystaf profiles.
5. Although the possibility of cocrystallization during Crystaf analysis has been considered before, it has not been previously reported as an important factor, as most previous studies considered only blends of polymers having very distinct crystallizabilities. The present work is the first comprehensive study of cocrystallization for polyolefin samples with varying crystallizabilities and comonomer types. It is demonstrated that cocrystallization during Crystaf analysis is a very important factor affecting Crystaf profiles and may adversely affect CCD

information obtained using Crystaf, even at traditional operating conditions. The results of this study also identify the factors that promote cocrystallization.

## 7.3 RECOMMENDATIONS FOR FUTURE WORK

1. It would be useful to extend the derivation of CCD for random multicomponent copolymers to the more general case of multicomponent copolymers that follow Markov statistics of higher orders. Such models could be used in the challenging task of constructing structure-property relationships for these copolymers.
2. The effect of molecular weight and comonomer content on Crystaf profiles has been clearly illustrated in this and previous studies. However, the role of comonomer type in the fractionation process remains unclear and is still debated in the literature. The effect of comonomer type on Crystaf data may be worth studying, as this effect has been reported to be important for Tref.
3. None of the existing Crystaf models, including the one proposed here, can explain the experimental findings of the present study, *e.g.* the effect of crystallization kinetics and cocrystallization. From an academic viewpoint, the understanding of the fractionation mechanism in Crystaf and the development of a good phenomenological model is a challenging task worth tackling. In order to simplify the problem, one might use polymers with simple, well-defined structures, such as nearly monodisperse HDPE.
4. In order to understand the complex nonisothermal crystallization process in Crystaf, it would be useful to study the simpler problem of isothermal crystallization in dilute solution. This could be done using a recently developed thermal characterization technique known as a solution DSC. The information obtained from isothermal crystallization could be used to determine the parameters of the phenomenological Crystaf model.
5. It would be interesting to investigate further cocrystallization in blends of different types of polymers, *e.g.* polyethylene/polypropylene blends. As the crystallite structures of these polymers are different, one could investigate the role of different monomeric structures on cocrystallization.

6. The major difficulty in obtaining quantitative CCDs from Crystaf profiles is the fact that the calibration curve depends on the type of polymer being analyzed. In order to obtain accurate CCDs, one must construct a calibration curve for each material of interest. This limitation could be eliminated by using two-detectors to measure simultaneously both concentration and comonomer content as functions of crystallization temperature. This would eliminate the need to prepare special calibration curves for each polymer.

# BIBLIOGRAPHY


Alizadeh A., Richardson L., Xu J., McCarrtney S., Marand H., Cheung Y.W. and Chum S., "Influence of Structure and Topological Constraints on the Crystallization and Melting Behavior of Polymer 1. Ethylene/1-Octene Copolymer", *Macromolecules*, **1999**, *32*, 6221.

Anantawaraskul S., Soares J.B.P. and Wood-Adams P.M., "Chemical Composition Distribution of Multicomponent Copolymers", *Macromolecular Theory and Simulation*, **2003**, *12*, 229.

Anantawaraskul S., Soares J.B.P., Wood-Adams P.M. and Monrabal B., "Effect of Molecular Weight and Average Comonomer Content on the Crystallization Analysis Fractionation (Crystaf) of Ethylene α-Olefin Copolymers", *Polymer*, **2003**, *44*, 2393.

Anantawaraskul S., Soares J.B.P. and Wood-Adams P.M., "Effect of Operation Parameters on Temperature Rising Elution Fractionation and Crystallization Analysis Fractionation", *Journal of Polymer Science: Part B: Polymer Physics*, **2003**, *41*, 1762.

Anantawaraskul S., Soares J.B.P. and Wood-Adams P.M., "An Experimental and Numerical Study on Crystallization Analysis Fractionation (Crystaf)", to appear in *Macromolecular Symposia.*

Anantawaraskul S., Soares J.B.P. and Wood-Adams P.M., "Chemical Composition Distribution of Multicomponent Copolymer Chains", to appear in *Macromolecular Symposia.*

Anantawaraskul S., Soares J.B.P. and Wood-Adams P.M., "A Study on the Cocrystallization of Blends of Ethylene/1-Olefin Copolymers during Crystallization Analysis Fractionation (Crystaf)", submitted to *Macromolecular Chemistry and Physics*.

Bensason S., Minick J., Moet A., Chum S., Hiltner A. and Baer E., "Classification of Homogeneous Ethylene-Octene Copolymers Based on Comonomer Content", *Journal of Polymer Science: Part B: Polymer Physics*, **1996**, *34*, 1301.

Beigzadeh D., Soares J.B.P. and Duever T.A., "Modeling of Fractionation in CRYSTAF Using Monte Carlo Simulation of Crystallizable Sequence Lengths: Ethylene/1-Octene Copolymers Synthesized with Single-Site-Type Catalysts", *Journal of Applied Polymer Science*, **2001**, *80*, 2200.

Beigzadeh D., "Long Chain Branching in Ethylene Polymerization Using Combined Metallocene Catalyst Systems", *PhD thesis*, University of Waterloo, Canada, 2000.

Borrajo J., Cordon C., Carella J.M., Toso S. and Goizueta G, "Modelling the Fractionation Process in TREF System: Thermodynamic Simple Approach", *Journal of Polymer Science: Part B: Polymer Physics*, **1995**, *33*, 1627.

Britto L.J.D., Soares J.B.P. and Penlidis A., "Observations on HDPE Characterization with a Microcalorimeter as a Complementary Tool to Tref and Crystaf", *Polymer Reaction Engineering*, **2000**, *8*, 159.

Britto L.J.D., Soares J.B.P., Penlidis A. and Monrabal B., "Polyolefin Analysis by Single-Step Crystallization Fractionation", *Journal of Polymer Science: Part B: Polymer Physics*, **1999**, *37*, 539.

Brull R., Grumel V., Pasch H., Raubenheimer H.G., Sanderson R. and Wahner U.M., "Analysis of Polyolefin Blends by CRYSTAF", *Macromolecule Symposium*, **2002**, *178*, 81.

Brull R., Pasch H., Ruaubenheimer H.G., Sanderson R., van Reenen A.J. and Wahner U.M., "Investigation of the Melting and Crystallization Behavior of Random

Propane/1-Olefin Copolymers by DSC and CRYSTAF", *Macromolecular Chemistry and Physics*, **2001**, *202*, 1281.

Burfield D.R. and Kashiwa N., "DSC Studies of Linear Low Density Polyethylene. Insights into the Disrupting Effect of Different Comonomers and the Minimum Fold Chain Length of the Polyethylene Lamellae", *Makromolecule Chemistry*, **1985**, *186*, 2657.

Cady L.D., "LLDPE Properties Tied to Branch Distribution", *Plastics Engineering*, **1987**, 25.

Chen F., Shanks R.A. and Amarasinghe G., "Crystallisation of Single-Site Polyethylene Blends Investigated by Thermal Fractionation Techniques", *Polymer*, **2001**, *42*, 4579.

Cheng H.N., Tam S.B. and Kasehagen L.J., "Compositional Heterogeneity in Polymers: Computer Simulation Approaches", *Macromolecules*, **1992**, *25*, 3779.

Cheng H.N. and Kasehagen, "Tacticity Distribution and Simulation", *Macromolecules*, **1993**, *26*, 4774.

Chiu F-C., Fu Q., Peng Y., Shih H-H., "Crystallization Kinetics and Melting Behavior of Metallocene Short-Chain Branched Polyethylene Fractions", *Journal of Polymer Science: Part B: Polymer Physics*, **2002**, *40*, 325.

Chu K.-J., Li Pi Shan C., Soares J.B.P. and Penlidis A., "Copolymerization of Ethylene and 1-Hexene with In-Situ Supported $Et[Ind]_2ZrCl_2$", *Macromolecular Chemistry and Physics*, **1999**, *200*, 2372.

Chu K.-J., Soares J.B.P. and Penlidis A., "Variation of Molecular Weight Distribution (MWD) and Short Chain Branching Distribution (SCBD) of Ethylene/1-Hexene Copolymers Produced with Different In-Situ Supported Metallocene Catalysts", *Macromolecular Chemistry and Physics*, **2000**, *201*, 340.

Chu K.-J., Soares J.B.P., Penlidis A. and Ihm S.-K., "The Influence of the $Ti^{3+}$ Species on the Microstructure of Ethylene/1-Hexene Copolymers", *Macromolecular Chemistry and Physics*, **1999**, *200*, 1298.

Costeux S., Anantawaraskul S., Wood-Adams P.M. and Soares J.B.P., "Distribution of the Longest Ethylene Sequence in Ethylene/1-Olefin Copolymers

Synthesized with Single-Site-Type Catalysts", *Macromolecular Theory and Simulation*, **2002**, *11*, 326.

da Silva Filho A.A., Soares J.B.P. and de Galland G.B., "Measurement and Mathematical Modeling of Molecular Weight and Chemical Composition Distributions of Ethylene/1-Olefin Copolymers Synthesized with A Heterogeneous Ziegler-Natta Catalyst", *Macromolecular Chemistry and Physics*, **2000**, *201*, 1226.

de Goede S., Brull R. and Pasch H., Marshall, "Monitoring Thermo-Oxidative Degradation of Polypropylene by Crystaf and SEC-FTIR", *Macromolecular Symposia*, **2003**, *193*, 35.

Devoy C., Mandelkern L. and Bourland L, " Crystallization Kinetics of Dilute Polyethylene Solutions", *Journal of Polymer Science: Part A-2*, **1970**, *8*, 869.

Elicabe G., Carella J. and Borrajo J., "Modelling the Fractionation Process in TREF System II. Numerical Analysis", *Journal of Polymer Science: Part B: Polymer Physics*, **1996**, *34*, 527.

Elicabe G., Borrajo J. and Carella J., "Modelling the Fractionation Process in TREF System III. Model Validation With Low Molecular Weight Homopolymers", *Journal of Polymer Science: Part B: Polymer Physics*, **1996**, *34*, 1147.

Faldi A. and Soares J.B.P., "Characterization of the Combined Molecular Weight and Composition Distribution of Industrial Ethylene/1-Olefin Copolymers", *Polymer,* **2001**, *42*, 3057.

Flory P.J., "Thermodynamics of High Polymer Solution", *Journal of Chemical Physics*, **1942**, *10*, 51.

Flory P.J., "Thermodynamics of Crystallization in High Polymers IV. A Theory of Crystalline States and Fusion in Polymers, Copolymers, and Their Mixtures with Diluents", *Journal of Chemical Physics,* **1949**, *17*, 223.

Flory P.J., "*Principles of Polymer Chemistry*", 1st edition, Cornell University Press **1953**.

Fonseca C.A. and Harrison I.R., "Temperature Rising Elution Fractionation", in: Modern Techniques for Polymer Characterization, R.A. Pethrick, J.V. Dawkins, Eds., John Wiley&Sons, **1999**, p. 1-14.

Gabriel C. and Lilge D., "Comparison of Different Methods for the Investigation of the Short-Chain Branching Distribution of LLDPE", *Polymer*, **2001**, *42*, 297.

Galante M.J., Mandelkern L. and Alamo R.G., "The Crystallization of Blends of Different Types of Polyethylene: The Role of Crystallization Conditions", *Polymer*, **1998**, *39*, 5105.

Gordon M., "Universality of the Stockmayer Distribution", *Macromolecules*, **1984**, *17*, 514.

Gownder M., "Branching of LLDPE as Studied by Crystallization Analysis Fractionation and Its Effect on Mechanical Properties of Films", *Journal of Plastic Film and Sheeting*, **2001**, *17*, 53.

Graef S.M., Brull R., Pasch H. and Wahner U.M., "Monitoring the Chemical Heterogeneity of Metallocene-Catalysed Copolymers of Ethylene and Higher 1-Olefins using CRYSTAF and SEC-FTIR", *e-Polymers*, **2003**, no 005.

Hawkins S.W. and Smith H., "The Fractionation of Polyethylene", *Journal of Polymer Science*, **1958**, *28*, 341.

Hosoda S., "Structural Distribution of Linear Low-Density Polyethylene", *Polymer Journal*, **1988**, *20*, 383.

Hosoda S., Nomura H., Gotoh Y. and Kihara H., "Degree of Branch Inclusion into the Lamellar Crystal for Various Ethylene/1-Olefin Copolymers", *Polymer*, **1990**, *31*, 1999.

Karbashewski E., Kale L., Rudin A., Tchir W.J., Cook D.G. and Pronovost J.O., "Characterization of Linear Low Density Polyethylene by Temperature Rising Elution Fractionation and by Differential Scanning Calorimetry", *Journal of Applied Polymer Science*, **1992**, *44*, 425.

Karbashewski E., Rudin A., Kale L., and Tchir W.J., "A Note on the Effect of Comonomer Sequence Distribution on TREF Branching Distributions", *Polymer Engineering and Science*, **1993**, *33*, 1370.

Karoglanian S.A. and Harrison I.R., "A Temperature Rising Elution Fractionation Study of Short Chain Branching Behavior in Ultra Low Density Polyethylene", *Polymer Engineering and Science*, **1996**, *36*, 731.

Kim J.D. and Soares J.B.P., "Copolymerization of Ethylene and 1-Hexene with Supported Metallocene Catalysts: Effect of Support Treatment", *Macromolecular Rapid Communication*, **1999**, *20*, 347.

Kim J.D. and Soares J.B.P., " Copolymerization of Ethylene and α-Olefins with Combined Metallocene Catalysts. III. Production of Polyolefins with Controlled Microstructures", *Journal of Polymer Science: Part A: Polymer Chemistry*, **2000**, *38*, 1427.

Kim M.-H. and Phillips P.J., "Nonisothermal Melting and Crystallization Studies of Homogeneous Ethylene/1-Olefin Random Copolymers", *Journal of Applied Polymer Science,* **1998**, *70*, 1893.

Kim Y.-M., Kim C.-H., Park J.-K., Kim J.-W. and Min T.-I., "Short Chain Branching Distribution and Thermal Behavior of High Density Polyethylene", *Journal of Applied Polymer Science*, **1996**, *60*, 2469.

Koenig J.L., "*Chemical Microstructure of Polymer Chains*", 1st edition, John Wiley&Sons 1980.

Li Pi Shan C., Chu K.-J., Soares J.B.P. and Penlidis A., "Using Alkyaluminium Activators to Tailor Short Chain Branching Distribution of Ethylene/1-Hexene Copolymers Produced with In-Situ Supported Metallocene Catalysts", *Macromolecular Chemistry and Physics*, **2000**, *201*, 2195.

Li Pi Shan C., Soares J.B.P. and Penlidis A., "Ethylene/1-Octene Copolymerization Studies with In Situ Supported Metallocene Catalysts: Effect of Polymerization Parameters on the Catalyst Activity and Polymer Microstructure", *Journal of Polymer Science: Part A: Polymer Chemistry*, **2002**, *40*, 4426.

Mandelkern L., "*Crystallization of Polymers*", 2nd edition, Cambridge University Press **2002**.

Mandelkern L., "Thermodynamic and Physical Properties of Polymer Crystals Formed from Dilute Solution", *Progress in Polymer Science*, **1970**, *2,* 165.

Mingozzi I. and Nascetti S., "Chemical Composition Distribution and Molecular Weight Distribution Determination of Ethylene, 1-Betene Linear Low-Density

Polyethylene (LLDPE)", *International Journal of Polymer Analysis and Characterization*, **1996**, *3*, 59.

Mirabella F.M. and Ford E.A., "Characterization of Linear Low-Density Polyethylene: Cross Fractionation According to Copolymer Composition and Molecular Weight", *Journal of Polymer Science: Part B: Polymer Physics*, **1987**, *25*, 777.

Monrabal B., "Crystallization Analysis Fractionation: A New Technique for the Analysis of Branching Distribution in Polyolefins", *Journal of Applied Polymer Science,* **1994**, *52*, 491.

Monrabal B., "CRYSTAF: Crystallization Analysis Fractionation. A New Approach to the Composition Analysis of Semicrystalline Polymers", *Macromolecular Symposia,* **1996**, *110*, 81.

Monrabal B., Blanco J., Nieto J. and Soares J.B.P, "Characterization of Homogeneous Ethylene/1-Octene Copolymers Made with a Single-Site Catalyst. CRYSTAF Analysis and Calibration", *Journal of Polymer Science: Part A: Polymer Chemistry*, **1999**, *37*, 89.

Montaudo M.S. and Montaudo G., "Bivariate Distribution in PMMA/PBA Copolymers by Combined SEC/NMR and SEC/MALDI Measurements", *Macromolecules*, **1999**, *32*, 7015.

Nakano S. and Goto Y., "Development of Automatic Cross Fractionation: Combination of Crystallizability Fractionation and Molecular Weight Fractionation", *Journal of Applied Polymer Science*, **1981**, *26*, 4217.

Nesarikar A., Crist B., and Davidovich A., "Liquid-liquid Phase Separation in Linear Low-Density Polyethylene", *Journal of Polymer Science: Part B Polymer Physics*, **1994**, *32*, 641.

Nieto J., Oswald T., Blanco F., Soares J.B.P. and Monrabal B., "Crystallizability of Ethylene Homopolymers by Crystallization Analysis Fractionation", *Journal of Polymer Science: Part B: Polymer Physics*, **2001**, *39*, 1616.

Pasch H., "Recent Developments in Polyolefin Characterization", *Macromolecular Symposium*, **2001**, *165*, 91.

Pasch H., Brull R., Wahner U. and Monrabal B., "Analysis of Polyolefins by Crystallization Analysis Fractionation", *Macromolecular Materials and Engineering*, **2000**, *279*, 46.

Pigeon M.G. and Rudin A., "Branching Measurement by Analytical TREF: A Fully Quantitative Technique", *Journal of Applied Polymer Science*, **1994**, *51*, 303.

Pigeon M.G. and Rudin A., "Comparison of Analytical and Preparative TREF Analysis: A Mathematical Approach to Correcting Analytical TREF Data", *Journal of Applied Polymer Science*, **1993**, 47, 685.

Prasad A. and Mandelkern L., "Equilibrium Dissolution Temperature of Low Molecular Weight Polyethylene Fractions in Dilute Solution", *Macromolecules*, **1989**, *22*, 914.

Rana S.K., "Effect of Cocrystallization on Kinetic Parameters of High-Density Polyethylene/Linear Low-Density Polyethylene Blend", *Journal of Applied Polymer Science*, **1996**, *61*, 951.

Riande E. and Fatou J.M.G., "Crystallization of Dilute Polyethylene Solution: Influence of Molecular Weight", *Polymer*, **1976**, *17*, 99.

Riande E. and Fatou J.M.G., "Effect of Solvent on the Crystallization from Dilute Polyethylene Solutions", *Polymer*, **1976**, *17*, 795.

Sarzotti D.M., "Heterogeneous Metallocene Catalysts for Olefin Polymerization: Effects of Support Material on Microstructure", *Master Thesis*, University of Waterloo, Canada, 2001.

Sarzotti D.M., Soares J.B.P. and Penlidis A., "Ethylene/1-Hexene Copolymers Synthesized with a Single-Site Catalyst: Crystallization Analysis Fractionation, Modeling, and Reactivity Ratio Estimation", *Journal of Polymer Science: Part B: Polymer Physics*, **2002**, *40*, 2595.

Savitski E.P., Caflisch G.B., Killian C.M., Meadows M., Merkley J.H. and Huff B.J., "Influence of the Short-Chain Branch Length on the Calibration of Temperature Rising Elution Fractionation Systems", *Journal of Applied Polymer Science*, **2003**, *90*, 722.

Schouterden P., Groeninckx., Van der Heijden B. and Jensen F., "Fractionation and Thermal Behavior of Linear Low Density Polyethylene", *Polymer*, **1987**, *28*, 2099.

Shanks R.A. and Amarasinghe G., "Comonomer Distribution in Polyethylenes Analysed by DSC After Thermal Fractionation", *Journal of Thermal Analysis and Calorimetry*, **2000**, *59*, 471.

Shirayama K., Kita S.-I. And Watabe H., "Effects of Branching on Some Properties of Ethylene/1-Olefin Copolymers", *Die. Makromolekilare Chemie,* **1972**, *151*, 97.

Simha R. and Branson H., "Theory of Chain Copolymerization Reactions", *Journal of Chemical Physics*, **1944**, *12*, 253.

Simon L.C., de Souza R.F., Soares J.B.P. and Mauler R.S., "Effect of Molecular Structure on Dynamic Mechanical Properties of Polyethylene Obtained with Nickel-Diimine Catalysts", *Polymer*, **2001**, *42*, 4885.

Simon L.C., Patel H., Soares J.B.P. and de Souza R.F., "Polyethylene Made with In Situ Supported Ni-Diimine/SMAO: Replication Phenomenon and Effect of Polymerization Conditions on Polymer Microstructure and Morphology", *Macromolecular Chemistry and Physics*, **2001**, *202*, 3237.

Soares J.B.P., "Mathematical Modeling of the Microstructure of Polyolefins Made by Coordination Polymerization: A Review", *Chemical Engineering Science*, **2001**, *56*, 4131.

Soares J.B.P., Abbott R.F., Willis J.N. and Liu X., "A New Methodology for Studying Multiple-Site-Type Catalysts for the Copolymerization of Olefins", *Macromolecular Chemistry and Physics*, **1996**, *197*, 3383.

Soares J.B.P., Monrabal B., Nieto J. and Blanco, "Crystallization Analysis Fractionation (CRYSTAF) of Poly(Ethylene-co-1-Octene) Made with Single-Site-Type Catalysts: A Mathematic Model for the Dependence of Composition Distribution on Molecular Weight", *Macromolecular Chemistry and Physics*, **1998**, *199*, 1917.

Soares J.B.P., Abbott R.F. and Kim J.D., "Environmental Stress Cracking Resistance of Polyethylene: the Use of CRYSTAF and SEC to Establish Structure-

Property Relationships", *Journal of Polymer Science: Part B: Polymer Physics*, **2000**, *38*, 1267.

Soares J.B.P. and Hamielec A.E., "Analyzing TREF Data by Stockmayer's Bivariate Distribution", *Macromolecular Theory and Simulation*, **1995**, *4*, 305.

Soares J.B.P. and Hamielec A.E., "Temperature Rising Elution Fractionation", in: *Modern Techniques for Polymer Characterization*, R.A. Pethrick, J.V. Dawkins, Eds., John Wiley&Sons, 1999, p. 15-55.

Soares J.B.P. and Hamielec A.E., "Temperature Rising Elution Fractionation of Linear Polyolefins", *Polymer*, **1995**, *36*, 1639.

Soares J.B.P. and Hamielec A.E., "Deconvolution of Chain-Length Distribution of Linear Polymers Made by Multi-Site-Type Catalysts", *Polymer*, **1995**, *36*, 2257.

Springer H., Hengse A. and Hinrichsen G., "Fractionation and Characterization of a 1-Butene Linear Low Density Polyethylene", *Journal of Applied Polymer Science*, **1990**, *40*, 2173.

Starck P., "Studies of the Comonomer Distributions in Low Linear Density Polyethylenes using Temperature Rising Elution Fractionation and Stepwise Crystallization by DSC", *Polymer International*, **1996**, *40*, 111.

Starck P., Lehmus P. and Seppala J.V., "Thermal Characterization of Ethylene Polymers Prepared with Metallocene Catalysts", *Polymer Engineering and Science*, **1999**, *39*, 1444.

Stejskal J., Kratochvil P. and Strakova D., "Study of the Statistical Chemical Heterogeneity of Copolymers by Cross-Fractionation", *Macromolecules*, **1981**, *14*, 150.

Stejskal J., Kratochvil P. and Jenkins A.D., "Graft Copolymer Statistics. 2. Application to Graft Copolymers Prepared from Macromonomers", *Macromolecules,* **1987**, *20*, 181.

Stejskal J. and Kratochvil P., "Statistical Chemical Heterogeneity of Copolymers. Modification of the Stockmayer Distribution Function of Chemical Composition", *Macromolecules*, **1987**, *20*, 2624.

Stockmayer W.H., "Distribution of Chain Lengths and Compositions in Copolymers", *Journal of Chemical Physics*, **1945**, *13*, 199.

Tacx J.C.J.F., Linssen H.N. and German A.L., "Effect of Molar Mass Ratio of Monomers on the Mass Distribution of Chain Lengths and Compositions in Copolymers: Extension of the Stockmayer Theory", *Journal of Polymer Science: Part A: Polymer Chemistry*, **1988**, *26*, 61.

Thomann Y., Sernetz F.G., Thomann R, Kressler J. and Mulhaupt R., "Temperature Rising Elution Fractionation of a Random Ethylene/Styrene Copolymer", *Macromolecular Chemistry and Physics*, **1997**, *198*, 739.

Tobita H., "Multivariate Composition Distribution in Free-Radical Multicomponent Polymerization, 1 Exact Calculation Method Using Generating Function", *Macromolecular Theory and Simulation*, **2003**, *12*, 463.

Tobita H., "Multivariate Composition Distribution in Free-Radical Multicomponent Polymerization, 2 Approximation Using Multivariate Normal Distribution", *Macromolecular Theory and Simulation*, **2003**, *12*, 470.

Tung L.H., "Fractionation of Polyethylene", *Journal of Polymer Science*, **1956**, *20*, 495.

Usami T, Gotoh Y. and Takayama S., "Generation Mechanism of Short-Chain Branching Distribution in Linear Low-Density Polyethylenes", *Macromolecules*, **1986**, *19*, 2722.

Wang W-J., Kolodka E., Zhu S., Hamilec A.E. and Kostanski K., "Temperature Rising Elution Fractionation and Characterization of Ethylene/Octene-1 Copolymers Synthesized with Constrained Geometry Catalyst", *Macromolecular Chemistry Physics*, **1999**, *200*, 2146.

Wardhaugh L.T. and Williams M.C., "Blockiness of Olefin Copolymers and Possible Microphase Separation in the Melt", *Polymer Engineering and Science*, **1995**, *35*, 18.

Wasiak A., Sajkiewicz P. and Wozniak A., "Effects of Cooling Rate on Crystallinity of i-Polypropylene and Polyethylene Terephthalate Crystallized in Nonisothermal Conditions", *Journal of Polymer Science: Part B: Polymer Physics*, **1999**, *37*, 2821.

Wignall G.D., Alamo R.G., Londono J.D., Mandelkern L. and Stehling F.C., "Small-Angle Neutron Scattering Investigations of Liquid-Liquid Phase Separation in Heterogeneous Linear Low-Density Polyethylene", *Macromolecules*, **1996**, *29*, 5332.

Wild L., "Temperature Rising Elution Fractionation", *Advances in Polymer Science*, **1990**, *98*, 1.

Wild L., Ryle D., Knobeloch D. and Peat I., "Determination of Branching Distributions in Polyethylene and Ethylene Copolymers", *Journal of Polymer Science: Part B: Polymer Physics*, **1982**, *20*, 441.

Wild L. and Blatz C., "Development of High Performance Tref for Polyolefin Analysis", in: *New Advances in Polyolefins*, T.C. Chung, Eds, Plenum Press 1993, p. 147-157.

Wilfong D.L., "Crystallization Mechanisms for LLDPE and Its Fractions", *Journal of Polymer Science: Part B Polymer Physics*, **1990**, *28*, 861.

Xu G., "Distribution of Chain Lengths and Composition in Terpolymers", *Journal of Polymer Science: Part A: Polymer Chemistry,* **1997**, *35*, 1161.

Zhang M., Lynch D.T. and Wanke S.E., "Characterization of Commercial Linear Low-Density Polyethylene by TREF-DSC and TREF-SEC Cross-Fractionation", *Journal of Applied Polymer Science*, **2000**, *75*, 960.

Zhang Y.-D., Wu C.-J. and Zhu S.-H., "Fractionation and Characterization for a Propylene-Ethylene Random Copolymer", *Polymer Journal*, **2002**, *34*, 700.

Zhou X.-Q. and Hay J.N., "Fractionation and Structural Properties of Linear Low Density Polyethylene", *European Polymer Journal*, **1993**, *29*, 291.

APPENDIX A

# DERIVATION OF CCD OF RANDOM BINARY COPOLYMERS

This appendix describes the derivation of the CCD of random binary copolymers using the same strategy used for the derivation of the CCD of random terpolymers described in detail in Section 3.4 and 3.5. The term random copolymers used here refer to the case where the inclusion of comonomer units is independent of the chain end type (i.e., a zero order Markov process).

The number and weight chain length distributions of linear binary polymers synthesized with single-site catalysts follow the most probable distribution:

$$f_N(r) = (1 - PP) \cdot PP^{r-1} \tag{A.1}$$

$$f_W(r) = r \cdot (1 - PP)^2 \cdot PP^{r-1} \tag{A.2}$$

where $r$ is the kinetic chain length and $PP$ is the probability of chain propagation.

If a specific kinetic chain length is considered, the number distribution function of chains having $N_A$ units of type A can be determined from

$$f_N(N_A \mid r) = C^r_{N_A} \cdot P[A]^{N_A} \cdot (1 - P[A])^{r-N_A} \tag{A.3}$$

where $N_A$ is the number of A units and $P[A]$ is the probability that monomer of type A will be incorporated into the molecule.

The first binomial coefficient in Equation (A.3), $C^{r}_{N_A}$, describes all possible arrangements of comonomer units in the chain having a kinetic chain length of $r$, $N_A$ units of A, and $r$-$N_A$ units of B. The remaining terms describe the probability that a particular molecule can be generated. A similar expression in terms of mole fraction ($n_A$) can be obtained:

$$f_N(n_A \mid r) = r \cdot C^{r}_{r-n_A} \cdot P[A]^{r-n_A} \cdot (1-P[A])^{r(1-n_A)} \tag{A.4}$$

A more general form of this distribution function can be obtained for the complete distribution of chain lengths:

$$f_N(r,n_A) = f_N(n_A \mid r) \cdot f_N(r) \tag{A.5}$$

where $f_N(r)$ is given by Equation (A.1). Equation (A.5) describes the number fraction of chains that have kinetic chain length $r$, and mole fractions of comonomers A and B, $n_A$ and 1-$n_A$ respectively.

Note that, the above distribution function satisfies the following condition:

$$\int_{r=1}^{\infty} \int_{n_A=0}^{1} f_N(r,n_A) \cdot dn_A dr = 1 \tag{A.6}$$

The weight distribution function of chemical composition can be calculated from the number distribution function by taking into account the weights of the chains. The weight distribution function of chains of kinetic chain length $r$ with mole fractions of $n_A$ is given by Equations (A.7).

$$f_W(n_A \mid r) = f_N(n_A \mid r) \cdot \left[ \frac{M_A \cdot n_A + M_B \cdot (1-n_A)}{M_A \cdot P[A] + M_B(1-P[A])} \right] \tag{A.7}$$

where $M_A$ and $M_B$ are molecular weight of monomer type A and B, respectively.

A more general form of Equation (A.7) can be obtained by considering the weight distribution function of chains having different kinetic chain lengths:

$$f_W(r,n_A) = f_W(n_A \mid r) \cdot f_W(r) \tag{A.8}$$

where $f_W(r)$ is given by Equation (A.2). Using Equation (A.2), (A.4), and (A.7), Equation (A.8) can be rewritten as:

$$f_{W,P}(r,n_A) = C^{r}_{r\cdot n_A} \cdot P[A]^{r\cdot n_A} \cdot (1-P[A])^{r\cdot(1-n_A)} \cdot r^2 \cdot (1-PP)^2 \cdot PP^{r-1} \times \left[ \frac{M_A \cdot n_A + M_B \cdot (1-n_A)}{M_A \cdot P[A] + M_B \cdot (1-P[A])} \right] \quad \text{(A.9)}$$

Equation (A.9) is identical to Equation (3.4) in Chapter 3.

APPENDIX B

# SAMPLE PREPARATION

This appendix briefly discusses the information related to sample preparation. For the polymerization, ethylene and nitrogen (Praxair) were purified by passing through packed beds of molecular sieves (a mixture of 4 Å and 13X sieves) and copper (II) oxide. Toluene was purified by distillation over a butyl lithium/styrene/sodium system. The 1-olefin comonomers (Aldrich) were dried over 4 Å molecular sieves and under nitrogen purge before use.

The cocatalyst, methylaluminoxane (MAO, 10 wt% solution in toluene from Aldrich), was used as received. The metallocene catalyst, rac-ethylene bis(indenyl)zirconium dichloride (rac-Et$(Ind)_2ZrCl_2$), was purchased as a crystalline solid from Boulder Scientific and was also used as received. For polymerization, a solution of rac-Et$(Ind)_2ZrCl_2$ was prepared at a concentration of 0.5 μmol/g in distilled toluene.

All ethylene/1-olefin copolymers were synthesized in semi-batch mode using a 300 mL Parr autoclave reactor by adding all components to the reactor (toluene, catalyst, cocatalyst and hydrogen) at the beginning of the polymerization and feeding ethylene on demand to keep a constant pressure. In this investigation, four comonomers were used: propylene, 1-hexene, 1-octene, and 1-dodecene. The

polymerizations were performed at 60 °C and 6.8 atm ethylene partial pressure. Approximately 0.25 μmol of Zr in form of rac-Et(Ind)$_2$ZrCl$_2$ was used in each reaction with MAO at an Al/Zr ratio of 2,000.

The amount of comonomer fed to the reactor was varied to obtain a series of copolymer samples with different average comonomer contents. Since all samples were synthesized with a single-site type catalyst, narrow and unimodal CCDs were expected. A more detailed description of the polymerization procedure has been given by Sarzotti et al. (2002) (see bibliography for reference).